AD_____

Award Number: DAMD17-01-1-0744

TITLE: Molecular Genetic Studies of Bone Mechanical Strain and of Pedigrees with Very High Bone Density

PRINCIPAL INVESTIGATOR: Subburaman Mohan, Ph.D.

CONTRACTING ORGANIZATION: Loma Linda Veterans Association for Research and Education
Redlands, CA 92373-5189

REPORT DATE: November 2006

TYPE OF REPORT: Annual

PREPARED FOR: U.S. Army Medical Research and Materiel Command
Fort Detrick, Maryland 21702-5012

REPORT DOCUMENTATION PAGE

Form Approved
OMB No. 0704-0188

1. REPORT DATE *(DD-MM-YYYY)*	**2. REPORT TYPE**	**3. DATES COVERED** *(From - To)*
01/1/06	Annual	15 May 2005 – 30 Oct 2006

4. TITLE AND SUBTITLE

Molecular Genetic Studies of Bone Mechanical Strain and of Pedigrees with Very High Bone Density

5a. CONTRACT NUMBER

5b. GRANT NUMBER
DAMD17-01-1-0744

5c. PROGRAM ELEMENT NUMBER

6. AUTHOR(S)
Subburaman Mohan, Ph.D.

E-Mail: Subburaman.Mohan@va.gov

5d. PROJECT NUMBER

5e. TASK NUMBER

5f. WORK UNIT NUMBER

7. PERFORMING ORGANIZATION NAME(S) AND ADDRESS(ES)

Loma Linda Veterans Association for Research and Education
Redlands, CA 92373-5189

8. PERFORMING ORGANIZATION REPORT NUMBER

9. SPONSORING / MONITORING AGENCY NAME(S) AND ADDRESS(ES)
U.S. Army Medical Research and Materiel Command
Fort Detrick, Maryland 21702-5012

10. SPONSOR/MONITOR'S ACRONYM(S)

11. SPONSOR/MONITOR'S REPORT NUMBER(S)

12. DISTRIBUTION / AVAILABILITY STATEMENT
Approved for Public Release; Distribution Unlimited

13. SUPPLEMENTARY NOTES

14. ABSTRACT: The primary goal of the proposed work on bone mechanical strain focuses on identifying the genes and their functions involved in mediating the anabolic skeletal response to mechanical stress. Two hypotheses have been proposed:1) Quantitative trait loci analysis using the four point bending technique in two strains of mice exhibiting extreme differences in loading response will lead to identification of chromosomal locations of genes involved in variation in skeletal response to mechanical loading. 2) Application of microarray and tyrosine phosphorylation studies using bone cells derived from inbred strains of mice exhibiting extreme differences to loading response and physiologically relevant fluid flow shear strain will lead to identification of key signaling genes and their pathways that contribute to variation in bone cell response to mechanical strain. During the last funding period, we proposed several specific objectives for each of the above-mentioned hypothesis. We have made considerable progress in accomplishing all of the specific objectives. Our work during this reporting period has resulted in two published manuscripts and three abstracts. We believe that successful accomplishment of the proposed studies will provide a better understanding of the molecular mechanisms involved in identifying the genes and their function as related to mechanical stress.

15. SUBJECT TERMS
Mechanical strain, quantitative trait loci analysis, microarray analysis, osteoblasts, signaling pathways, bone formation

16. SECURITY CLASSIFICATION OF:			**17. LIMITATION OF ABSTRACT**	**18. NUMBER OF PAGES**	**19a. NAME OF RESPONSIBLE PERSON**
a. REPORT	**b. ABSTRACT**	**c. THIS PAGE**			USAMRMC
U	U	U	UU	91	**19b. TELEPHONE NUMBER** *(include area code)*

Table of Contents

Molecular Genetic Studies of Bone Mechanical Strain – In Vivo Studies

Introduction

Mechanical stimulation is one of the important factors in the development and maintenance of skeletal tissues [1, 2]. Several *in-vivo* studies have shown that increased mechanical stress on bone tissue changes the bone density and morphology, resulting in an increased bone mass and biomechanical strength, whereas lack of mechanical stress leads to a rapid bone loss as evidenced by immobilization and bed rest studies [3-7]. Thus, physical exercise has been perceived as an important therapeutic strategy in humans to maintain bone mass and prevent osteoporosis. Recent studies in humans have also shown that bone anabolic response to a given mechanical load is highly variable, with some individuals exhibiting robust bone anabolic response with others responding modestly [8-10]. A similar variation has been observed among inbred strains of mice. We [11, 12] and others have shown that mouse strains such as C57BL/6J (B6) respond with a much higher increase in bone density (BMD) and bone cross-sectional area as compared to the C3H/HeJ (C3H) strain of mouse in response to a similar amount of *in-vivo* loading. These data suggest that variations in skeletal response to mechanical loading (ML) in humans and mice are largely determined by genetic factors. However, very little is known about the genetic regulation of mechanical loading and, so far, not a single gene has been identified that influences the skeletal response to mechanical loading.

Quantitative trait loci (QTL) analyses in inbred strains of mice provide a powerful and practical approach to perform a genome-wide search for genetic loci that contribute to variation in a quantitative phenotype. This approach has been used extensively to study genetic regulation of bone density and other related traits, such as bone metabolism, strength, quality, and size, using an intercross of two inbred strains of mice that exhibit extreme differences in the phenotype of interest[13-15]. In this study, we used two inbred strains, C57BL/6J and C3H/HeJ, good and poor responder strains respectively, to perform a genome-wide search for loci regulating bone adaptive response to exercise.

Body: Our goals for the first year of this continuation proposal for the in-vivo studies for the revised Technical Objective-I, as well as our progress for each of the specific objectives in Technical Objective-I, are described below.

Our specific objectives for the first 12 months of the funding period for the in vivo studies are as follows:

1) To cross two strains of mice (a poor responder strain and a good responder strain) to produce F1 mice.
2) To intercross F1 mice from these two strains to produce about 300 F2 mice.
3) To begin phenotyping the 300 F2 mice with our newly validated phenotype (i.e. realtime PCR of bone marker genes)
4) To begin genotyping the 300 F2 mice.
5) To determine the fate of new bone gained during 2 weeks of mechanical loading (i.e. to determine how long the bone density and/or bone strength gained during 2 weeks of mechanical loading is maintained after termination of 4-point bending).
6) To determine if the load applied to increase optimal anabolic response causes micro cracks in loaded bone.

Specific objective 1: To cross two strains of mice (a poor responder strain and a good responder strain) to produce F1 mice.

In the previous report, we demonstrated that the B6 mouse is a good responder to mechanical loading and C3H is a poor responder in terms of BMD response. We therefore selected these two inbred strains of mice for our QTL study to localize the genetic regions responsible for increasing bone's anabolic response to mechanical stress. We crossed female B6 with male C3H mice and generated 100F1s (a mix of male & female).

Specific objective 2: To intercross F1 mice from these two strains to produce about 300 F2 mice.

A population of 329 F2 female mice was generated from 100 F1s (brother-sister mating). We used female mice for our study in the F2 population for three reasons: 1) There was no difference in the bone response to mechanical loading between the sexes in the parental strains (B6 and C3H mice); 2) The males are aggressive and territorial compared to females; and 3) All our previous experiments to establish the phenotypic difference between the B6 and C3H mice to mechanical load were carried out in females.

Specific objective 3: To continue the phenotyping of about 300 F2 mice

The F2 animals, after reaching 10-weeks, were mechanically loaded for 12 days using four-point bending according to our optimized regimen (9N load at 2Hz, 36 cycles). We used halothane [95% Oxygen and 5% Halothane] for 2-3 minutes to anesthetize the mice and performed mechanical loading while the mice were anesthetized. Prior to loading and while the mice were anesthetized, we used the ankle of the tibia that sits on the lower secondary immobile point as a reference which allowed us to position the loading region of the tibia similarly for each mouse. The right tibia was used for loading and the left tibia was used as an internal control. Two days after the last loading regimen, changes in the bone parameters were measured *in vivo* in the loaded vs. unloaded tibia using the pQCT system from Stratec XCT Research. The mice were anesthetized using a solution of sterile water, ketamine (16.6 mg/mL), and xylazine (3.3 mg/mL). The mice were weighed and the ketamine/xylazine solution was injected in cubic centimeters (ccs) based on the gram weight of the mice [gram weight multiplied by 0.0036 (0.06 mg ketamine/g mouse, 0.012 mg xylazine/g mouse)]. The bone measurements were then taken using pQCT while the mice were anesthetized and afterwards the mice recovered from the anesthesia near a heat source.

To minimize the measurement errors caused by positioning of the tibia for pQCT, we used the tibia-fibular junction as the reference line in all F2 mice. We selected two-slices (1mm intervals) that were 4 mm proximal from the tibia-fibular junction for pQCT measurement. The reasons for selecting the two slices were as follows: 1) this region corresponds to the loading zone based on our preliminary study; 2) To complete pQCT scanning of more than two slices would take 25 minutes and longer for one mouse; 3) Since we are performing *in vivo* pQCT, straight positioning (90° angle) of the tibia in our scout view was very important for measuring the transverse-cross section accurately, which also consumes time; and 4) Long duration of ketamine/xylazine anesthesia can lead to death in the mice, which would have reduced the number of mice in our F2s. We next analyzed the pQCT data for the changes in the bone parameters such as vBMD, cortical vBMD, bone size and cortical thickness in the non-loaded and loaded bones of F1 and F2 animals. We used two thresholds that have been selected based on preliminary studies. A

180-730 mg/cm^3 threshold was used to measure total area, total mineral content, periosteal circumference, and endosteal circumference in the loaded vs. non-loaded bones. A 730-730-mg/cm^3 threshold was used to measure cortical thickness, total volumetric density, and material bone mineral density.

We now, have completed the pQCT measurement of bone parameters, followed by the data analysis and organization. The mean percent increase in response to loading in the female F1 mice (n=100) was 2.8% for total vBMD, 0.8% for cortical vBMD, 8.0% for PC and 11.7% for CTh. These loading-induced increases in various skeletal parameters in F1 mice were intermediate between parent strains based on results published previously [11]. In the F2 mice (n=329), the mean increase in total vBMD was 5%, and that of cortical vBMD, PC, CTh, were 1.5%, 9%, and 14%, respectively.

Specific objective 4: To continue the genotyping of the F2 mice

Two-days after the last loading, we scarified the mice and collected tissues such as liver, tibia, and muscle and stored at -80°C for later use. Genomic DNA was extracted from liver tissue of 329 F2 mice using a Qiagen DNA extraction kit. The quality and quantity of the DNA was analyzed using bio-analyzer and Nana-Drop respectively. We selected 111 markers, which were chosen depending upon the position on the chromosome in an effort to distribute then at <15cM to generate a complete genome wide scan. Polymerase Chain Reaction (PCR) primers were purchased from Applied Biosystems (ABIPRISM, Foster City, CA) to perform the genome-wide genotyping scan of the F2 population. PCR reaction conditions allowed 3-4 microsatellite markers to be multiplexed in a single electrophoretic lane. The pooled products were analyzed for fragments size on the ABI 3100 Sequence Detection System and Gene Scan software was used to detect size of the alleles. Allele calls and edits were performed using Genotyper software and in house software, and exported as text files for downstream analysis. We have completed genotyping for all the F2 mice.

Before proceeding with the QTL study, previously, we have reported that mechanical loading by four-point bending caused greater changes in the BMD and bone size in B6 mice after 12 days of 9N load. In order to determine if the increase in bone anabolic response induced by bending are not due to periosteal pad pressure, we performed sham-bending in 10-week old female B6 mice for 12 days using 9N load at 2Hz for 36 cycles. The results from our pQCT analysis revealed no significant changes in the BMD, periosteal circumference and other bone parameters (**Table-1**). This finding implies that changes in bone parameters induced by bending are not due to periosteal pad pressure as evidenced from sham-loading study. We have therefore used four-point bending as a loading model in our QTL study.

Table-1 Changes in the bone parameters in response to 12 days of sham-bending at 9N load in 10-week female B6 mice.

Bone parameters	Mean ± SD		
	Non-loaded	Loaded	p-value
Total Area, mm^2	2.01 ± 0.11	2.07 ± 0.10	0.30
Total Mineral content, mg/mm	1.08 ± 0.04	1.10 ± 0.04	0.46
Periosteal. Circum, mm	5.02 ± 0.14	5.10 ± 0.12	0.29
Endosteal. Circum, mm	4.09 ± 0.15	4.17 ± 0.12	0.31
Total vBMD, mg/cm^3	649 ± 14.64	663.7 ± 19.7	0.15
Cortical vBMD, mg/cm^3	1031 ± 9.8	1038 ± 13.5	0.26

N=7

Using the above phenotype (bone parameters) and genotype data, we next performed classical QTL analysis to identify the loci regulating the bone anabolic response to loading. The bone anabolic response to mechanical loading in the F2 mice was calculated from measurements of well-established parameters, such as total vBMD, cortical vBMD, PC and CTh, in loaded tibia. Results for each parameter were expressed as percent change from identical measurements performed on non-loaded left tibia in each F2 mouse. Analysis of percent change from non-loaded bone was based on the rationale that variable genetic background in each F2 mouse would affect the bone morphology (such as cross sectional area) and influence the skeletal response independently of genetic regulation of loading. In addition, there are naturally segregating allelic variations between C3H and B6 mice that could affect BMD and bone size traits. Therefore, the use of absolute changes in BMD or periosteal circumference phenotype to study linkage would identify common, rather than specific, genetic components relevant for response to loading. Subsequently, genotyping for 329 F2 mice was completed. Alleles were called, edited using in house and ABI genotyper software.

We then used parametric mapping (a mapping strategy that requires the assumption of normal distribution for the quantitative trait investigation) for total vBMD, Cortical vBMD, PC and CTh in our QTL analysis. Because the distribution of the PC showed some significant skewing, analysis was also performed on log transformed PC data. The log transformation normalized the distribution but did not alter the identification of QTL and produced only slight changes in LOD scores. The interval mapping was performed by using a MapQTL software program (Verison 5.0; Wageningen, The Netherlands). The threshold values for significance of association were determined by a 1000 permutation test. QTLs with a genome wide error of 1%, 5% and 32% were classified as highly significant, significant and suggestive, respectively.

The linkage map, constructed using 111 markers (average marker density: 15 cM) and loading-induced changes in total vBMD, cortical vBMD, PC, and CTh phenotypes in 329 female F2 mice, revealed evidence for the presence of several significant and suggestive loci as shown in **Table-2 and Figure 1**. Loci regulating total vBMD (and cortical vBMD) were located on Chromosome (Chr) 1, 3, 8, and 9, whereas loci regulating bone size, which includes periosteal circumference and cortical thickness were located on

Chrs 8, 9, 11, 17, and 18. The strongest linkage was observed on chromosome 8 for total vBMD (LOD score 4.2, 60 cM) (**Figure 1**). **Figure 2** shows posterior probability density plots for QTLs located on Chrs 1, 3, and 8. The posterior probability density plot is a likelihood statistic that gives rise to the 95% confidence intervals for QTL peak indicated by a horizontal bar in the plot. The four BMD QTLs (includes total vBMD and cortical vBMD) on Chrs 1, 3, 8, and 9 accounted for 19% of the variance in response to ML. Loci on Chrs 8, 9, 11, 17, and 18 regulating bone size (includes PC and CTh) accounted for the 16% variance in the F2 mice (**Table-2**). Chrs 8 and 9 QTL for BMD, PC and CTh were colocalized, whereas loci on Chrs 1 and 3 were specific for BMD, and Chrs 11, 17 and 18 loci were specific for bone size. Because there was a slight negative correlation between % changes in BMD response in loaded bones versus body weight, we performed QTL analysis after adjusting for body weight in the F2 mice. We found that body weight adjustment yielded an additional locus (Chr17) in addition to loci on Chr 1, 8 and 9.

Table-2 Significant and suggestive QTLs for the mechanical load-induced phenotypes in the B6xC3H F2 female mice.

Phenotype	Chromosome	Locus	cM	LOD score	% Variation
Total vBMD	1	D1Mit113	91.8	3.4[a]	5.5
	8	D8Mit88	60.1	4.2[a]	8.5
	9	D9Mit336	33.9	2.5[c]	4.8
Cortical vBMD	1	D1Mit113	91.8	2.3[c]	3.6
	3	D3Mit320	50.3	3.6[a]	7.3
	9	D9Mit355	49.2	2.5[c]	3.4
Periosteal	8	D8Mit49	68.9	3.0[b]	4.3
circumference	9	D9Mit97	24	2.2[c]	3.3
	11	D11Mit333	69.9	2.1[c]	3.3
	18	D18Mit64	0	3.0[b]	4.4
Cortical thickness	8	D8Mit88	60.1	3.6[a]	5.7
	9	D9Mit2	13.1	3.0[b]	3.2
	11	D11Mit333	69.9	2.5[c]	4.2
	17	D17Mit93	39.3	3.0[b]	4.2

[a]The threshold for the highly significant LOD score is $p<0.01$
[b]The threshold for the significant LOD score is $p<0.05$
[c]The threshold for the suggestive LOD score is $p<0.1$
Variances explained are from the peak LOD score in each phenotype

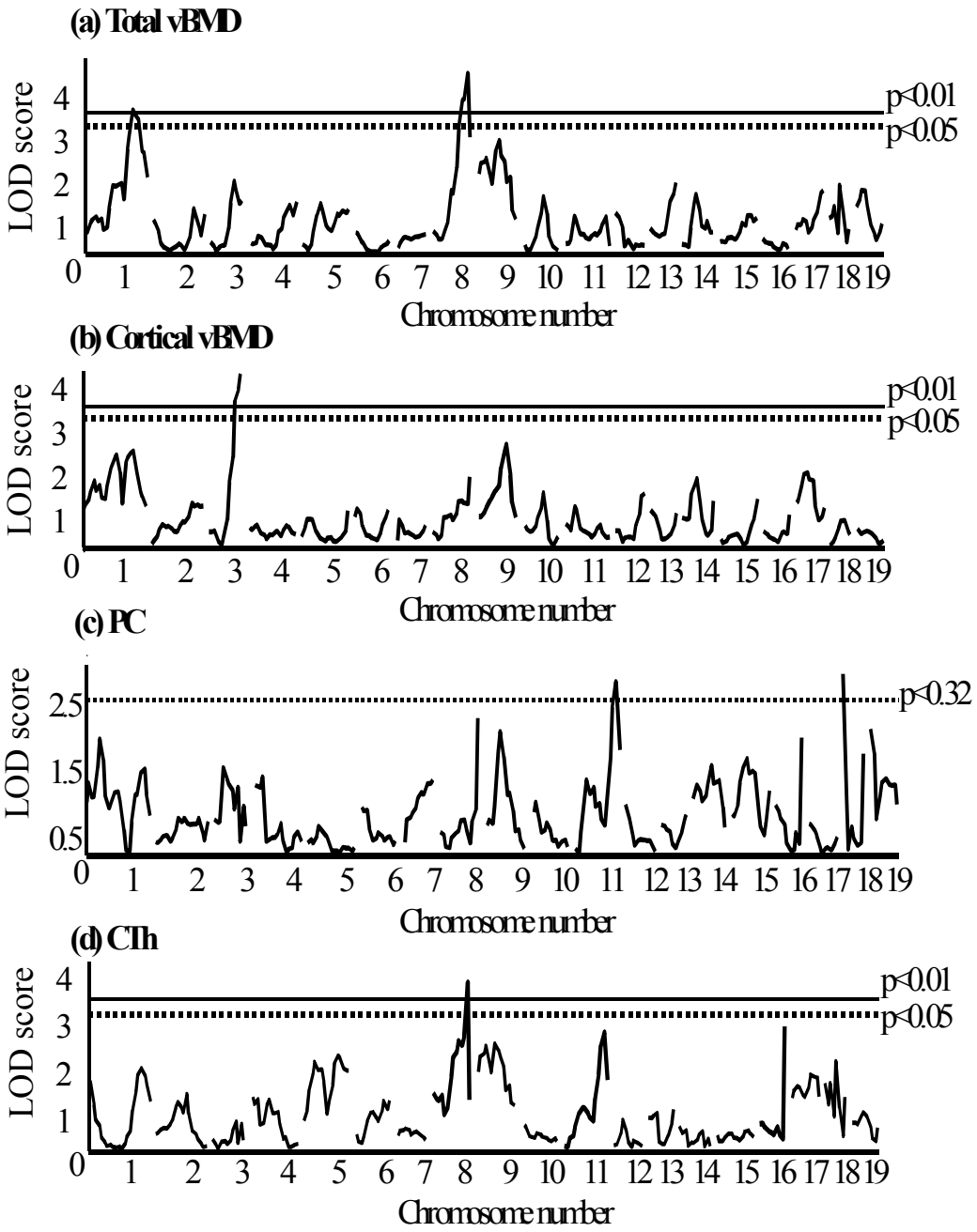

Figure 1: Genome-wide scan for percent change in (a) Total vBMD, (b) Cortical vBMD and (c) PC and (d) CTh induced by mechanical loading in the F2 population of B6xC3H intercross. The y-axis indicates LOD score and x-axis represent chromosomes. The solid line indicates genome-wide thresholds for significant QTL and broken links indicate thresholds for suggestive QTL.

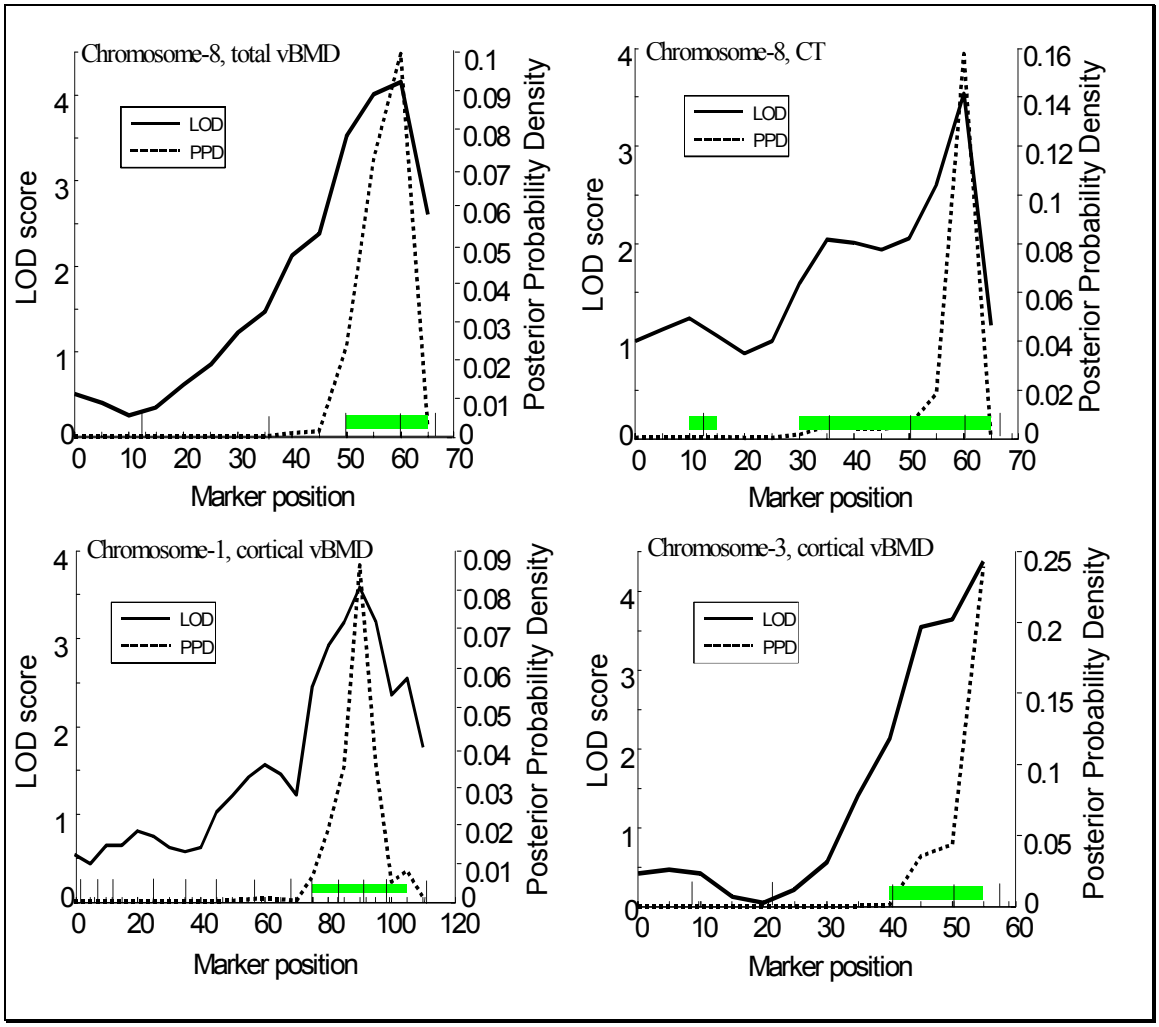

Figure 2: Detailed map for chromosomes 8, 1 and 3 showing significant QTLs for total vBMD, cortical thickness and cortical vBMD. LOD scores between markers were determined using Pseudomarker MAINSCAN program with a default setting of 2.5cM between steps. The markers positions are highlighted as vertical lines in the x-axis. Posterior probability density (shown on right y-axis) plots allow best estimate of putative QTL position on the marker map.

In addition to loci regulating response to loading, we used data from non-loaded tibia to identify linkage to BMD and bone size parameters. All four traits (total vBMD, cortical vBMD, PC, and CTh) showed normal distribution. Since there was a significant positive correlation (r-value range from 0.13 to 0.55, $p<0.05$) between the body weight and PC, and body weight and BMD, we performed QTL analyses after adjustment for body weight. We identified 13 chromosomes that regulate changes in BMD and bone size including Chrs 1, 2, 3, 4, 6, 10, 11, 12, 15, 16, 17, 18, and 19 (**Table-3, Figure 3**). Table-3 provides a list of QTLs that showed significant and suggestive linkages, the closest markers on peak QTL, and the percent variance explained by each QTL for different phenotypes. Some of the QTLs observed for the non-loaded phenotypes that include BMD and bone size, are similar to the previously published QTLs [16-19]. In addition, we identified novel QTL for BMD on Chr 3 (LOD score 2.8, 59.0cM), 10 (LOD score 3.8, 63.4cM) and 17 (LOD score 5.4, 39.0cM), and PC QTL on Chrs 3 (LOD score 4.0, 46.4 cM), 10 (LOD score 2.4, 57.3 cM), 11 (LOD score 4.3, 49.2 cM), 15 (LOD score 3.1, 41.5

cM), 16 (LOD score 3.1, 24.0 cM), 17 (LOD score 5.1, 39.3 cM), and CTh QTL on Chrs 1, 3, 10, 16, 17, 18, and 19 (Table-3). Together, data from the loaded and non-loaded tibia, we found that ML BMD QTL for Chr. 8 and 9 and bone size QTL for Chr. 8 and 18 could not be detected using phenotype data from non-loaded bones, suggesting that these QTLs are unique to ML phenotypes.

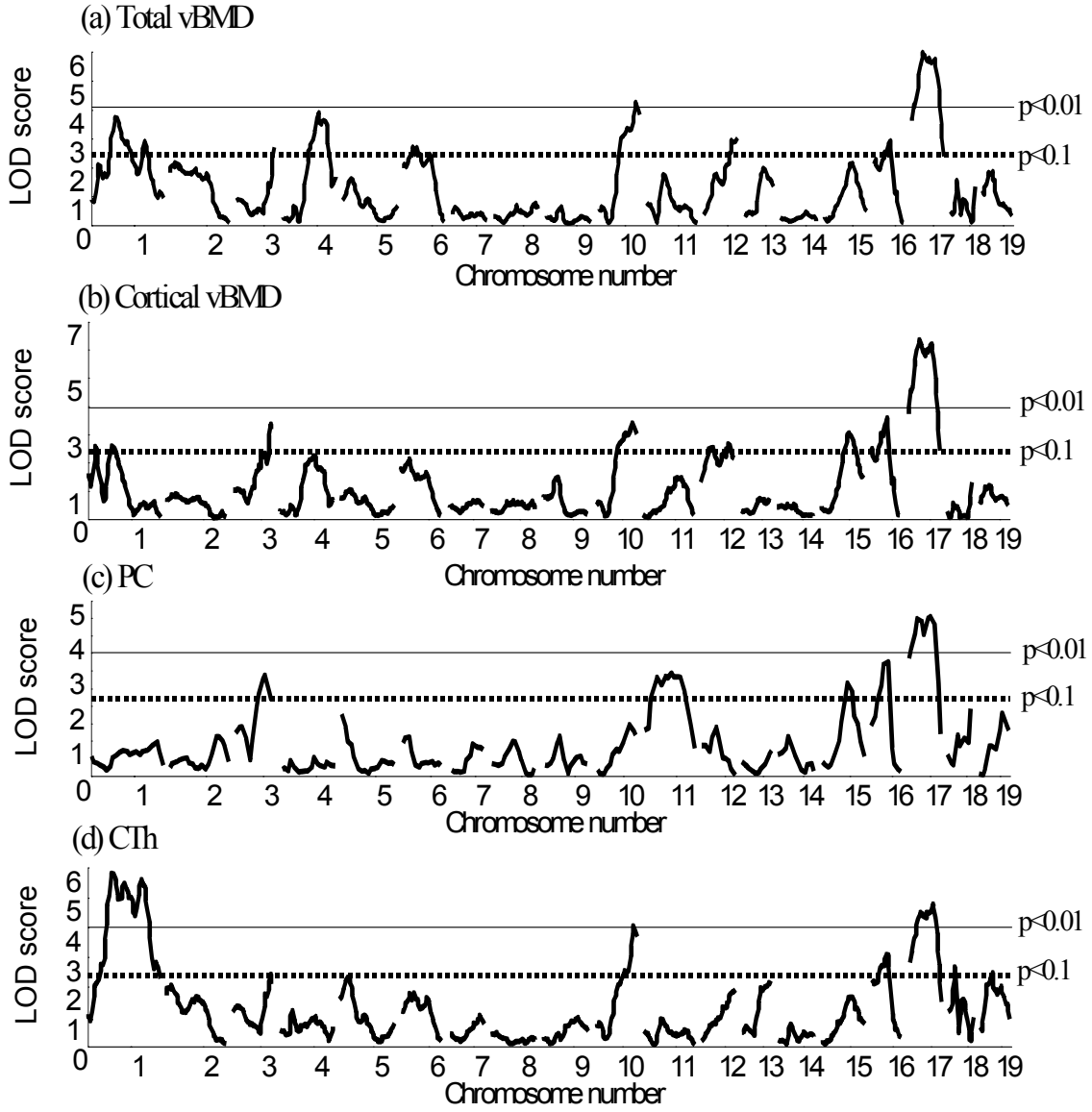

Figure 3: Genome-wide scan associated with non-loaded (a) Total vBMD, (b) Cortical vBMD, (c) PC and (d) CTh in the F2 population of B6-C3H intercross. The y-axis indicates LOD score and x-axis represents chromosomes. The solid line indicates genome-wide threshold for significant QTL and broken lines indicate thresholds for suggestive QTL.

Table-3 Significant and suggestive QTLs for the non-loaded phenotypes in the B6xC3H F2 female mice.

Phenotypes	Chromosome	Locus	cM	LOD score	% Variation
Total vBMD	1	D1Mit380	37.1	3.8[a]	5.3
		D1Mit106	83.1	2.8[c]	3.9
	2	D2Mit1*	14.2	2.3[c]	4.6
	3	**D3Mit147**	**59.0**	**2.8[c]**	**3.9**
	4	D4Mit251	66.7	3.6[a]	5.4
	6	D6Mit209*	16.9	2.9[c]	4.8
	10	**D10Mit233**	**63.4**	**3.8[a]**	**5.3**
	12	D12Mit16*	44.5	3.3[a]	5.9
	16	D16Mit60	24.0	2.9[c]	4.0
	17	**D17Mit93**	**39.0**	**5.4[a]**	**7.4**
Cortical vBMD	1	D1Mit380	37.2	2.7[c]	3.8
	3	**D3Mit147**	**59.1**	**3.2[a]**	**4.6**
	10	**D10Mit95**	**50.3**	**3.0[b]**	**4.2**
	12	D12Mit16*	40.5	2.9[c]	5.7
	15	D15Mit107	41.5	3.0[b]	4.5
	16	D16Mit60	24.0	3.6[a]	4.9
	17	**D17Mit93**	**39.3**	**5.9[a]**	**8.0**
	3	**D3Mit320***	**46.4**	**4.0[a]**	**7.2**
Periosteal	**10**	**D10Mit233***	**57.3**	**2.4[c]**	**3.9**
circumference	**11**	**D11Mit285**	**49.2**	**4.3[a]**	**6**
	15	**D15Mit107**	**41.5**	**3.1[b]**	**4.7**
	16	**D16Mit60**	**24.0**	**3.1[b]**	**4.3**
	17	**D17Mit93**	**39.3**	**5.1[a]**	**7**
	1	**D1Mit380**	**37.2**	**5.9[a]**	**8**
Cortical thickness		**D1Mit106**	**83.1**	**5.4[a]**	**7.3**
	3	**D3Mit147***	**55.3**	**2.5[c]**	**4.2**
	10	**D10Mit233**	**63.4**	**3.7[a]**	**5.1**
	16	**D16Mit60**	**24.0**	**3.1[b]**	**4.2**
	17	**D17Mit93**	**39.3**	**4.7 [a]**	**6.5**
	18	**D18Mit12**	**9.8**	**2.7[c]**	**3.8**
	19	**D19Mit28***	**9.8**	**2.8[c]**	**6**

[a]The threshold for the highly significant LOD score is $p<0.01$
[b]The threshold for the significant LOD score is $p<0.05$
[c]The threshold for the suggestive LOD score is $p<0.1$
Novel QTLs are highlighted in bold
* Corresponds to marker closer to the peak LOD score

The genome-wide search for associations between marker genotypes and the quantitative phenotypes of bone anabolic response to loading resulted in the localization of several QTLs in C3HxB6 F2 mice. The primary mechanism by which mechanical loading induces increases in BMD is believed to involve Periosteal modeling [11], leading to increased cortical thickness and an eventual increase in volumetric BMD. Based on this hypothesis, the QTLs identified in this study can be grouped into three categories: 1) QTLs that affect both BMD and bone size response to ML; 2) QTLs that affect only BMD response to ML; and 3) QTLs that only influence bone size response to ML.

Our findings that genetic loci in Chrs 8 and 9 show significant linkage with multiple measures of skeletal response to loading (total vBMD, PC and CTh), even though our analysis eliminated effects of confounding factors, such as bone size, suggest that these loci may contain genes that play a key role in mediating bone cell response to loading by regulating both BMD and bone size. Consistent with this idea, previous studies have shown that Chrs 8 and 9 contain genetic loci that regulate biomechanical and femur breaking strength in the multiple inbred mouse strain crosses including B6xC3H (Chr 8, 30-90 cM) [20], B6XD2 F2 mice (Chr 8, 30-57 cM) [21, 22] and MRLXSJL (30-60cM) [13, 23]. Taken together, these data may suggest genes in these regions regulate biomechanical strength possibly with consequence of superior (or more favorable) response to exercise.

In addition to the ML QTL that regulated both BMD and bone size, Chr 1 (91.8 cM) and Chr 3 (50.3 cM) QTL specifically affected BMD but not bone size. ML QTL in Chr 1 (91.8 cM) colocalizes with a major QTL identified earlier for total vBMD and other structural properties in the congenic and B6xC3H F2 mice [20, 24]. Accordingly, QTL analysis of the BMD phenotype for non-loaded bones in the present study revealed a major QTL on Chr 1 at 83.1 cM, which is closer to the previous published BMD QTL. While the B6 alleles in Chr 1 contributed to higher BMD response to four-point bending (Figure 5), C3H alleles contributed to higher BMD in non-loaded bone (data not shown). Thus, Chr 1 QTL may contain genes: 1) that contribute to natural variation in BMD between B6 and C3H strains; and 2) that respond to mechanical loading by increasing the vBMD. Our linkage analysis also identified loci on Chr 11 (69.9 cM), Chr 17 (39.3 cM), and Chr 18 (0 cM) that only influence bone size in response to mechanical loading. Furthermore, several novel loci regulating bone size on Chrs 3, 10, 11, 15, 16, 17, 18, and 19 were discovered using data from non-loaded bones. Based on these findings, it can be concluded that complex genetic mechanisms regulate variations in BMD and bone size in non-loaded and loaded bones. Another finding that provides substantial support for this concept of complex regulation of BMD and bone size is appearance of novel QTLs (Chr 5 and Chr 13) in the interaction study mentioned below but not in the mainscan.

We next determined the contribution of alleles from B6 and C3H mice for the major QTL affecting BMD and PC. As shown in Figure 5, for Chr 1 BMD QTL, homozygous B6 alleles at marker *D1Mit113* showed dominant effect over C3H homozygous mice and were 5.6% (Figure 5) higher than the homozygotes for C3H alleles. Although the response to mechanical loading was higher in the B6 strain, it is noteworthy that C3H alleles at Chr 8 increased BMD in response to mechanical loading (**Figure 4**). Thus, homozygous C3H alleles at marker *D8Mit88* had 5.8% higher BMD than the homozygous B6 alleles. For this QTL, the C3H alleles best fit a recessive mode of inheritance. For PC QTL, homozygous alleles from B6 mice at marker *D8Mit49* showed 10% higher PC values than the mice with homozygous C3H alleles. The Chr 8 loci regulating PC inherited in dominant mode. It is noteworthy that a previous study reported that a congenic strain in which a small fragment of C3H Chr 4 (40-80 cM) was introgressed in a B6 background showed increased mechanosensitivity to loading [25]. Our study, however, did not identify any QTL on Chr 4. There are several possible explanations for why we did not find a QTL in chromosome 4: 1) the two models of loading used to study the bone anabolic responses are different. 2) The number of F2 mice used may not be adequate to identify all of the mechanical loading QTL and 3) While many of the mechanical loading QTL may regulate anabolic response to four-point bending at multiple skeletal sites, there may be some QTL that are site specific i.e. regulate

anabolic response in some but not other skeletal sites. In this regard, it is known that there common BMD QTL that regulate BMD at multiple skeletal sites and site specific BMD QTL that regulate BMD at some but not other site. Consistent with the previous study, we did observe that the BMD response to mechanical loading was higher for C3H alleles on Chr 8 QTL as compared to B6 alleles. Since C3H mice demonstrate poor adaptation to mechanical loading as compared to the B6 mice, these findings of high response alleles in C3H were unexpected. It is possible that C3H alleles at these loci are phenotypically silent in the context of the C3H genome but increase BMD in response to four-point bending in the presence of one or more B6 alleles.

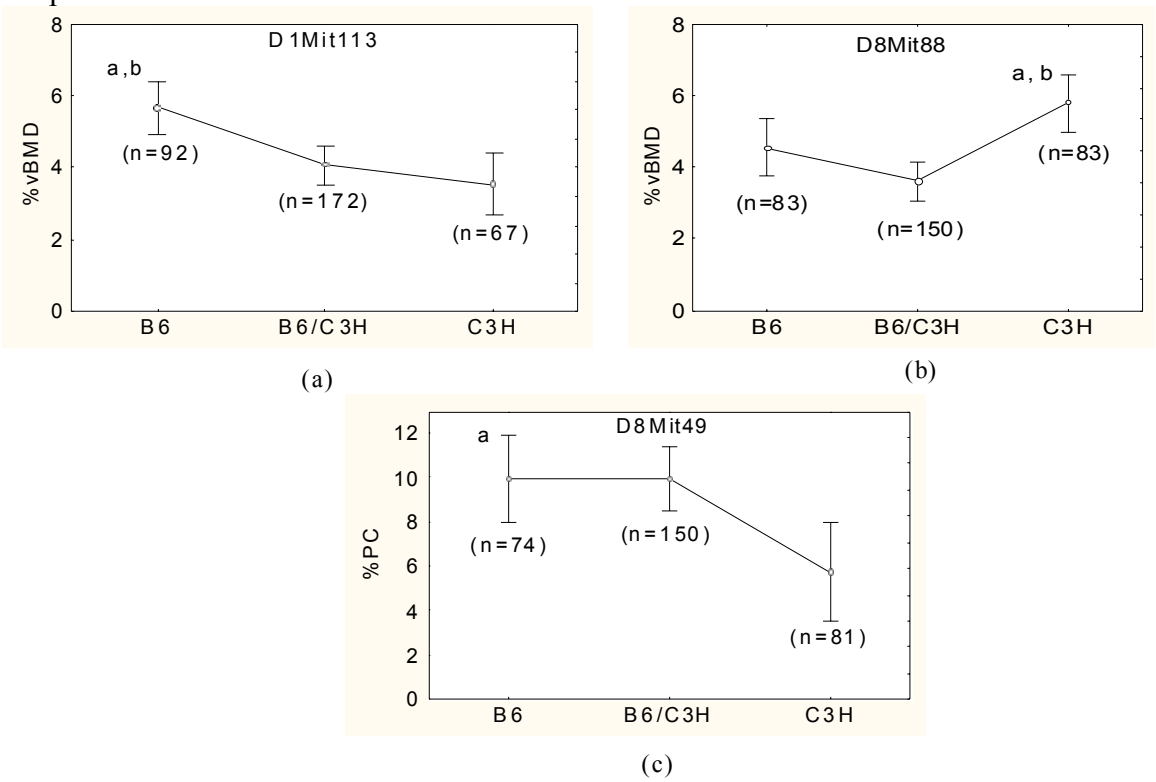

Figure 4: Effect of B6 vs. C3H alleles at the major QTLs affecting total vBMD and bone size phenotypes on chromosome 1 and 8. Significant differences ($p<0.01$) are indicated by the lowercase letters, where "a" indicates the B6 or C3H allele is significantly different than mice with C3H or B6 allele and "b" indicates that the B6 or C3H allele differs from mice with B6C3H allele. The values shown here are mean ± SD. The y-axis represents percent change of vBMD and PC in the F2 population and x-axis represents mouse genotypes. The total number of mice was 329 but due to missing data the number of genotype marker data varied.

To determine the genetic variance that remains unaccounted in our study we performed PAIRSCAN analysis in search of loci-loci interaction. Interaction was observed between loci on Chr 8 with other loci on Chr 13 and 5 for total vBMD and cortical thickness (**Table-4**). Similarly, Chr 1 locus interacted with loci on Chr 3 and 13 for vBMD and cortical vBMD (**Table-4)**. These four interactions combined together accounted for approximately 11% of the variance in loading induced changes in BMD (includes total vBMD and cortical vBMD) and CTh (calculated by Pseudomarker FITQTL algorithm). It was interesting to note that Chr 13 and 5 loci did not show significant main effect for

BMD and cortical thickness, but showed significant interaction LOD score with Chr 8 and 1 that showed significant QTL for BMD and cortical thickness in the main effect. We believe that the two novel loci may contain genes that are closely associated with the candidate genes, but not genetically inherited, within the other locus identified in the main scan. These associated genes can be in the same signaling pathways, either upstream or downstream. The expression of the associated genes can be regulated or modified by the candidate genes responsible for the mechanical loading. Further functional screening of candidate genes from the QTL regions may provide more substantive data to answer the mechanisms of gene-gene interactions.

Table-4 List of significant marker pairs showing interaction from genome-wide analysis of multiple phenotypes in B6xC3H F2 female mice.

Phenotype	Chr pairs	cM1	cM2	LOD Full	LOD Int	p-value (interaction)
Total vBMD	8 × 13	60	45	9.10	2.96	0.008
	1 × 13	90	45	7.57	2.65	0.01
Cortical vBMD	1 × 3	75	55	8.72	2.17	0.04
CT	5 × 8	80	10	7.41	4.50	0.004

For vBMD full LOD score threshold (effect of both markers in affecting the bone phenotype) significant was 7.68 ($p<0.05$) and for cortical vBMD full LOD score threshold significant was 7.95 ($p<0.05$). Suggestive threshold was 7.32 ($p<0.1$) for vBMD and 6.83 ($p<0.6$) for CT Full LOD score effect.

While QTL analysis leads to precise mapping of the genetic loci that contribute to a phenotype of interest, the next phase lies in identifying the potential candidate genes within the region of a QTL, which is the first step in understanding the underlying molecular mechanisms responsible for increasing the bone adaptive response to ML. Each of the QTL regions identified in this study is more than 15 cM in length and contains hundreds of genes. To identify potential candidate genes for the ML QTL, we used several criteria including findings from clinical association studies, gene knock out studies and *in-vitro* studies on the effects of mechanical strain on bone cells [26-29]. Candidate genes for locus on Chr 8 (38–68.9 cM) include carboxypeptidase E (cpe), annexin A10 (Anxa10), SH3 multiple domains 2 (Sh3md2), chloride channel 3 (Clcn3), ATPase, H+ transporting, V1 subunit B, isoform 2 (Atp6v1b2), high mobility group box 2 (Hmgb2), vascular endothelial growth factor C (Vegfc), ectonucleotide pyrophosphatase/phosphodiesterase 6 (Enpp6) and Lrp2 binding protein. Candidate genes for the Chr 9 locus include calponin 1 (Cnn1), and 5-hydroxytryptamine (serotonin) receptor 3A&B (Htr3a&b). The Chr 3 (41-59 cM) contains possible candidate genes protocadherin (Pcdh) 10, 18, OSF (postn), transient receptor potential cation channel, subfamily C, member 4 (Trpc4), Smad8 and Vpurinergic receptor P2Y, G-protein coupled 12, 13 and 14 (P2ry). Possible candidate genes on Chr 11 (64-71cM) include mitogen activated protein kinase kinase 4 (Map2k4), fibroblast growth factor 11 (fgf11), and synataxin (Stx8). The loci on Chr 17 include FK506 binding protein 5 (Fkbp5), opsin 5 (opn5), and runt related transcription factor 2 (Runx2), and Chr 18 include mitogen activated protein kinase kinase kinase 8 (Map3K8) and BMP and activin

membrane-bound inhibitor (Bambi). Further studies are needed to determine if any of the above candidate genes, is in, fact a ML QTL gene.

Although this first genome-wide research for mechanical loading QTL using C3H and B6 strains of mice has revealed evidence for the presence of multiple genetic loci regulating the skeletal response to loading, our findings should be viewed in the context of the following limitations. The use of growing mice rather than mature mice may have confounded the response. In this regard, we have recently found that four-point bending significantly increased bone density in B6 mice compared to C3H mice at 10-, 16- and 36-week (11), regardless of age. In addition, the non-loaded contralateral bone was used to control for growth effects. Second, in our recent study, we observed that the amount of strain in C3H and B6 mice was similar at 9N force. However, the variable genetic background in each F2 mouse resulted in mice with variable cross-sectional area of tibia. With a fixed amount of force (9N), the amount of strain experienced by each mouse will depend on cross-sectional area (moment of inertia), suggesting that a mouse with a large cross-sectional area will experience lower strain and vice versa. This would generate a variable response to loading independent of genetic response to loading. The results from our study showed a weak correlation between bone size and loading response and our quartile analysis showed that the increase in bone size response to loading in the F2 mice varied somewhat depending on the size of bone (**Figure 5**). We therefore performed QTL analysis after adjustment with non-loaded PC bone which produced the same QTL as unadjusted data suggesting that loading response in F2 mice is largely genetically determined. Third, in the phenotype distribution, we found some of the F2 mice showed negative BMD response to mechanical loading. Whether the negative BMD response is due to loading induced changes in architecture/shape or due to rapid increase in poorly mineralized bone at the periosteum remain unknown. Fourth, our study used a relatively low number of F2 mice (n=329) to perform the QTL analysis. This was mainly due to practical difficulties in performing four-point bending-based loading in a large number of mice. Therefore, the power to detect QTL was less than studies with 600-1000 animals. Thus, there are likely additional chromosomal regions that affect the bone response to loading which were undetected in this study. This was further evident by the loci interactions that showed only 11% variance. Finally, hormonal status is shown to significantly influence the response to loading, therefore the QTLs identified in this study could be specific to female mice. In this regard, mapping of each locus in the male mice will provide more definitive proof as to whether the same loci or closely linked loci underlie the QTLs mapped to overlapping chromosomal regions using only females.

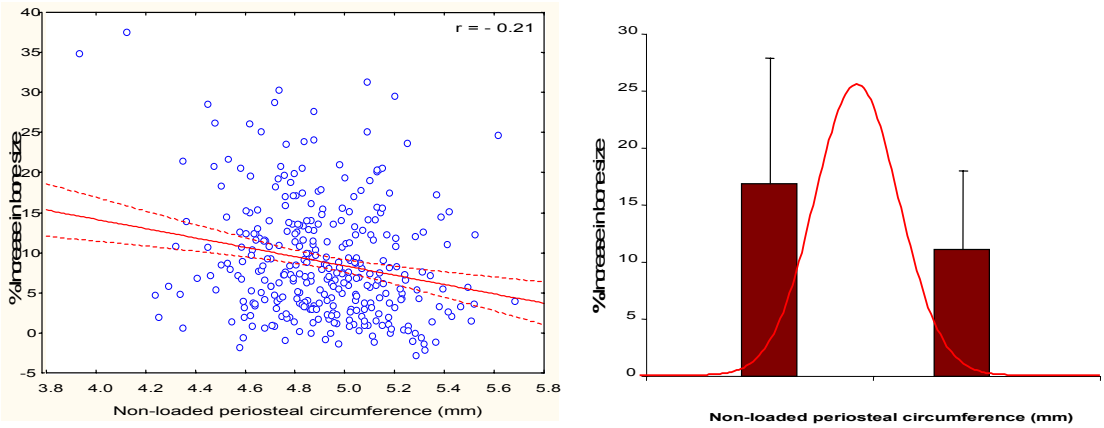

Figure 5: Correlation of non-loaded PC values (mm) vs. percent change in bone size in response to loading (A) and quartile analysis of the bone size response to mechanical loading in the B6XC3H F2 population (B).

<u>Specific objective 5</u>: **To determine the fate of new bone gained during 2 weeks of mechanical loading (i.e. to determine how long the bone density and/or bone strength gained during 2 weeks of mechanical loading is maintained after termination of 4-point bending).**

At present, we carrying out this experiment, we will include the data of this proposed specific objective in our next annual progress report.

<u>Specific objective 6</u>: To determine if the load applied to increase optimal anabolic response causes micro cracks in loaded bone

We performed four-point bending for 12 days at 9N load in 10-week old female B6 and C3H mice and 2 days after last loading tibias were collected and stored at 10% formalin. One thick cross-section was obtained on the loaded and unloaded bones, and both sides were measured for micro-cracks (Bone area mm^2). In order to rule out the possibility that the changes on bone parameters induced by a load of 9N are due to micro-crack induced healing, we measured micro-cracks by histological analysis. The micro-cracks area (mm^2) was not significantly different between the loaded vs unloaded bones (n=5) for either B6 (0.82 ± 0.05 vs. 0.60 ± 0.04) or C3H (0.87 ± 0.07 vs 0.95 ± 0.02) mice. Furthermore, the micro-crack area was not significantly different between the two strains in either the loaded or unloaded bone suggesting that the bone anabolic response produced by 9N are not due to microcracks.

Key Research Accomplishments

1) We provide evidence from sham-bending study that four-point bending induced changes in bone parameters are due to bending and not due to periosteal pad pressure.
2) We provide evidence from our microcrack experiment that bone anabolic response induced by 9N load on tibia of B6 mice was not due to pathological changes.
3) Although bone response to mechanical loading is dependent on the size of the bone, it is largely determined by genetic factors.

4) We identified six loci that regulating the bone adaptive response to loading using classical QTL approach.
5) We found that ML BMD QTL for Chrs. 8 and 9 and bone size QTL for Chrs. 8 and 18 could not be detected using phenotype data from unloaded bones, suggesting that these QTLs are unique to ML phenotypes.
6) Our study has identified known (Chrs 10, 11, 15, 16, and 17) and novel QTL on Chr 3 for the periosteal circumference (PC) or bone size trait in the B6XC3H F2 mice. Chrs 10 and 11 have been identified in multiple strain crosses, suggesting the importance of this QTL in PC regulation.
7) QTL identified for non-loaded tibia PC are the same as QTL previously identified for femur, suggesting that the same mechanisms are involved in the regulation of bone size in both femur and tibia.

Reportable Outcomes

1. Chandrasekhar K, Baylink DJ, Apurva K. Srivastava, Susanna O, Hongrun Yu, Jon E. Wergedal and Mohan S. Identification of genetic loci that regulate bone adaptive response to loading in C57BL/6J and C3H/HeJ intercross. Bone 39(3): 634-44.
2. Chandrasekhar K, S Mohan, H Yu, S Oberholtzer, J.E Wergedal, D.J.Baylink. Novel Mechanoresponsive BMD and Bone Size QTL Identified In A Genome Wide Linkage Study Involving C57BL/6J-C3H/HeJ Intercross. ASBMR 27th Annual Meeting, 2005.
3. Chandrasekhar K, D. J Baylink, K. Susanna, J. E. Wergedal, H. Yu, and S. Mohan. Quantitative Trait loci for Tibia Periosteal Circumference in the C57BL/6J-C3H/HeJ mice intercross. ASBMR 28th Annual Meeting, 2005.

Conclusion

Our results confirm that response to mechanical loading has a strong genetic component with several loci regulating loading induced bone modeling. The future discovery of genes at these loci could provide a basis for the observed variability in bone mass accretion and maintenance due to exercise in normal healthy individuals.

References:

1. Borer, K.T., *Physical activity in the prevention and amelioration of osteoporosis in women : interaction of mechanical, hormonal and dietary factors.* Sports Med, 2005. **35**(9): p. 779-830.
2. Bailey, D.A. and R.G. McCulloch, *Bone tissue and physical activity.* Can J Sport Sci, 1990. **15**(4): p. 229-39.
3. Bikle, D.D., T. Sakata, and B.P. Halloran, *The impact of skeletal unloading on bone formation.* Gravit Space Biol Bull, 2003. **16**(2): p. 45-54.
4. Bikle, D.D. and B.P. Halloran, *The response of bone to unloading.* J Bone Miner Metab, 1999. **17**(4): p. 233-44.
5. Umemura, Y., et al., *A time course of bone response to jump exercise in C57BL/6J mice.* J Bone Miner Metab, 2002. **20**(4): p. 209-15.
6. Kodama, Y., et al., *Exercise and mechanical loading increase periosteal bone formation and whole bone strength in C57BL/6J mice but not in C3H/Hej mice.* Calcif Tissue Int, 2000. **66**(4): p. 298-306.

7. Kodama, Y., et al., *Cortical tibial bone volume in two strains of mice: effects of sciatic neurectomy and genetic regulation of bone response to mechanical loading.* Bone, 1999. **25**(2): p. 183-90.
8. Dhamrait, S.S., et al., *Cortical bone resorption during exercise is interleukin-6 genotype-dependent.* Eur J Appl Physiol, 2003. **89**(1): p. 21-5.
9. Dalsky, G.P., et al., *Weight-bearing exercise training and lumbar bone mineral content in postmenopausal women.* Ann Intern Med, 1988. **108**(6): p. 824-8.
10. Snow-Harter, C., et al., *Effects of resistance and endurance exercise on bone mineral status of young women: a randomized exercise intervention trial.* J Bone Miner Res, 1992. **7**(7): p. 761-9.
11. Kesavan, C., et al., *Mechanical loading induced gene expression and BMD changes are different in two inbred mouse strains.* J Appl Physiol, 2005.
12. Akhter, M.P., et al., *Bone response to in vivo mechanical loading in two breeds of mice.* Calcif Tissue Int, 1998. **63**(5): p. 442-9.
13. Li, X., et al., *Chromosomal regions harboring genes for the work to femur failure in mice.* Funct Integr Genomics, 2002. **1**(6): p. 367-74.
14. Masinde, G.L., et al., *Quantitative trait loci for periosteal circumference (PC): identification of single loci and epistatic effects in F2 MRL/SJL mice.* Bone, 2003. **32**(5): p. 554-60.
15. Srivastava, A.K., et al., *Mapping quantitative trait loci that influence blood levels of alkaline phosphatase in MRL/MpJ and SJL/J mice.* Bone, 2004. **35**(5): p. 1086-94.
16. Beamer, W.G., et al., *Quantitative trait loci for femoral and lumbar vertebral bone mineral density in C57BL/6J and C3H/HeJ inbred strains of mice.* J Bone Miner Res, 2001. **16**(7): p. 1195-206.
17. Turner, C.H., et al., *Congenic mice reveal sex-specific genetic regulation of femoral structure and strength.* Calcif Tissue Int, 2003. **73**(3): p. 297-303.
18. Shultz, K.L., et al., *Congenic strains of mice for verification and genetic decomposition of quantitative trait loci for femoral bone mineral density.* J Bone Miner Res, 2003. **18**(2): p. 175-85.
19. Bouxsein, M.L., et al., *Mapping quantitative trait loci for vertebral trabecular bone volume fraction and microarchitecture in mice.* J Bone Miner Res, 2004. **19**(4): p. 587-99.
20. Koller, D.L., et al., *Genetic effects for femoral biomechanics, structure, and density in C57BL/6J and C3H/HeJ inbred mouse strains.* J Bone Miner Res, 2003. **18**(10): p. 1758-65.
21. Lang, D.H., et al., *Quantitative trait loci analysis of structural and material skeletal phenotypes in C57BL/6J and DBA/2 second-generation and recombinant inbred mice.* J Bone Miner Res, 2005. **20**(1): p. 88-99.
22. Volkman, S.K., et al., *Quantitative trait loci that modulate femoral mechanical properties in a genetically heterogeneous mouse population.* J Bone Miner Res, 2004. **19**(9): p. 1497-505.
23. Li, X., et al., *Genetic dissection of femur breaking strength in a large population (MRL/MpJ x SJL/J) of F2 Mice: single QTL effects, epistasis, and pleiotropy.* Genomics, 2002. **79**(5): p. 734-40.
24. Yershov, Y., et al., *Bone strength and related traits in HcB/Dem recombinant congenic mice.* J Bone Miner Res, 2001. **16**(6): p. 992-1003.

25. Robling, A.G., et al., *Evidence for a skeletal mechanosensitivity gene on mouse chromosome 4.* Faseb J, 2003. **17**(2): p. 324-6.
26. Riechman, S.E., et al., *Association of interleukin-15 protein and interleukin-15 receptor genetic variation with resistance exercise training responses.* J Appl Physiol, 2004. **97**(6): p. 2214-9.
27. McCole, S.D., et al., *Angiotensinogen M235T polymorphism associates with exercise hemodynamics in postmenopausal women.* Physiol Genomics, 2002. **10**(2): p. 63-9.
28. Kapur, S., et al., *Fluid shear stress synergizes with insulin-like growth factor-I (IGF-I) on osteoblast proliferation through integrin-dependent activation of IGF-I mitogenic signaling pathway.* J Biol Chem, 2005. **280**(20): p. 20163-70.
29. Hens, J.R., et al., *TOPGAL mice show that the canonical Wnt signaling pathway is active during bone development and growth and is activated by mechanical loading in vitro.* J Bone Miner Res, 2005. **20**(7): p. 1103-13.
30. Kesavan et al., *Identification of genetic loci that regulate bone adaptive response to mechanical loading in C57BL/6J and C3H/HeJ mice intercross*. Bone 2006 (In Press).

Molecular Genetic Studies on Bone Mechanical Strain - In Vitro Studies

Introduction:

This portion of the report summarizes our progress made during the past year on the identification of mechanosensitivity genes and the mechanotransduction mechanism(s) involved in mediating the anabolic skeletal response to mechanical stimulation, using an in vitro fluid shear stress model generated by the Cytodyne flow chamber system.

A major focus of this work was to address the potential role of a candidate mechanosensitivity modulating genes and its mechanotransduction, leptin receptor.

Body:

In our original experimental approach, we plan to identify potential candidate genes from our microarray data and to determine the effect of suppression of expression of the candidate gene in osteoblasts by the siRNA technology on their anabolic response to fluid shear stress. However, because the siRNA approach is time-consuming and technically labor-intensive, we intentionally delayed the siRNA studies until we have more information about the identity potential candidate mechanosensitivity genes through a more systematic analysis, instead of arbitrarily choosing one or more novel genes whose expression was altered by the fluid shear stress. We believe that this alternative approach would be more productive. Accordingly, during the past year, we focused on two modified Technical Objectives: 1) to identify a candidate mechanosensitivity gene that may contribute at least in part the differential anabolic response to fluid shear stress between osteoblasts of C57BL/6J (B6) and those of C3H/HeJ (C3H) inbred mouse strains, and 2) to determine the molecular mechanism (i.e., mechanotransduction) whereby the candidate gene acts to regulate the anabolic response in osteoblasts.

Technical Objectives: The original specific objectives for the in vitro studies during the past year of this grant are as follows:

1. To optimize the in vitro siRNA techniques for the application to mouse osteoblasts in conjunction with our shear stress technology.
2. To select one or more ESTs (or known genes) for further study from our microarray data.
3. To apply the siRNA technique to suppress the candidate EST expression or known gene and then evaluate the functional role of this EST or known gene in osteoblast proliferation, differentiation, and apoptosis.
4. To continue to advance our protein-tyrosine phosphorylation studies in order to identify signaling proteins that show differences in protein-tyrosine phosphorylation levels in response to mechanical strain in bone cells isolated from those mouse strains which exhibit differential responses to the in vitro mouse strains. Changes in protein-tyrosine phosphorylation levels will be compared to in vitro parameters of osteoblast proliferation, differentiation, and apoptosis.

Specific Objective #1. To identify candidate mechanosensitivity genes in osteoblasts. B6 mice respond to mechanical stimulation with an increase in bone formation and C3H mice did not. Similarly, osteoblasts of B6 mice respond to fluid shear with an increase in cell proliferation and ALP activity *in vitro*, but the same fluid shear did not produce anabolic effects in C3H osteoblasts. Thus, we believe that comparison of the differential gene expression in osteoblasts of these two inbred mouse strains would give important insights into the identity of potential candidate mechanosensitivity genes and the mechanotransduction involved in the anabolic response to the fluid shear stress. Accordingly, we had performed an in-house microarray analysis on B6 and C3H osteoblasts. As resported in our previous progress report, the fluid shear stress differentially upregulated the expression of a number of genes associated with at least 4 anabolic pathways [the canonical Wnt, IGF-I, estrogen receptor (ER), and BMP/TGFβ pathways] in B6 but not in C3H osteoblasts (1). We also confirmed that *in vivo* loading to the tibia also led to upregulation of the expression of these genes in B6 but not in C3H mice (1). Thus, we conclude that the "mechanosensitivity" genes contributing to the good and poor bone formation response in B6 and C3H mice, respectively, are upstream to these four pathways. We also showed that the mechanism leading to the fluid shear-induced upregulation of these 4 pathways involved two early mechanoresponsive genes, integrin β1 and cyclooxygenase (Cox)-2 and that the "mechanosensitivity" genes are upstream to these two genes (1). Thus, these studies indicate that the "mechanosensitivity" genes responsible for the differential mechanical response in this pair of mouse strains are upstream even to these early mechanoresponsive genes.

Several genetic approaches have been attempted to identify genetic loci of "mechanosensitivity" genes in the C3H/B6 pair of mouse strains. A study with the B6.C3H-4T mouse strain, which was genetically identical to B6 except that it carried a segment of C3H chromosome 4 (between 40 and 80 cM), showed that these congenic mice were more responsive to mechanical stimulation in periosteal bone formation than B6 mice (2), suggesting that this C3H chromosome 4 region contains one or more genetic loci that would enhance bone mechano-sensitivity in B6 mice. While these findings are exciting, it is also puzzling as to why the transfer of a DNA fragment from the nonresponsive C3H mice into B6 mice would increase their bone formation response. The mechanistic reason(s) for this seemingly contradictory finding is unclear. We interpret these findings as that there must be interactions among various "mechanosensitivity" modulating genes

located at various loci, such that the interaction between genes of this C3H chromosome 4 locus with other mechanosensitivity genes in the C3H background yielded a negative response, while that in the B6 background produced an enhanced response. Nevertheless, our initial work to identify candidate mechanosensitivity gene focused on upstream signaling genes located within the 40-80 cM locus of mouse chromosome 4, since this DNA segment is currently the only genetic locus that has demonstrated ability to modulate mechanosensitivity in this pair of mouse strains. This locus is large and contains several hundreds of genes. Because the mechanosensitivity of the rat skeleton has been shown to be markedly reduced after a long period of sustained loading (3) and the lost of responsiveness after sustained activation is a hallmark characteristic of desensitization of receptor-mediated events, we were particularly interested in receptor genes or receptor-associated upstream genes.

Some of the receptor and upstream genes located in this locus are: *Lepr*, *Tie1*, *Il22ra1*, *Ptafr*, *Oprd1*, *Htr6*, *Htr1d*, *Ephb2*, *Epha2*, *Tnfrsfa*, *Tnfrsf1*b, *Tnfrst4*, *Tnfrst8*, *Agtrap, Sh3gl2*, *Tek*, *Plaa*, *Jun*, *Foxd3*, *Jak1*, *Pde4b*, *Ak2*, *Ak3*, *Ror1*, *Ppap2b*, *Inpp5b*, *Guca2a*, *Guca2b*, *Gjb3*, *Lck*, *Ptpru*, *Fdpsl2*, *Rap1ga1*, *Pla2g5*, *Pla2g2a*, *Pla2g2c*, *Frap1*, and *Gnb1*. Of these potential receptor or receptor-associated upstream genes, we were particularly interested in the *Lepr* gene as a candidate "mechanosensitivity" modulating gene. In this regard, a recent preliminary genome-wide screen study in the rat (4) has suggested that the *Lepr* gene (located within a bone-strength QTL of rat chromosome 5) was associated strongly with bone architecture and strength. Although the leptin signaling is an important regulator of bone formation, its effects can be stimulatory or inhibitory, depending on whether the administration is peripheral or central in nature. Leptin may stimulate bone formation through direct angiogenic and chondro-osteogenic effects (5), but it may also exert negative effects on bone formation through a hypothalamic pathway mediated downstream by the sympathetic nervous system (6). Accordingly, leptin exerts dual effects depending on bone tissue, skeletal maturity, or signaling pathway. Because of this unique dual action of the *Lepr* signaling pathway on bone formation, it has been suggested that the *Lepr* pathway may have a critical role in the "Mechanostat" theory in the overall regulation of bone mass and integrity (7).

To test whether *Lepr* may be a candidate mechanosensitivity gene, we evaluated the effects of mechanical loading on bone formation in leptin-deficient *ob/ob* mice. We reasoned that if *Lepr* or its signaling pathway indeed plays a role in determination of bone cell mechanosensitivity, the bone formation response in bone of *ob*/*ob* mice would be significantly altered. Our investigation of the bone phenotype of *ob/ob* mice revealed a previously undisclosed, but very interesting, observation (8). In this regard, androgen functions produce sex-related differences in several tissues, including bones, leading to the greater periosteal expansion in the males, but these sex-related differences in bone parameters were surprisingly absent in the femur of male *ob/ob* mice. Accordingly, pQCT measurements of the periosteal circumference revealed that the significant differences between male and female B6 mice were not seen between male *ob/ob* and female *ob/ob* mice. The same was true of the endosteal circumference in B6 male and female mice (3.6 vs 3.3 mm^2, $p<0.0002$); male and female *ob*/*ob* mice showed no significant differences (3.4 vs 3.3 mm^2). The difference in the trabecular area of the male and female B6 mice (0.73 vs 0.56 mm^2, $p<0.0002$) was not significant in the male and female *ob/ob* mice (0.64 vs 0.61

mm^2). There were no differences in the bone parameters between B6 and *ob/ob* females. The loss of androgen effects in male *ob/ob* mice could not be explained by a decrease in free serum testosterone or estrogen levels, since it was higher in male *ob/ob* mice (313 vs 693 pg/ml, $p<0.005$) than in B6 mice and since serum estradiol was also increased in female *ob/ob* mice relative to B6 mice (67 vs 100 pg/ml, $p<0.0001$). It is also not due to the loss of *Lepr*, since *Lepr* mRNA levels in bones of *ob/ob* mice (by real-time PCR) were not different from those in bones of B6 mice. Preliminary real-time PCR measurements of bone expression of several androgen responsive genes suggested that their levels were lower in male *ob/ob* bones than in male B6 bones (data not shown). Although these data need to be confirmed, our results suggest that the lost of androgen-specific effects on bone in male ob/ob mice may be due to a defect in the androgen signaling.

Because the *ob/ob* males appear to have a defective androgen signaling in the bones, we used only female *ob/ob* and B6 mice to determine the bone response (by pQCT) to a 2-

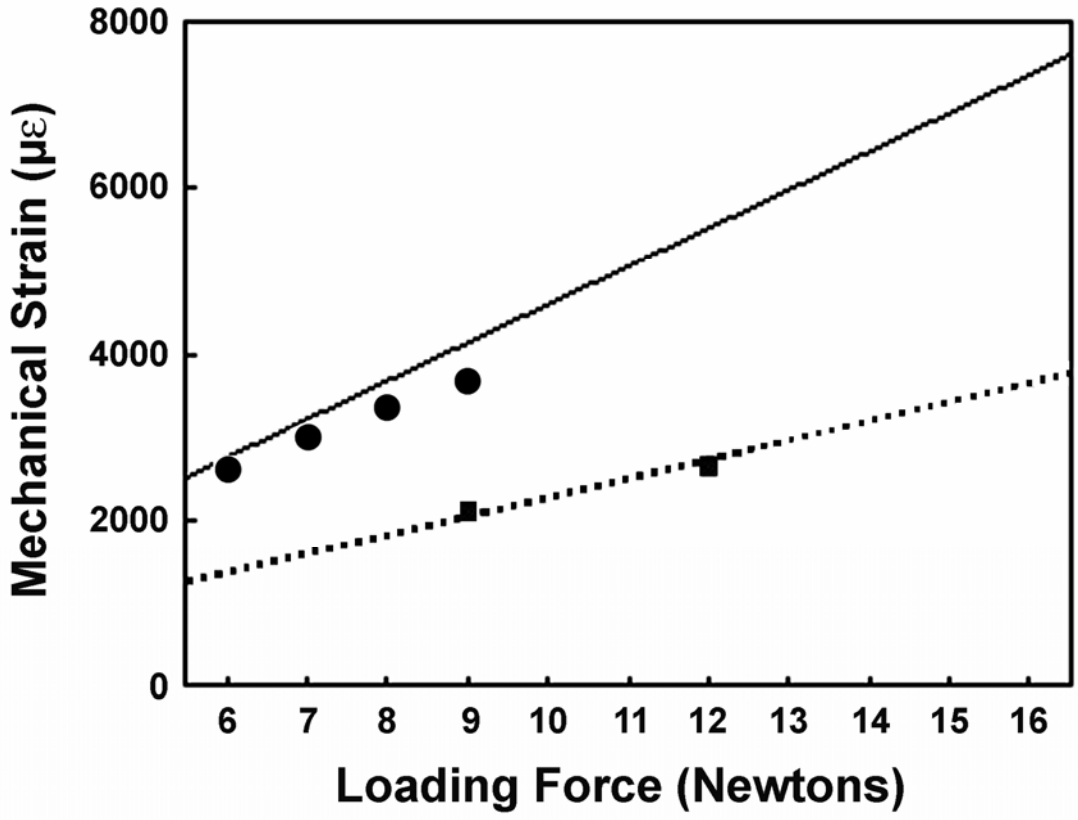

Figure 1. The calculated and experimental relationship between loading force (in Newtons) and mechanical strain sensed by the bone (in με) in female B6 mice and *ob/ob* mice. The solid line represents the calculated strain for each loading force in female B6 mice, and the dotted line is the calculated strain for each loading force for female *ob/ob* mice. The filled circles are the actual strain sensed by the bone of female B6 mice measured with a strain gauge, whereas the filled squares are the actual strain sensed by the bone of the female *ob/ob* mice.

week four-point bending exercise regimen. We chose the four-point bending exercise model as the *in vivo* loading model because this model provides: 1) a controlled external

loading of an intact long bone; and 2) the contralateral limb can be used as the control to determine the loading response. This loading regimen also caused a massive increase in cancellous bone formation at the periosteum of the loaded tibia of B6 mice, but not in the loaded tibia of C3H mice (1).

The bone formation response is determined by mechanical strain sensed by the bone rather than the loading force *per se* and the strain created by a given load is influenced by the bone size. Because the size of tibia of adult female *ob/ob* mice is significantly bigger than that of B6 mice (periosteal circumference: 5.66 ± 0.21 vs. 4.94 ± 0.21 mm, $p<0.0001$), we measured the actual strain sensed by the loaded bones of 10-week-old female *ob/ob* mice as opposed to female B6 mice at a given load with a strain gauge. The predicted strain at various loading forces on each mouse strain based on their bone size was also calculated for comparison. As shown in **Fig. 1**, the bones of B6 mice would experience a significantly higher strain at any given load than bones of *ob*/*ob* mice. Hence, the loading force needed to be adjusted to ensure that a similar strain is applied to B6 and *ob/ob* mice. Accordingly, a load of 9N produced ~2100 με in female adult *ob/ob* mice, which was in a similar range as that (~2500 με) produced by a 6N load in adult female B6 mice. Therefore, we used a 9 N load for ob/ob mice and a 6 N load for B6 mice.

In our experiments, the Instron four-point bending device consisted of two upper vertically movable points covered with rubber pads (4-mm apart), and two 12-mm lower non-movable points covered with rubber pads. During the bending exercise, the two upper pads touched the lateral surface of the tibia through overlaying muscle and soft tissue, while the lower pads touched the medial surface of the proximal and distal parts of the tibia. The loading protocol consisted of a 9-N load (for *ob/ob* mice) or a 6-N load (for B6 mice) at a frequency of 2 Hz for 36 cycles and the exercise was performed once daily. The right tibia was subjected to the loading exercise, while the left tibia was used as an internal unloaded control. Upon anesthesia, the ankle of the tibia was positioned on the second lower immobile points of the Instron equipment, such that the region of tibia loaded did not vary from mouse to mouse. The loading was applied for 6 days/week with a day rest for 2-weeks. Mice were sacrificed 48 hrs after the final loading and tibias were collected for pQCT measurements. As shown in **Fig. 2**, this dosage of strain had no stimulatory effect on any of the pQCT bone parameters in B6 mice. This is not surprising, since our previous data indicated that the 6N force is insufficient to produce a bone formation response in adult B6 mice (not shown). In contrast, this mechanical strain significantly increased total bone mineral content, cortical area, cortical content, cortical thickness, mBMD and vBMD at the site of loading in *ob/ob* mice. These findings indicate that female *ob/ob* mice showed an enhanced sensitivity to mechanical stimuli in tibia compared to female B6 mice.

To further test if deficiency of leptin expression would lead to an enhanced osteogenic response to mechanical stimuli, we examined the effects of a steady fluid shear on [^{3}H]thymidine incorporation and Erk1/2 phosphorylation in osteoblasts isolated from adult female *ob/ob* mice as opposed to those in adult female B6 osteoblasts *in vitro*. Osteoblasts were isolated as previously described (1) and pooled cells were used. For comparison, osteoblasts of the WT littermates of *ob*/*ob* mice (ob^+/ob^+) were included. **Fig. 3** confirms that a 30-min steady fluid shear of 20 dynes/cm^2 significantly stimulated[^{3}H]thymidine incorporation and Erk1/2 phosphorylation in female B6 osteoblasts. The same shear stress produced significantly greater increases in [^{3}H]thymidine incorporation and Erk1/2 phosphorylation in ob^-/ob^- osteoblasts than those in B6 osteoblasts and osteoblasts of WT ob^+/ob^+ littermates. The shear stress-induced [^{3}H]thymidine incorporation and Erk1/2 phosphorylation in WT ob^+/ob^+ osteoblasts were not different from those in B6 osteoblasts. These results are highly reproducible and were seen in every repeat experiment. While these preliminary findings are exciting and support our overall hypothesis, it is also somewhat puzzling to observe an enhanced mitogenic response in the isolated *ob*/*ob* osteoblasts to the fluid shear, since as shown in **Fig. 5** below, these osteoblasts were deficient only in leptin production but not in the *Lepr* expression.

A potential explanation for this observation is that primary B6 mouse osteoblasts,

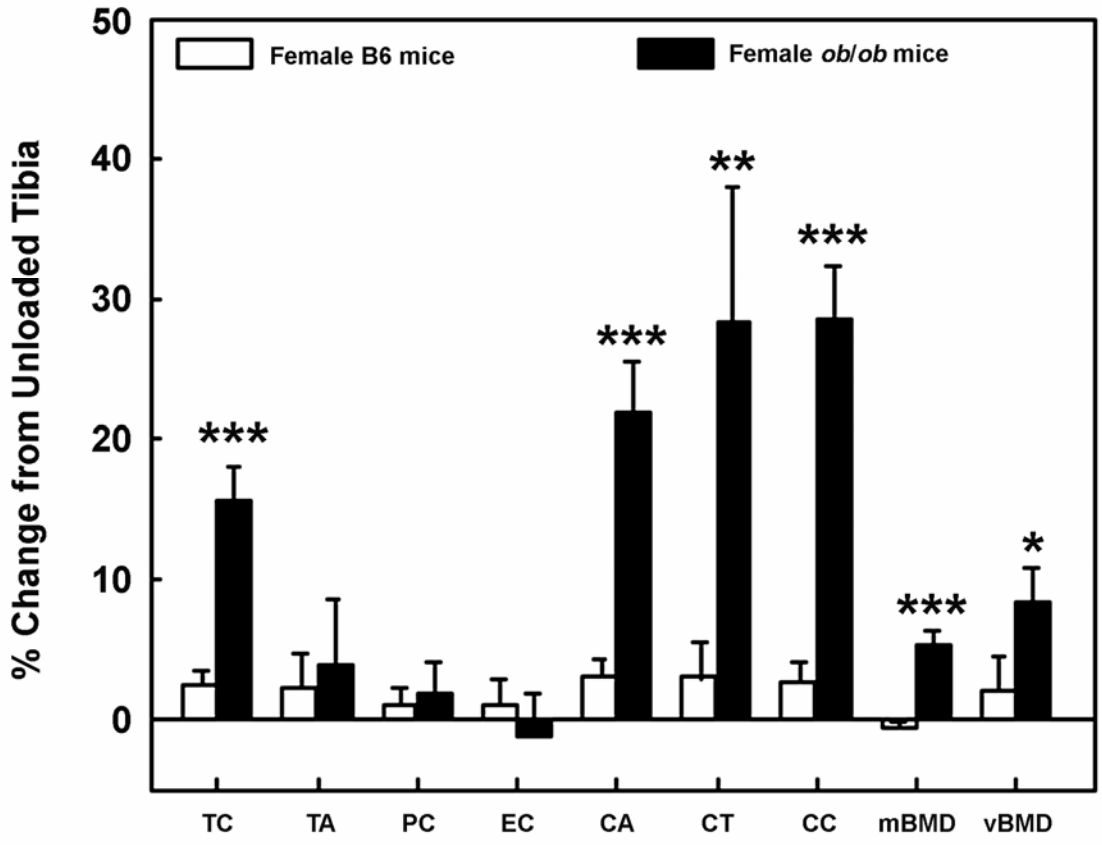

Figure 2. The bone responses in the tibia (determined by pQCT) of adult female *ob/ob* mice (filled bars) after a 2-week four-point bending exercise as opposed to those in the tibia of adult female B6 mice (open bars). The bending exercise was performed in 6 ob/ob mice and 12 B6 mice. The results are shown as relative percent change from the unloaded tibia of each individual mouse (mean ± SEM). TC = total bone mineral content; TA = total area; PC = periosteal circumference; EC = endosteal circumference; CA = cortical area; CT = cortical thickness; CC = cortical content; mBMD = material bone mineral density; vBMD = volumetric BMD. *p<0.05; **p<0.01; and ***p<0.001.

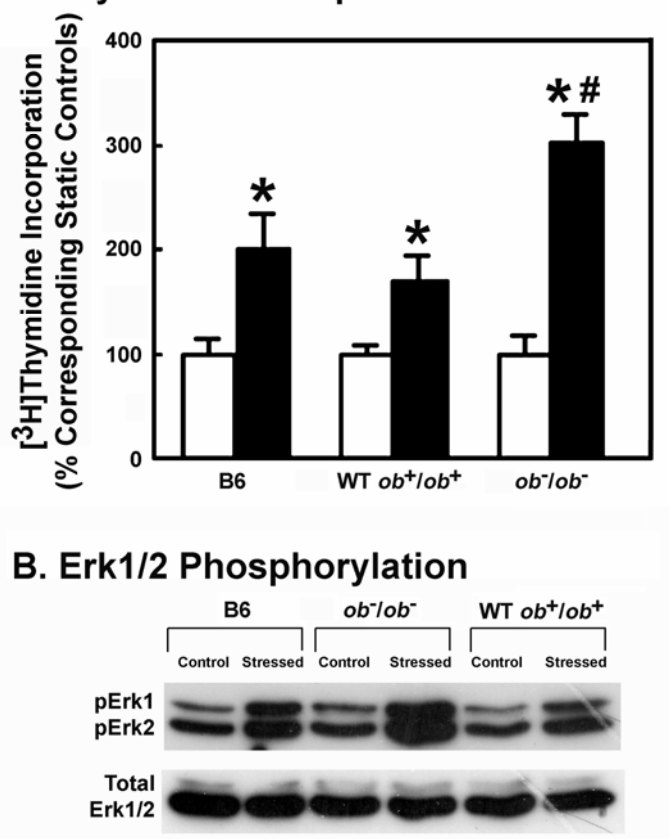

Figure 3. Effects of fluid shear on [^{3}H]thymidine incorporation (panel A) or Erk1/2 phosphorylation levles (panel B) of osteoblasts isolated from adult female B6 mice, wild-type littermates of *ob/ob* mice (WT ob$^+$/ob$^+$), or *ob/ob* (ob$^-$/ob$^-$) mice. In A, Results are shown as relative percentage of corresponding static cells (mean ± S.D., n = 3 for each). *p<0.05 compared to corresponding static control (by Student's t-test), and #p<0.05 compared to the B6 and WT ob/ob cells (by ANOVA). In B, top lane was a representative blot of phosphorylated Erk1/2 (pErk1 and pErk2) using an anti-pErk1/2 antibody, and bottom lane was a representative blot of total Erk1/2 using an anti-panErk antibody.

especially after exposure of the fluid shear, may produce sufficient amounts of leptin to suppress the *Lepr* signaling. The lack of the leptin production in *ob*/*ob* osteoblasts may thus alleviate the suppressive effects of the endogenous leptin, resulting in an enhanced mitogenic response to mechanical stimulation. Leptin is primarily synthesized by adipose tissues. We are currently test the hypothesis that primary mouse osteoblasts may produce significant amounts of leptin, especially after the fluid shear. These *in vitro* data are consistent with the *in vivo* loading data that deficiency of leptin expression or *Lepr* signaling enhanced the osteogenic response to mechanical stimulation.

If the observed enhanced mitogenic response of *ob*/*ob* osteoblasts to fluid shear was indeed due to the deficiency in the *Lepr* signaling, we reason that pretreatment of *ob*/*ob* osteoblasts with an effective dose of leptin prior to the fluid shear would block the enhanced response. Thus, we assessed the effects of a 2-hr pretreatment with 100 ng/ml of leptin prior to the 30-min steady shear stress of 20 dynes/cm^2 on [^{3}H]thymidine incorporation in osteoblasts of *ob*$^-$/*ob*$^-$ mice. **Fig. 4** shows that *ob*/*ob* osteoblasts without the leptin pretreatment, again, showed a significantly greater response to the shear stress than B6 osteoblasts. The mitogenic response of *ob*/*ob* osteoblasts to the same shear stress was markedly reduced by the leptin treatment and was now no longer different from that of B6 osteoblasts, indicating that the enhanced mitogenic response to fluid shear in ob/ob osteoblasts was completely obliterated by the leptin pretreatment. These preliminary data suggest that the *Lepr* signaling has a negative regulatory role in the context of mechanotransduction.

A corollary to our hypothesis that the mechanosensitivity genes contributing to the good and poor bone formation response, respectively, in B6 and C3H mice are upstream to

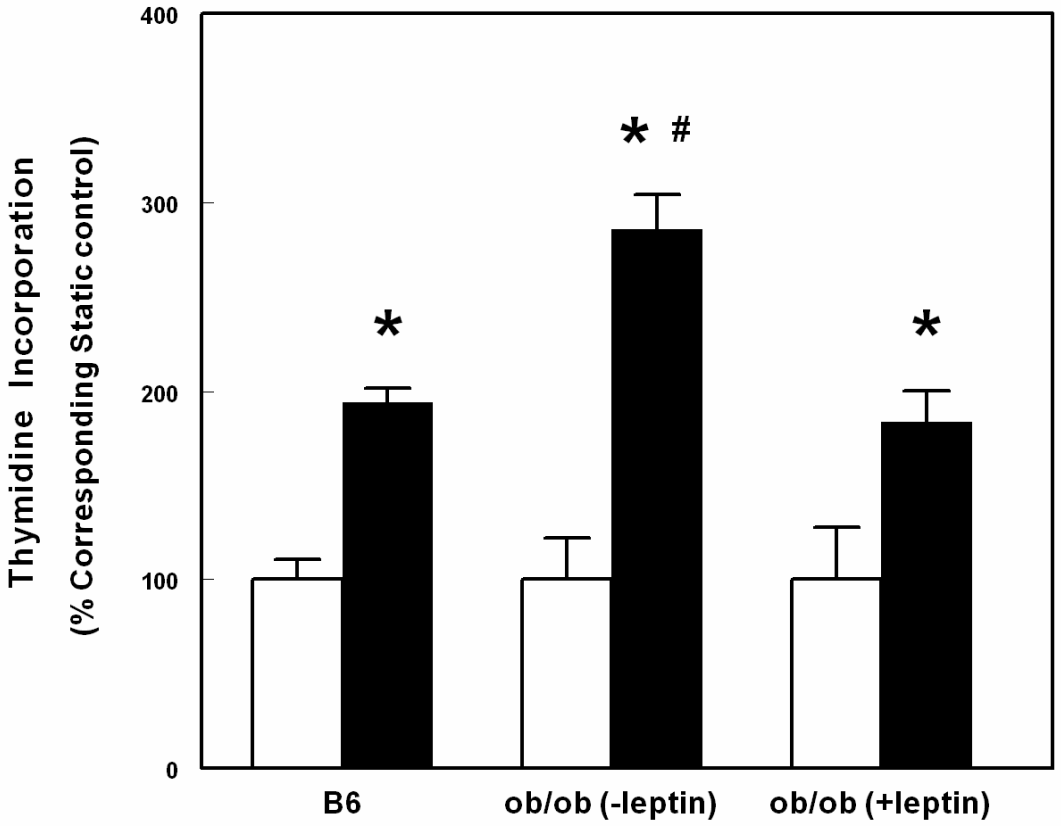

Figure 4. The leptin pretreatment of *ob*/*ob* osteoblasts abolished their enhanced mitogenic response to the fluid shear *in vitro*. Primary osteoblasts of *ob/ob* mice were pretreated for 2-hrs with or with 100 ng/ml leptin. Immediately after the pretreatment, these *ob*/*ob* osteoblasts along with B6 osteoblasts were subjected to the 30-min fluid shear stress of 20 dynes/cm^2. [^{3}H]Thymidine incorporation was determined 24 hrs after the stress. The results are shown as % corresponding static controls (mean ± SD, n = 6). *p<0.05, compared to corresponding static control; $^{\#}$p<0.05, compared to B6 osteoblasts.

the 4 anabolic pathways-of-interest is that the ability to upregulate these 4 pathways in response to mechanical stimulation may be used as a screening test for candidate mechanosensitivity modulating genes. Thus, if *Lepr* is indeed a "mechanosensitivity" modulating gene in these mouse strains, it follows that the enhanced mitogenic response to fluid shear in *ob*/*ob* osteoblasts should be accompanied by an enhanced response in the upregulation of expression of genes associated with the four anabolic signaling pathways-of-interest. Thus, we next compared levels of upregulation in expression of several genes associated with the IGF-I (*Igf1r*, *c-fos*), ER (*Era*, *Ncoa1*), BMP/TGFβ (*Dlx1*), and canonical Wnt (*Ctnnb1*, *Wnt1*, *Wnt3a*) pathways 4 hr after the fluid shear (by real-time PCR). **Table 1** shows that, while the 30-min steady fluid shear significantly upregulated the expression of the test genes in B6 and *ob*/*ob* osteoblasts, the upregulation of each test gene in *ob*/*ob* osteoblasts was significantly greater than that in B6 osteoblasts. These results are consistent with our hypothesis that the lack of the leptin gene or the *Lepr*

signaling in osteoblasts would enhance the upregulation of expression of genes associated with the 4 pathways-of-interest in response to mechanical stimulation and that these four pathways are downstream to the *Lepr* signaling.

If the *Lepr* signaling has a negative regulatory role on the mechanosensitivity in osteoblasts, then activation of the *Lepr* signaling should blunt the effect of shear stress on the upregulation of expression of genes associated with these 4 pathways-of-interest. Thus,

Table 1: Effect of the 30-min fluid shear of 20 dynes/cm^2 on the expression of genes of the IGF-I, BMP/TGFβ, ER, and Wnt signaling pathways in B6 osteoblasts and *ob*/*ob* osteoblasts measured by real-time PCR 4 hrs after the stress (n = 3 for each).

Gene	B6 osteoblasts (Stressed/Static Control, Fold changes, mean ± SD)	*ob*/*ob* osteoblasts (Stressed/Static Control, Fold changes, mean ± SD)
Era	2.04 ± 0.30*	3.31 ± 0.20*,#
Igf1r	2.38 ± 0.32*	4.49 ± 0.71*,#
Dlx1	2.09 ± 0.42*	3.23 ± 0.65*,#
Ncoa1	1.90 ± 0.78*	3.74 ± 0.88*,#
c-fos	1.95 ± 0.42*	2.56 ± 0.29*,#
Ctnnb1	2.71 ± 0.95*	3.80 ± 0.62*,#
Wnt1	2.16 ± 0.22*	3.65 ± 0.52*,#
Wnt3a	2.04 ± 0.22*	3.00 ± 0.62*,#

*$p<0.05$, compared to the corresponding static control.
#$p<0.05$, compared to B6 osteoblasts.

we evaluated the effect of the overnight pretreatment of B6 osteoblasts with 100 ng/ml leptin on the expression of the test genes 4 hrs after the stress. **Table 2** shows that the 2-hr pretreatment with 100 ng/ml leptin drastically suppressed the shear stress-induced upregulation of expression of the test genes. Along with our findings in **Figs. 3-4**, we conclude that the *Lepr* signaling functions as a negative regulatory pathway in the context of mechanotransduction in osteoblasts.

If our hypothesis that the differential bone formation response to mechanical stimuli between B6 and C3H mice is in part due to a "defective" *Lepr* signaling in C3H osteoblasts has merit, we would expect a difference in either the expression of *Lepr* gene or the effectiveness of the *Lepr* pathway between B6 and C3H osteoblasts. Thus, we evaluated if there were a difference in the basal and/or fluid shear-induced expression of *Lepr* between B6 and C3H osteoblasts. To quantitatively measure the *Lepr* mRNA levels in B6 and C3H osteoblasts, real-time PCR was performed using the following primer set for *Lepr* mRNA [forward primer: 5'-ACG TGG TGA AGC ATC GTA CT-3' and reverse primer: 5'-GGC CAT GAG AAG GTA AGG TT-3'] with an annealing temperature of 53^{o}C. There was no difference in basal *Lepr* mRNA expression levels [reported as ΔC_T (the difference between the threshold cycle (C_T) of *Lepr* and that of β-actin)] between the two osteoblasts (left panel of **Fig. 5**). The shear stress slightly increased the *Lepr* mRNA levels by ~40% in B6 osteoblasts and ~25% in C3H osteoblasts. The increase in C3H osteoblasts approached, but did not reach, the significant level (right panel). Thus, the basal and the shear stress-induced *Lepr* mRNA expression levels in C3H and B6 osteoblasts were not significantly different.

We next assessed the possibility that polymorphisms might exist in the coding region of the *Lepr* gene between C3H and B6 mice. We cloned the full-length *Lepr* mRNA from both C3H and B6 osteoblasts by long-PCR and the DNA sequence of the entire open

Table 2: Effect of the overnight pretreatment with 100 ng/ml leptin on the shear stress-induced expression of genes of the IGF-I, BMP/TGFβ, ER, and Wnt signaling pathways in B6 osteoblasts by real-time PCR 4 hrs after the fluid shear (n=3 for each).

Gene	Stressed/Static Control (No leptin pretreatment, Fold changes, mean ± SD)	Stressed/Static Control (+ leptin pretreatment, Fold changes, mean ± SD)
Era	2.40 ± 0.75*	1.39 ± 0.25#
Igf1r	3.30 ± 0.36*	1.55 ± 0.29#
Dlx1	1.68 ± 0.48*	0.75 ± 0.10#
Ncoa1	2.89 ± 0.11*	1.34 ± 0.60#
c-fos	3.06 ± 0.68*	1.25 ± 0.22#
Ctnnb1	2.62 ± 0.54*	0.90 ± 0.30#
Wnt1	2.71 ± 0.74*	0.93 ± 0.09#
Wnt3a	2.56 ± 0.75*	1.66 ± 0.25#

*$p<0.05$, compared to the corresponding static control.
#$p<0.05$, compared to those without the leptin pretreatment.

reading frame (ORF) of both strands of the *Lepr* gene of both C3H and B6 osteoblasts were determined and compared (**Fig. 6**). We found that there were three single nucleotide differences in the *Lepr* ORF between B6 and C3H osteoblasts. The differences in these single nucleotides were not due to mutations introduced by the long PCR amplification, and the same variations also existed in some of the *Lepr* ORF sequences in the PubMed database. Thus, we conclude that these are SNPs: 1) G→A SNP at nucleotide 594; 2) T→C SNP at nucleotide 1041, and 3) A→G SNP at nucleotide 1075. [The nucleotide numbering system referred to that of the ORF]. Two of the SNPs are silent and are located at the wobble base, but the A→G SNP at nucleotide 1075 yielded an Ile→Val substitution at amino acid residue 359. Although the physiological significance of this substitution is unclear, we postulate that this substitution may affect the ligand binding and, thus, the *Lepr* signaling, since the substitution is located within the ligand binding domain. Although it is beyond the scope of this proposal, it would be interesting to see if osteoblasts of other mouse strains that do not respond anaboically to the fluid shear, such as 129J and AKR (reported previously), would also exhibit this same A→G SNP at nucleotide 1075 of the *Lepr*. Our future work will address this possibility.

Specific Aim #2: Determination of the molecular mechanism whereby the candidate gene

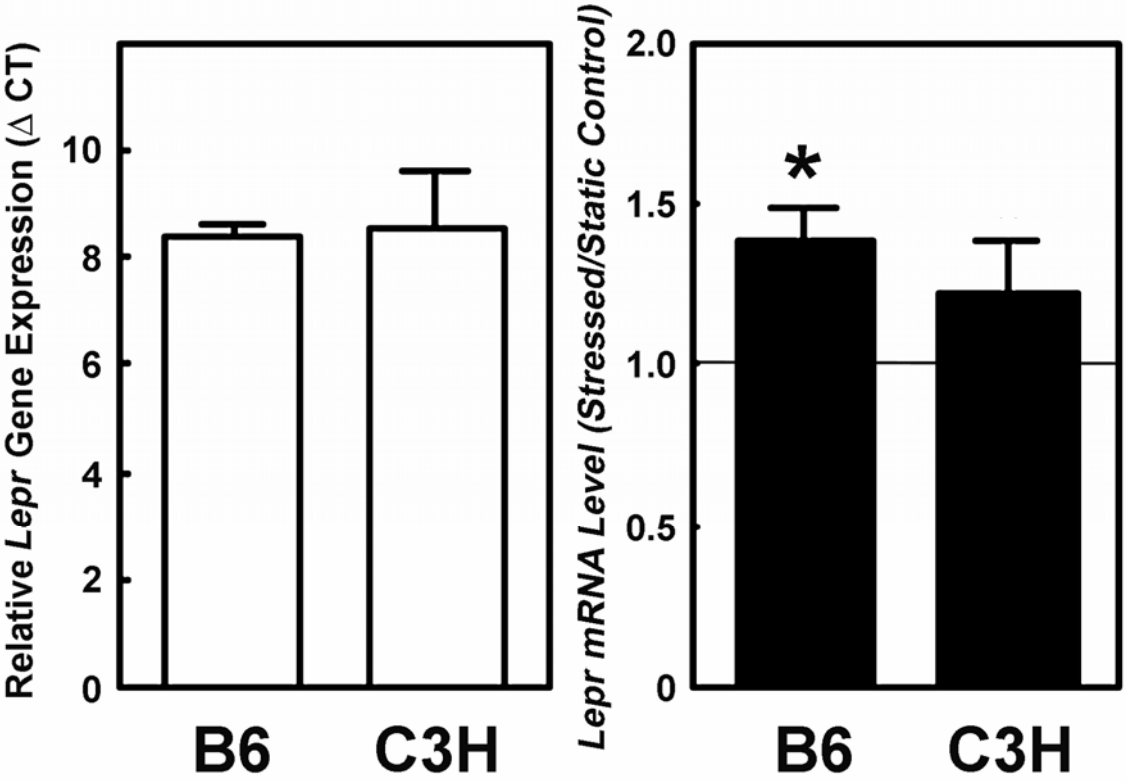

Figure 5. Basal (left panel) and shear-stress-induced (right panel) *Lepr* mRNA expression levels in B6 and C3H osteoblasts. The relative *Lepr* mRNA expression levels were determined by real-time PCR normalized against β-actin mRNA levels. Forward *Lepr* primer: ACG TGG TGA AGC ATC GTA CT; and the reverse primer: GGC CAT GAG AAG GTA AGG TT. The annealing temperature was 53^{o}C. On the left panel, the mRNA levels were assessed by the ΔCT method. The basal *Lepr* mRNA expression levels were reported as ΔCT compared to β-actin. On the right panel, osteoblasts were subjected to a 30-min steady shear stress of 20 dynes/cm^2 and the fold changes in Lepr mRNA levels in response to the shear stress were determined by ΔΔCT. The results were shown as ratio of the stressed cells/respective static control cells. (mean ± SD, n = 3 each). *p<0.05.

(i.e., *Lepr*) acts to regulate the anabolic response in osteoblasts. The mechanism(s) whereby the *Lepr* signaling pathway negatively regulates mechanotransduction in osteoblasts is unknown. Because fluid shear only slightly increased *Lepr* mRNA expression in both B6 and C3H osteoblasts (**Fig. 5**), we conclude that the inhibitory effect of fluid shear on the *Lepr* signaling is not mediated by suppression of the *Lepr* expression. *Lepr* is a member of the class I cytokine receptor family (9) and uses Janus kinase (JAK)2-signal transducers and activators of transcription (STAT) 3 as the primary signaling (10). As schematically shown in **Fig. 7**, the binding of leptin to *Lepr* results in transphosphorylation and activation of JAK2 and the subsequent phosphorylation of tyrosine residues in the cytoplasmic part of *Lepr*, which provide docking sites for SH2-containing signaling proteins, including STAT3, SHP2, suppressor of cytokine signaling 3

(SOCS3), and PTP1B. Recruitment of STAT3 to the phosphorylated tyr(pY)-1138 residue leads to its rapid phosphorylation, dimerization, and translocation to the nucleus to activate transcription of STAT3-inducible genes, including SOCS3. The pY-985 residue recruits either SHP2 or SOCS3. Binding of SOCS3 attenuates leptin signaling by inhibiting the receptor-associated JAKs. Recruitment of SHP2 can have both positive and negative

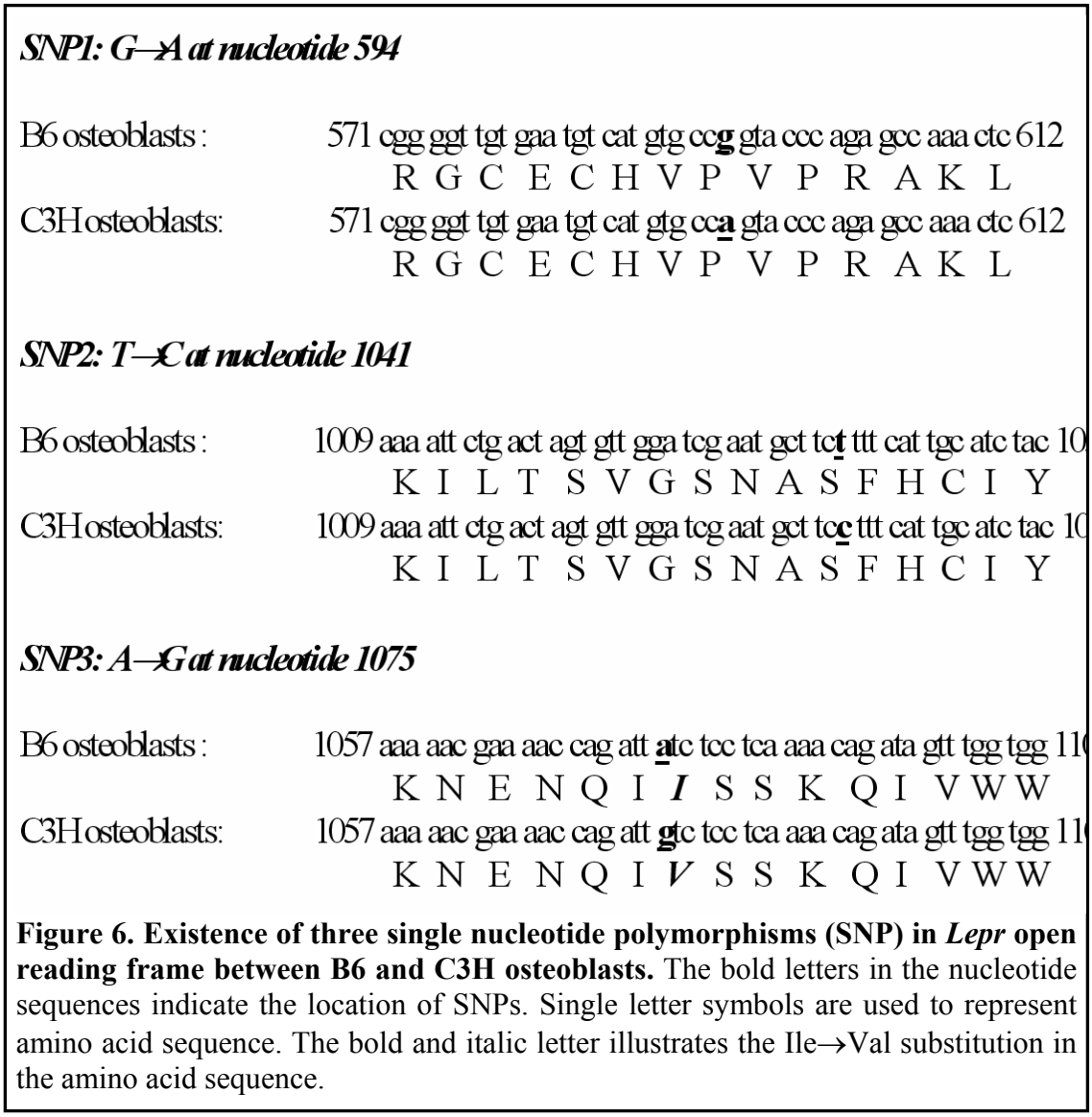

Figure 6. Existence of three single nucleotide polymorphisms (SNP) in *Lepr* open reading frame between B6 and C3H osteoblasts. The bold letters in the nucleotide sequences indicate the location of SNPs. Single letter symbols are used to represent amino acid sequence. The bold and italic letter illustrates the Ile→Val substitution in the amino acid sequence.

effects on the *Lepr* signaling. On the one hand, the SHP2 binding results in binding of Grb2 to SHP2 and subsequent activation of the Ras/Raf/Erk signaling pathway, leading to, among others, the expression of c-fos. On the other hand, SHP2 dephosphorylates and inactivates JAK2, leading to termination of the *Lepr* signaling. PTP1B is a critical downstream negative regulator of the *Lepr* pathway. Deletion of PTP1B gene enhanced leptin sensitivity in mice (11). PTP1B decreased JAK2 phosphorylation and blocked leptin-induced transcription of SOCS3 and c-fos (12). The *Lepr* signaling pathway also regulates other key anabolic pathways through crosstalks, including the integrin, IGF-I, ER, BMP/TGFβ, and canonical Wnt signaling pathways. **Fig. 7** shows some of the interactions between the *Lepr* and the integrin signaling pathways. Specifically, the recruitment of SHP2 and/or PTP1B to integrin is essential for the integrin signaling (13,14). Recruitment of these PTPs would lead to c-Src activation (by dephosphorylating

its inhibitory pY-527 residue), which in turn activates the Grb2/Ras/RAF/Erk signaling. We surmise that there is a competition between integrins and Lepr for recruitment of SHP2 and/or PTP1B (indicated by the thick arrows in **Fig. 7***)*, and that the *Lepr* pathway inhibits the mechanical stimulation of bone formation in part through sequestering SHP2 and/or PTP-1B from binding to integrins. We further postulate that the mechanism(s) leading to the preferential recruitment of SHP2 and PTP-1B to integrins in response to mechanical stimuli is defective in C3H osteoblasts.

As a preliminary test of our model, we determined and compared the basal and shear stress-induced levels of leptin-dependent activation of JAK2/STAT3 in C3H osteoblasts and B6 osteoblasts. We reasoned that if the I359V substitution alters the efficiency of the *Lepr* signaling in C3H osteoblasts, the basal and/or shear stress-induced leptin-mediated activation of the *Lepr* signaling in the two osteoblasts should be different. As a preliminary test for this hypothesis, we measured the relative levels of total and the tyrosine phosphorylated JAK2 and total and tyrosine phosphorylated STAT3 in C3H and B6 osteoblasts with or without the 30-min steady fluid shear. We also included osteoblasts of *ob*/*ob* mice for comparison. **Fig. 8** shows that the basal leptin-mediated increases in p-JAK2 and p-STAT3 levels in the C3H were higher than those in the B6 and *ob*/*ob* osteoblasts. While this finding needs to the confirmed, it is entirely consistent with our premise that the I359V substitution in *Lepr* in C3H osteoblasts leads to an enhanced basal leptin-mediated activation of the Lepr signaling pathway. It is also interesting to note that the basal total JAK2 and STAT3 levels appeared to be several fold higher in C3H osteoblasts than in B6 and *ob*/*ob* osteoblasts. It raises the possibility that other genetic differences between B6 and C3H mice might cause the greater levels of JAK2 and STAT3 in C3H osteoblasts, which might in part be responsible for the differential osteogenic response to mechanical stimulation in the two mouse strains. Because there does not appear to have a significant difference in the *Lepr* mRNA expression level between the two mouse osteoblasts (**Fig. 5**), the enhanced *Lepr* signaling seen with the C3H osteoblasts is probably related to an enhanced ligand binding affinity and/or a more efficient transduction of signals in C3H osteoblasts compared to B6 osteoblasts. The 30-min steady shear stress markedly suppressed the leptin-mediated increases in the p-JAK2 and p-STAT3 levels in all three test osteoblasts. The shear stress-mediated suppression appeared to be bigger in *ob*/*ob* osteoblasts compared to that in B6 and C3H osteoblasts. Although the fluid shear suppressed the leptin-mediated p-JAK2 and p-STAT3 levels in C3H osteoblasts, the resulting p-JAK2 and p-STAT3 levels were still several folds higher than the basal levels of these proteins in B6 and *ob*/*ob* osteoblasts. It may be speculated that the shear stress produced by physiologically relevant levels of loading might not be sufficient to reduce the *Lepr* signaling to a level that would yield an anabolic response. The past findings that high levels of mechanical strains were able to elicit an osteogenic response in C3H mice (15) are consistent with this possibility. Moreover, because the shear stress increased the *Lepr* mRNA levels in these osteoblasts (**Fig. 5**), the suppression of p-JAK2/p-STAT3 phosphorylation levels is not due to a reduction in the number of *Lepr*, but may be due to an inhibition of the *Lepr* signaling. While these findings need to be confirmed, these results suggest that the leptin signaling pathway is a negative pathway in the context of mechanotransduction and that mechanical stimulation activates the mechanotransduction in part by suppressing this negative pathway.

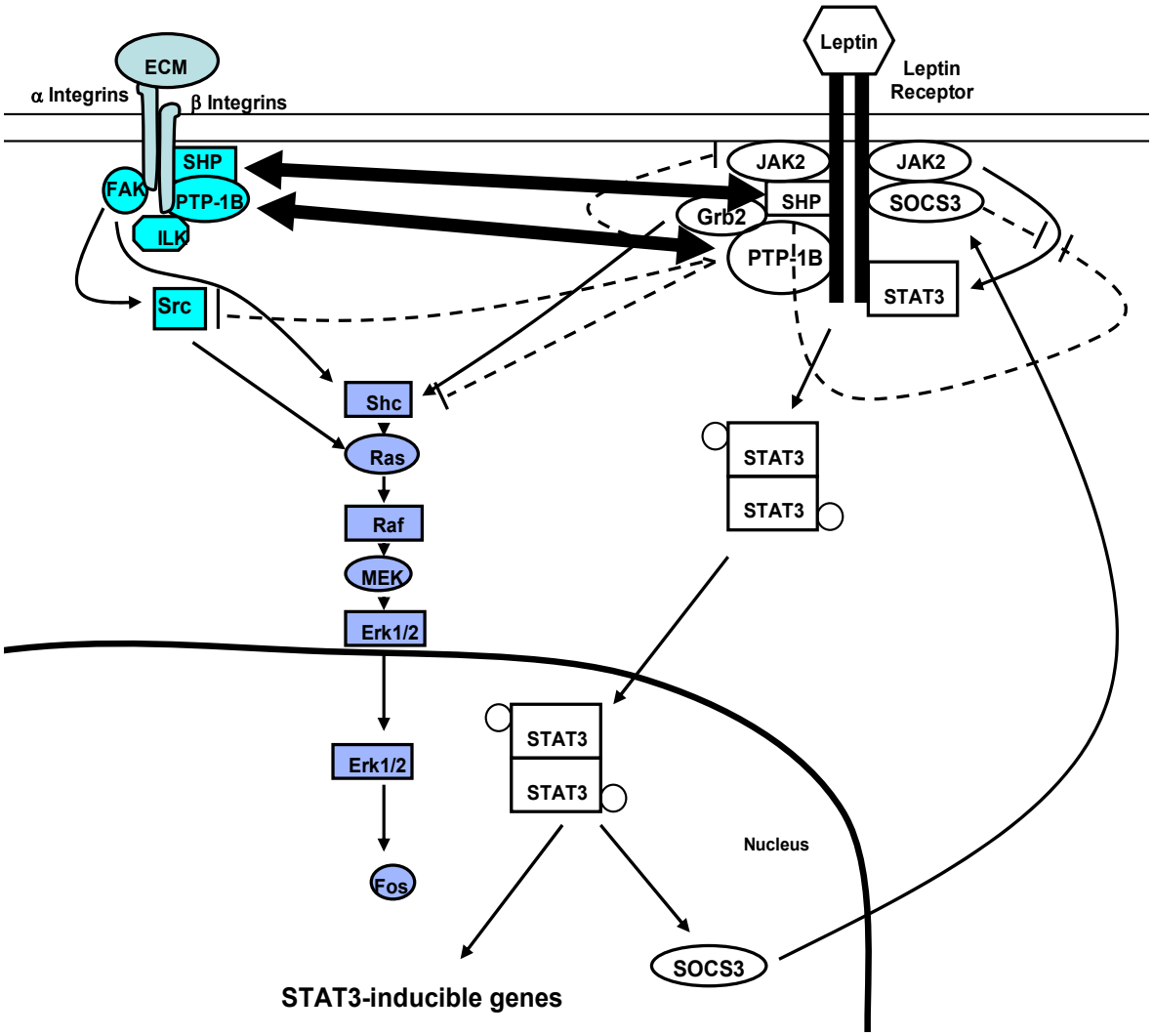

Figure 7. Molecular mechanism of the leptin receptor signaling pathway and its potential interactions with the integrin signaling pathway. Please refer to text for a detailed description. The solid lines represent upregulation; while the dashed lines indicate negative regulation. The thick arrows indicates shuffling of SHP2 and/or PTP1B between Lepr and integrins.

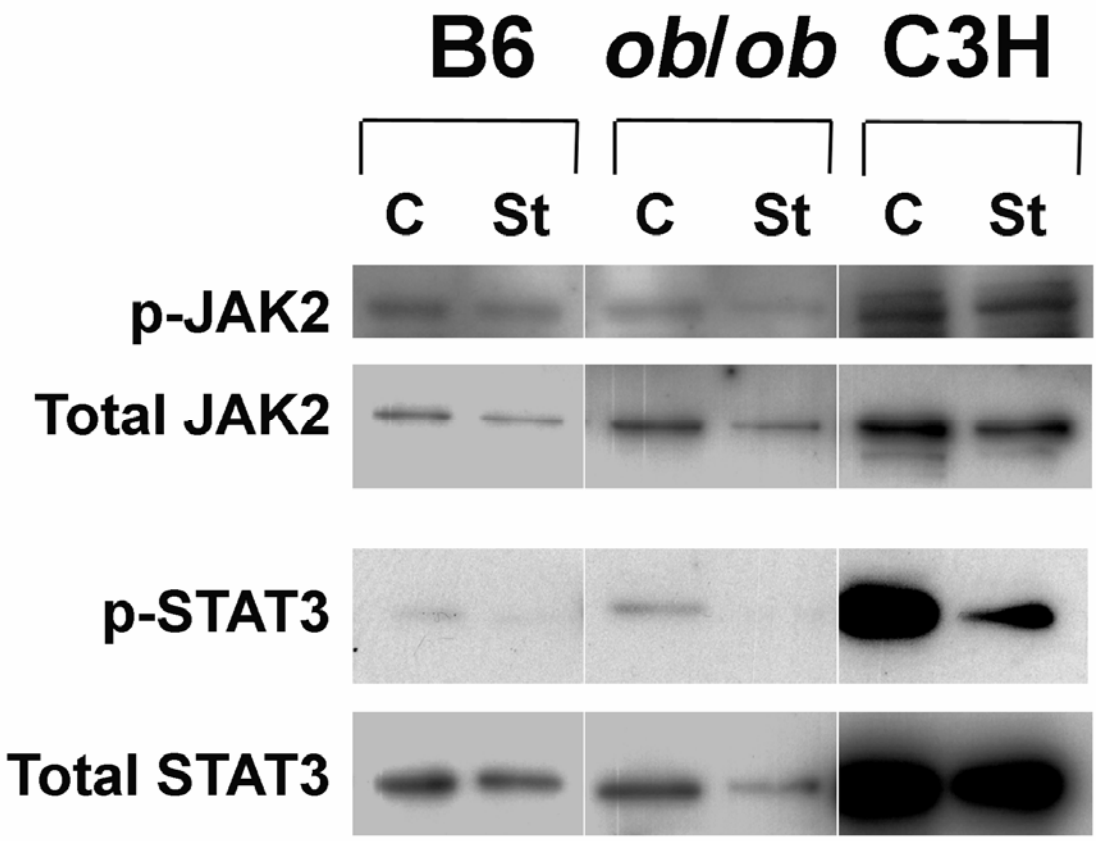

Figure 8. Effects of the steady fluid shear on leptin-mediated induced phosphorylation of JAK2 and STAT3. Primary osteoblasts isolated from B6, *ob*/*ob*, and C3H mice were each treated with 100 ng/ml leptin with or without the 30-min steady fluid shear stress of 20 dynes/cm^2. Ten minutes after the shear stress, the stressed cells (St) and the corresponding static control cells (C) were lyzed in RIPA, and the relative levels of tyrosine phosphorylated (p-JAK2) and total JAK2 as well as those of tyrosine phosphorylated (p-STAT3) and total STAT3 were analyzed by Western blot. This composite figure shows a representative blot.

Key Research Accomplishments:

1. We have obtained strong circumstantial evidence that the *Lepr* signaling pathway is a negative regulator of mechanical stimulation of bone formation.
2. We have shown that there are three SNPs in the coding region of *Lepr* between B6 and C3H mice, and that one of the SNPs resulted in the change of the amino acid sequence of the *Lepr* protein.
3. We have obtained preliminary evidence that leads to our hypothesis that the *Lepr* signaling pathway in osteoblasts negatively regulate the anabolic response to mechanical stimuli through sequestering SHP2 and/or PTP-1B from binding to integrins.

Reportable Outcomes:

1. Lau K-HW, Kapur S, Kesavan C, and Baylink DJ (2006) Upregulation of the wnt, estrogen receptor, insulin-like growth factor-I and bone morphogenetic protein pathways in C57BL/6J osteoblasts as opposed to C3H/HeJ osteoblasts in part contributes to the differential anabolic response to fluid shear. ***J Biol Chem*** 281(14), 9576-9588.
2. Kapur S, Baylink DJ, and Lau K-HW (2005) The canonical Wnt pathway is downstream to the BMP signaling pathway in mediating fluid shear stress-induced osteoblast proliferation. ***J Bone Miner Res*** 20 (Suppl 1), S240, abstract # SU219.

Conclusion:

In summary, these data provide strong supports for our conclusions that 1) the *Lepr* and its signaling pathway acts as a negative regulator of mechanosensitivity, 2) the *Lepr* in osteoblasts of B6 and C3H mice might have different functional activity due to a SNP in the coding region, and the different functional activity of *Lepr* in osteoblasts of these two mouse strains may in part be responsible for the differential anabolic response to mechanical stimuli in these two mouse strains, and 3) the *Lepr* signaling pathway in osteoblasts negatively regulate the anabolic response to mechanical stimuli through sequestering SHP2 and/or PTP-1B from binding to integrins. We are now in position to apply the siRNA technology to definitively evaluate whether *Lepr* or its signaling mechanism is involved in the regulation of the osteogenic response to mechanical stimulation.

References:

1. Lau K-HW, Kapur S, Kesavan C, and Baylink DJ (2006) Upregulation of the Wnt, estrogen receptor, insulin-like growth factor-I, and bone morphogenetic protein pathways in C57BL/6J osteoblasts as opposed to C3H/HeJ osteoblasts in part contributes to the differential anabolic response to fluid shear. *J Biol Chem* **281**, 9576-9588.
2. Robling AG, Li J, Shultz KL, Beamer WG, and Turner CH (2003) Evidence for a skeletal mechanosensitivity gene on mouse chromosome 4. *FASEB J* **17**, 324-326.
3. Saxon LK, Robling AG, Alam I, Turner CH (2005) Mechanosensitivity of the rat skeleton decreases after a long period of loading, but is improved with time off. *Bone* **36**, 454-464.
4. Turner CH, Alam I, Sun O, Li J, Fuchs RK, Edenberg HJ, Koller DL, Foroud T, Econs MJ (2005) The leptin receptor strongly influences bone structure and strength: results from a genome-wide screen in rats. *J Bone Miner Res* 20 (Suppl 1), S28, abstract 1108.
5. Thomas T (2004) The complex effects of leptin on bone metabolism through multiple pathways. *Curr Opin Pharmacol* **4**, 295-300.
6. Ducy P, Amling M, Takeda S, Priemel M, Schilling AF, Beil FT, Shen J, Vinson C, Rueger NM, Karsenty G (2000) Leptin inhibits bone formation through a hypothalamic relay: a central control of bone mass. *Cell* **100**, 197-207.

7. Gordeladze JO, Reseland JE (2003) A unified model for the action of leptin on bone turnover. *J Cell Biochem* **88**, 706-712.
8. Rundle CH, Wang X, Wergedal JE, Srivastava AK, Davis EI, Lau K-HW, Mohan S, Baylink DJ (2006) Loss of sex-specific differences in bone size in leptin-deficient (*ob/ob*) mice. *Transactions to the 52nd Annual meeting of Orthopaed Res Soc* abstract # 188.
9. Tartaglia LA, Dembski M, Weng X, Deng N, Culpepper J, Devos R, Richards GJ, Campfield LA, Clark FT, Deeds J (1995) Identification and expression cloning of a leptin receptor, OB-R. *Cell* **83**, 1263-1271.
10. Hekerman P, Zeidler J, Bamberg-Lemper S, Knobelspies H, Lavens D, Tavernier J, Joost H-G, Becker W (2005) Pleitrophy of leptin receptor receptor signaling is defined by distinct roles of the intracellular tyrosines. *FEBS J* **272**, 109-119.
11. Zabolotny JM, Bence-Hanulee KK, Stricker-Krongrad A, Haj F, Wamg Y, Minokoshi Y, Kim YB, Elmquist JK, Tartaglia LA, Kahn BB, Neel BG (2002) PTP1B regulates leptin signal transduction in vivo. *Dev Cell* **2**, 489-495.
12. Zabeau L, Lavens D, Peelman F, Eyckerman S, Vandekerckhove J, Tavernier J (2003) The ins and outs of leptin receptor activation. *FEBS Lett* **546**, 45-50.
13. Oh E-S, Gu H, Saxton TM, Timms JF, Hausdorff S, Frevert EU, Kahn BB, Pawson T, Neel BG, Thomas SM (1999) Regulation of early events in integrin signaling by protein tyrosine phosphatase SHP-2. *Mol Cell Biol* **19**, 3205-3215.
14. Arias-Salgado EG, Haj F, Dubois C, Moran B, Kasirer-Friede A, Furie BC, Furie B, Neel BG, Shattil SJ (2005) PTP-1B is an essential positive regulator of platelet integrin signaling. *J Cell Biol* 170, 837-845.
15. Pedersen EA, Akhter MP, Cullen DM, Kimmel DB, Recker RR (1999) Bone response to in vivo mechanical loading in C3H/HeJ mice. *Calcif Tissue Int* **65**, 41-46.

APPENDICES

In Vivo Studies

1. Chandrasekhar K, Baylink DJ, Apurva K. Srivastava, Susanna O, Hongrun Yu, Jon E. Wergedal and Mohan S. Identification of genetic loci that regulate bone adaptive response to loading in C57BL/6J and C3H/HeJ intercross. Bone 39(3): 634-64, 2006.

2. Chandrasekhar K, S Mohan, H Yu, S Oberholtzer, J.E Wergedal, D.J.Baylink. Novel Mechanoresponsive BMD and Bone Size QTL Identified In A Genome Wide Linkage Study Involving C57BL/6J-C3H/HeJ Intercross. ASBMR 27th Annual Meeting, 2005.

3. Chandrasekhar K, D. J Baylink, K. Susanna, J. E. Wergedal, H. Yu, and S. Mohan. Quantitative Trait loci for Tibia Periosteal Circumference in the C57BL/6J-C3H/HeJ mice intercross. ASBMR 28th Annual Meeting, 2005.

In Vitro Studies

4. Lau K-HW, Kapur S, Kesavan C, and Baylink DJ (2006) Upregulation of the wnt, estrogen receptor, insulin-like growth factor-I and bone morphogenetic protein pathways in C57BL/6J osteoblasts as opposed to C3H/HeJ osteoblasts in part contributes to the differential anabolic response to fluid shear. ***J Biol Chem*** 281(14), 9576-9588.

5. Kapur S, Baylink DJ, and Lau K-HW (2005) The canonical Wnt pathway is downstream to the BMP signaling pathway in mediating fluid shear stress-induced osteoblast proliferation. ***J Bone Miner Res*** 20 (Suppl 1), S240, abstract # SU219.

Identification of genetic loci that regulate bone adaptive response to mechanical loading in C57BL/6J and C3H/HeJ mice intercross

Chandrasekhar Kesavan[1], Subburaman Mohan[1, 2], Apurva K. Srivastava[1], Susanna Kapoor[1], Jon E Wergedal[1, 2], Hongrun Yu[1], and David J Baylink[1, 2]

[1]Musculoskeletal Disease Center, VA Loma Linda Healthcare System, Loma Linda, CA
[2]Department of Medicine, Loma Linda University, Loma Linda, CA

Running title: QTLs affecting bone anabolic response to loading

Corresponding Author: Subburaman Mohan, Ph.D.
Research Professor of Medicine and Biochemistry
Loma Linda University
Musculoskeletal Disease Center (151)
Jerry L. Pettis Memorial VA Medical Center
11201 Benton Street
Loma Linda, CA 92357
Phone: 909-825-7084, ext. 2932
FAX: 909-796-1680
E-Mail: Subburaman.Mohan@med.va.gov

Appendix-1

Abstract

Strain-dependent differences in bone adaptive responses to loading among inbred mouse strains suggest that genetic background contributes significantly to adaptation to exercise. To explore the genetic regulation of response to loading, we performed a genome-wide search for linkage in a cross between two strains, a good responder, C57BL6/J (B6), and poor responder, C3H/HeJ (C3H). Using a four-point bending model, the right tibia was loaded by applying 9N force for 36 cycles for 12-days in 10-week old female B6×C3H F2 mice. Changes in bone density (BMD) and bone size were evaluated *in-vivo* by pQCT. Measurements from non-loaded left tibia were used as an internal control to calculate loading-induced percent increase in BMD and bone size, thus excluding the possibility of identifying background QTL(s) due to natural allelic variation in mapping strains. A genome-wide scan was performed using 111 micro-satellite markers in DNA samples collected from 329 F2 mice. Heritability of bone adaptive response to loading was between 70-80%. The mean increase, expressed as percent of unloaded tibia, was 5% for BMD, 9% for periosteal circumference (PC), and 14% for cortical thickness in F2 mice (n=329). All these phenotypes showed normal distributions. Absence of significant correlation between BMD response to four-point bending and body weight or bone size suggested that the bone adaptive response was independent of bone size. Interval mapping revealed that BMD response to four-point bending was influenced by three significant loci on Chrs 1 (Log-of-odds ratio score (LOD) 3.4, 91.8 cM), 3 (LOD 3.6, 50.3 cM), and 8 (LOD 4.2, 60.1 cM), and one suggestive QTL on Chr 9 (LOD 2.5, 33.9 cM). Loading-induced increases in PC and Cth were influenced by four significant loci on Chrs 8

(LOD 3.0, 68.9 cM), 9 (LOD 3.0, 13.1cM), 17 (LOD 3.0, 39.3cM) and 18 (LOD 3.0, 0 cM) and two suggestive loci on Chr 9 (LOD 2.2, 24 cM) and 11 (LOD 2.1, 69.9 cM). Pairwise analysis showed the presence of several significant and suggestive interactions between loci on Chrs 1, 3, 8, and 13 for BMD trait. This is the first study that provides evidence for the presence of multiple genetic loci regulating bone anabolic responses to loading in the B6xC3H intercross. Knowledge of the genes underlying these loci could provide novel approaches to improve skeletal mass.

Keywords: mechanical loading, four-point bending, quantitative trait loci, Mice, vBMD

Introduction

Mechanical stimulation is one of the important factors in the development and maintenance of skeletal tissues [1-4]. Several *in-vivo* studies have shown that increased mechanical stress on bone tissue changes the bone density and morphology, resulting in an increased bone mass and biomechanical strength, whereas lack of mechanical stress leads to a rapid bone loss as evidenced by immobilization and bed rest studies [5-14]. Thus, physical exercise has been perceived as an important therapeutic strategy in humans to maintain bone mass and prevent osteoporosis. Recent studies in humans have also shown that bone anabolic response to a given mechanical load is highly variable, with some individuals exhibiting robust bone anabolic response with others responding modestly [15-18]. A similar variation has been observed among inbred strains of mice [19-21]. We [6,19] and others [21] have shown that mouse strains such as C57BL/6J (B6) respond with a much higher increase in bone density (BMD) and bone cross-sectional area as compared to the C3H/HeJ (C3H) strain of mouse in response to a similar amount of *in-vivo* loading. These data suggest that variations in skeletal response to mechanical loading in humans and mice are largely determined by genetic factors [12,21]. However, very little is known about the genetic regulation of mechanical loading and, so far, not a single gene has been identified that influences the skeletal response to mechanical loading [22].

One approach often used to perform genome-wide searches of genetic loci that contribute to differences in phenotypic variation is the quantitative trait loci (QTL) technique. This approach has been used in experimental animal models and in humans to study genetic regulation of bone density [23,24], bone metabolism [25], strength [26], quality, and size [27] and other traits [28]. By utilizing the QTL technique one could a) identify the regions within chromosomes that contain the functional genes of interest for a given phenotype; 2)

estimate the influence of genetic variation on within-species phenotypic variation; and 3) evaluate QTL-QTL interactions for the effect on phenotypic variation. The limitations of the QTL approach include: 1) it is technically time-consuming and expensive; 2) initial QTL analysis does not allow high resolution mapping and further fine mapping is required to narrow down the loci containing possible candidate genes; and 3) many genes in a particular chromosomal interval may not be relevant for a specific trait. Despite the drawback that the relevance of QTL genes identified using mouse models to explain the phenotypic variation in humans remains to be established, the availability of genomic (sequences, SNPs) and animal resources (congenic lines, chromosomal substitution strains, recombinant inbred strains) facilitates the identification and functional testing of QTL of candidate genes and therefore has attracted attention among molecular geneticists to use mice for QTL studies. In this study, we used two inbred strains, C57BL/6J and C3H/HeJ, good and poor responder strains respectively, to perform a genome-wide search for loci regulating bone adaptive response to mechanical loading.

Materials and methods

Mice

Female B6 and male C3H mice were obtained from the Jackson Laboratory (Bar Harbor, Me) to produce C3HB6 F1 mice, which were intercrossed to generate F2 mice. At 10-weeks of age the mice were subjected to mechanical loading using a four-point bending model described previously [19,21]. All mice were housed under the standard conditions of 14-hour light and 10-hour darkness, and had open access to food and water. The experimental protocols were in compliance with animal welfare regulation and approved by local IACUC.

In-vivo loading model/ regimen

The four-point bending device [Instron, Canton, MA] consists of two upper movable points covered with rubber pads, which are 4 mm (millimeter) apart, and two lower non-movable points covered with rubber pads, which are 12 mm apart. After anesthetizing the mice, the ankle of the tibia was positioned on the second lower immobile points of instron such that the region of tibia loaded did not vary in different mice. During bending, the two upper pads touch the lateral surface of the tibia through overlaying muscle and soft tissue, while the lower pads touch the medial surface of the proximal and distal parts of the tibia. One of the limitations of this model is that force applied over soft tissue may have some local effects on blood and fluid flow. We took efforts to minimize this by changing the rubber pads frequently in the Instron mechanical tester. The loading protocol for this study consisted of a 9 Newton (N) force at a frequency of 2 Hz for 36 cycles performed at the same time once a day under inhaleable (5% halothane and 95% oxygen) anesthesia. The loading procedure was repeated for 6 days/week with 1 day of rest for 2-weeks. On the 15th day, *in-vivo* pQCT measurements were performed on the loaded and non-loaded tibia of all F2 mice. Sham-bending was performed as described previously (1).

Peripheral quantitative computed tomography (pQCT) measurements

To measure loading-induced changes in the bone density and geometry in loaded and non-loaded tibias, we used pQCT (Stratec XCT 960M, Norland Medical System, Ft. Atkinson, WI) as described previously [19,29]. Calibration was performed daily with a defined

standard provided by the manufacturer. Mice were anesthetized and a two-dimensional scout view was taken first, which permits the identification of landmarks and a precise selection of the appropriate site for measurement. In order to minimize the measurement errors caused by positioning of tibia for pQCT, we used the tibia-fibular junction as the reference line. We selected two-slices that start 4 mm proximal from tibia-fibular junction for pQCT measurement. This region corresponds to the loading zone. Each slice is at a 1mm interval and the values presented in the Results are an average of these two slices [19]. To minimize exposure time of animals to anesthesia for *in-vivo* pQCT measurements, we choose to scan only the loading zone in the F1 or F2 mice. Based on our previous findings [19], we used two thresholds to analyze the pQCT data; a 180-730 mg/cm^3 threshold was used to measure periosteal circumference (PC) and a 730-730-mg/cm^3 threshold was used to measure total volumetric density (vBMD), cortical volumetric bone mineral density (cortical vBMD), and cortical thickness (CTh). Cortical vBMD is defined as cortical content/cortical volume excluding the marrow cavity.

PCR based Genetic Analysis

Two days after the last loading, the mice were sacrificed and tissues such as liver and tibia were collected and stored at -80ºC. Genomic DNA was extracted from the liver of each F2 mouse using a Maxi prep DNA extraction kit (Qiagen) and stored at -80°C. The quality and quantity of DNA was measured by Nano drop and Bio-analyzer (Agilent Technologies, Inc, CA). Polymerase Chain Reaction (PCR) primers were purchased from Applied Biosystems (ABIPRISM, Foster City, CA) to perform the genome-wide genotyping scan of the F2 population. PCR reaction conditions allowed 3-4 microsatellite markers to be multiplexed in a single

electrophoretic lane. The pooled products were analyzed for fragments size on the ABI 3100 Sequence Detection System and Gene Scan software was used to detect size of the alleles. Allele calls and edits were performed using Genotyper software and in house software, and exported as text files for downstream analysis.

QTL analysis

We used parametric mapping (a mapping strategy that requires the assumption of normal distribution for the quantitative trait investigation) for total vBMD, Cortical vBMD, PC and CTh in our QTL analysis. Because the distribution of the PC showed some significant skewing, analysis was also performed on log transformed PC data. The log transformation normalized the distribution but did not alter the identification of QTL and produced only slight changes in LOD scores. The interval mapping was performed by using a MapQTL software program (Verison 5.0; Wageningen, The Netherlands). The significant levels of the LOD scores used in this study were obtained by the permutation test on the studied population. By conducting a certain number of permutations (usually 1000), a threshold LOD score can be established based on the chosen probability level. As we understand, in the human genetics, the threshold LOD score is usually 3, i.e. $p<0.01\%$, depending on the sample size. The permutation analysis is done by the well-established software, which has been extensively used in QTL analyses in mice and other animal models. QTLs with a genome wide error of 1%, 5% and 32% were classified as highly significant, significant and suggestive, respectively [30,31]. To study genome-wide interactions between QTLs, we used a Pseudomarker algorithm written for the MATLAB (Mathworks Inc., Natick, MA,

USA) programming environment (obtained from www.jax.org/research/churchill). This program analyzes the phenotypic effect of each marker taken individually (MAINSCAN run by pseudomarker program) and also the phenotypic effects of pairs of markers or intervals (PAIRSCAN) taken jointly for their effects on the trait. In the PAIRSCAN analysis, we tested the combined (or full model) effects on a trait for a marker pair, which reflects the main the effects of both markers plus their interaction. Thresholds for significance were estimated by a 200-permutation test carried out on F2 data. The MapQTL and Pseudomarker Main scan analyses gave similar results. The broad sense of heritability index of each phenotype was calculated using a formula as mentioned earlier [26].

Statistical Analysis

Phenotypic response to mechanical loading (e.g. BMD) was calculated using the following formula: % response = [(BMD of loaded tibia – BMD of non-loaded tibia)/BMD of non-loaded tibia x 100]. We used Statistica software to perform correlation analysis, phenotype distribution, and Regression analysis, and two-way ANOVA. Data were analyzed using Graphpad Prism (Windows version 3.0, San Diego, CA). Correlation coefficients between phenotypes were obtained using Pearson's correlation.

Results

Sham-Bending

Previously, we have reported that mechanical loading by four-point bending caused greater changes in the BMD and bone size in B6 mice after 12 days of 9N

load. In order to confirm that the increase in bone anabolic response induced by bending is not due to periosteal pad pressure, we performed sham-bending in 10-week old female B6 mice for 12 days using 9N load at 2Hz for 36 cycles. The results from our pQCT analysis revealed no significant changes in the BMD, periosteal circumference and other bone parameters (Table-1). This finding implies that changes in bone parameters induced by bending are not due to periosteal pad pressure as evidenced from our sham-loading study.

Bone response to mechanical loading is a heritable trait

The bone response to mechanical loading was calculated from measurements of well-established parameters, such as total vBMD, cortical vBMD, PC and CTh, in loaded tibia. Results for each parameter were expressed as percent change from identical measurements performed on non-loaded left tibia in each F2 mouse. The mean percent increase in response to loading in the female F1 mice (n=100) was 2.8% for total vBMD, 0.8% for cortical vBMD, 8.0% for PC and 11.7% for CTh. These loading-induced increases in various skeletal parameters in F1 mice were intermediate between parent strains based on results published previously [19]. In the F2 mice (n=329), the mean increase in total vBMD was 5%, and that of cortical vBMD, PC, CTh, were 1.5%, 9%, and 14%, respectively (Figure 1). The distributions of total vBMD, cortical vBMD, PC, and CTh among female F2 mice shown in Figure 1 indicate that bone responses to mechanical loading were variable. The distributions of all four phenotypes approached normality (n=329) but values were predominantly positive, indicating most mice responded to loading. These wide ranges of bone adaptive responses displayed by F2 mice are probably due to the variable genetic background of each F2 mouse. The broad sense of heritability, calculated as described earlier [26], of the loading-induced changes in the vBMD, cortical vBMD, PC, and CTh was 82%, 70%, 86%, and 82%, respectively.

Due to natural allelic variation in bone size between C3H and B6 strains, we expected the F2 mice to exhibit differences in cross-sectional area. The mice with a smaller cross-sectional area receive greater mechanical strain than mice with larger cross sectional area for the same load. In order to determine if variations in strain difference caused by difference in cross sectional area contribute to a variation in BMD response, we performed

correlation analysis between periosteal circumferences of non-loaded bones versus % BMD changes in corresponding loaded bones. The results from our study showed no significant correlation (r = -0.09) between loading induced percent changes in total vBMD and periosteal circumference. Furthermore, moment of inertia of non-loaded bones did not show significant correlation with percent changes in vBMD response. However, there could have been some difference in the shape of the bones in F2 mice whose possible effect on strain levels in affecting the BMD response to loading has not been determined in this study. Since the pQCT measurement was done *in-vivo*, we could not evaluate if variations in strain difference caused by differences in bone shape contribute to a variation in BMD response. On the other hand, there was a slight negative correlation (r = -0.18, $p<0.05$) between body weight and percent change in total vBMD in response to four- point bending in the F2 mice. These data suggest that variation in anabolic response to mechanical load was largely independent of body weight or bone size in female C3HxB6 F2 mice.

QTL for bone response to Mechanical loading

The linkage map, constructed using 111 markers (average marker density: 15 cM) and loading-induced changes in total vBMD, cortical vBMD, PC, and CTh phenotypes in 329 female F2 mice, revealed evidence for the presence of several significant and suggestive loci as shown in Table-2 and Figure 2. Loci regulating total vBMD (and cortical vBMD) were located on Chromosome (Chr) 1, 3, 8, and 9, whereas loci regulating bone size, which includes periosteal circumference and cortical thickness were located on Chrs 8, 9, 11, 17, and 18. The strongest linkage was observed on chromosome 8 for total vBMD (LOD score 4.2, 60 cM). Figure 3

shows posterior probability density plots for QTLs located on Chrs 1, 3, and 8. The posterior probability density plot is a likelihood statistic that gives rise to the 95% confidence intervals for QTL peak indicated by a horizontal bar in the plot. The four BMD QTLs (includes total vBMD and cortical vBMD) on Chrs 1, 3, 8, and 9 accounted for 19% of the variance in response to mechanical loading. Loci on Chrs 8, 9, 11, 17, and 18 regulating bone size (includes PC and CTh) accounted for the 15% variance in the F2 mice (Table-2). Chrs 8 and 9 QTL for BMD, PC and CTh were colocalized, whereas loci on Chrs 1 and 3 were specific for BMD, and Chrs 11, 17 and 18 loci were specific for bone size. Because there was a slight negative correlation between % changes in BMD response in loaded bones versus body weight, we performed QTL analysis after adjusting for body weight in the F2 mice. We found that body weight adjustment yielded an additional locus (Chr17) in addition to loci on Chr 1, 8 and 9.

Allele contribution to the peak QTLs

Figure 4 shows the contribution of alleles from B6 and C3H mice for the major QTL affecting BMD and PC. For Chr 1 BMD QTL, homozygous B6 alleles at marker *D1Mit113* showed dominant effect over C3H homozygous mice and were 5.6% (Figure 4) higher than the homozygotes for C3H alleles. Although the response to mechanical loading was higher in the B6 strain, it is noteworthy that C3H alleles at Chr 8 increased BMD in response to mechanical loading (Figure 4). Thus, homozygous C3H alleles at marker *D8Mit88* had 5.8% higher BMD than the homozygous B6 alleles. For this QTL, the C3H alleles best fit a recessive mode of inheritance. For PC QTL, homozygous alleles from B6 mice at marker *D8Mit49*

showed 10% higher PC values than the mice with homozygous C3H alleles. The Chr 8 loci regulating PC inherited in dominant mode.

QTL-QTL Interactions

Two loci show interaction when the genotype of one locus affects the effect of other locus. PAIRSCAN analysis revealed four significant interactions (Table-3) involving loci on Chrs 8 (60cM), 13 (45cM), 1 (90cM), and 13 (45cM) and one suggestive interaction involving loci on Chrs 5 (80cM) and 8 (10cM). These four interactions combined together accounted for approximately 11% of the variance in loading induced changes in BMD (includes total vBMD and cortical vBMD) and CTh (calculated by Pseudomarker FITQTL algorithm).

QTL analyses for bone density and size parameters using non-loaded bone

In addition to loci regulating response to loading, we used data from non-loaded tibia to identify linkage to BMD and bone size parameters. All four traits (total vBMD, cortical vBMD, PC, and CTh) showed normal distribution. Since there was a significant positive correlation (r-value range from 0.13 to 0.55, $p<0.05$) between the body weight and PC, and body weight and BMD, we performed QTL analyses after adjustment for body weight. We identified 13 chromosomes that regulate changes in BMD and bone size including Chrs 1, 2, 3, 4, 6, 10, 11, 12, 15, 16, 17, 18, and 19 (Table-4, Figure 5). Table-4 provides a list of QTLs that showed significant and suggestive linkages, the closest markers on peak QTL, and the percent variance explained by each QTL for different phenotypes. Some of the QTLs observed for the non-loaded phenotypes that include BMD and bone size,

are similar to the previously published QTLs [24,32-34]. In addition, we identified novel QTL for BMD on Chr 3 (LOD score 2.8, 59.0cM), 10 (LOD score 3.8, 63.4cM) and 17 (LOD score 5.4, 39.0cM), and PC QTL on Chrs 3 (LOD score 4.0, 46.4 cM), 10 (LOD score 2.4, 57.3 cM), 11 (LOD score 4.3, 49.2 cM), 15 (LOD score 3.1, 41.5 cM), 16 (LOD score 3.1, 24.0 cM), 17 (LOD score 5.1, 39.3 cM), and CTh QTL on Chrs 1, 3, 10, 16, 17, 18, and 19 (Table-4).

Discussion

Despite the fact that mechanical loading is an important regulator of bone mass, very little is known about the loci that contribute to the variation in bone anabolic response. Past research towards understanding the genetic variation in bone response to mechanical loading has been mainly focused on hypotheses concerning known candidate genes. To our knowledge, this is the first genome-wide search for loci that regulate bones anabolic response to mechanical loading. To evaluate loading-induced changes in bone adaptive response, our study design employed several selective criteria. Rationales for each of these criteria were based on evidence accumulated in previous studies [19]. The four-point bending model was used as a surrogate for other *in vivo* loading models, such as wheel running or jump training, because this model provided: 1) an extremely controlled external loading of an intact long bone; and 2) a controlateral control limb from each of the F2 mouse that can be used as a baseline to determine the loading response in the loaded limb. A criticism of using four-point bending is that it increases periosteal bone formation through pressure applied by pads as tested by sham loading rather than due to bending in mice and rats [21,35]. However,

subsequent studies in mice comparing periosteal bone response in sham loaded vs. loaded bones revealed that the magnitude of increase in bone formation was much greater in tibia subjected to four-point bending compared to sham loading. Raab-Cullen et al., reported a similar finding, using a four-point bending device in the rat model [36,37]. In this study we have also provided evidence by performing sham-bending in B6 mice. These studies are consistent with the possibility that loading induced strain but not periosteal pressure contributed mainly to increase in periosteal bone formation in response to four-point bending. We have therefore used four-point bending as a loading model in our QTL study.

Several phenotypic end points have been used in the literature to measure the efficacy of loading-induced changes in bone parameters [6,10,19,21,38]. Based on results of previous studies, including our recent study, we selected four parameters (total vBMD, cortical vBMD, PC and CTh) to define the bone adaptive response. Analysis of percent change from non-loaded bone was based on the rationale that variable genetic background in each F2 mouse would affect the bone morphology (such as cross sectional area) and influence the skeletal response independently of genetic regulation of loading. In addition, there are naturally segregating allelic variations between C3H and B6 mice that could affect BMD and bone size traits. Therefore, the use of absolute changes in BMD or periosteal circumference phenotype to study linkage would identify common, rather than specific, genetic components relevant for response to loading.

As observed with skeletal traits, response to four-point bending had a high index of heritability (70-80%). These heritability estimates were in agreement with those reported

recently by Massett et al., [39] for various traits in mouse strains. Our results also agree with the 40-80% heritability estimates in humans [40] determined for physical activity. Thus, variance in bone response to mechanical loading in mice is strongly influenced by genetic factors.

The genome-wide search for associations between marker genotypes and the quantitative phenotypes of bone anabolic response to loading resulted in the localization of several QTLs in C3HxB6 F2 mice. The primary mechanism by which mechanical loading induces increases in BMD is believed to involve periosteal modeling [19], leading to increased cortical thickness and an eventual increase in volumetric BMD. Based on this hypothesis, the QTLs identified in this study can be grouped into three categories: 1) QTLs that affect both BMD and bone size response to mechanical loading; 2) QTLs that affect only BMD response to mechanical loading; and 3) QTLs that only influence bone size response to mechanical loading.

Our findings that genetic loci in Chrs 8 and 9 show significant linkage with multiple measures of skeletal response to loading (total vBMD, PC and CTh), even though our analysis eliminated effects of confounding factors, such as bone size, suggest that these loci may contain genes that play a key role in mediating bone cell response to loading by regulating both BMD and bone size. Consistent with this idea, previous studies have shown that Chrs 8 and 9 contain genetic loci that regulate biomechanical and femur breaking strength in the multiple inbred mouse strain crosses including B6xC3H (Chr 8, 30-90 cM) [23] , B6xD2 F2 mice (Chr 8, 30-57 cM) [41,42] and MRLxSJL (30-60cM) [26,43]. Taken together, these data may suggest genes in these regions regulate

biomechanical strength possibly with consequence of superior (or more favorable) response to exercise.

In addition to the mechanical loading QTL that regulated both BMD and bone size, Chr 1 (91.8 cM) and Chr 3 (50.3 cM) QTL specifically affected BMD but not bone size. Mechanical loading QTL in Chr 1 (91.8 cM) colocalizes with a major QTL identified earlier for total vBMD and other structural properties [23,44] in the congenic and B6xC3H F2 mice. Accordingly, QTL analysis of the BMD phenotype for non-loaded bones in the present study revealed a major QTL on Chr 1 at 83.1 cM, which is closer to the previous published BMD QTL. While the B6 alleles in Chr 1 contributed to higher BMD response to four-point bending (Figure 5), C3H alleles contributed to higher BMD in non-loaded bone (data not shown). Thus, Chr 1 QTL may contain genes: 1) that contribute to natural variation in BMD between B6 and C3H strains; and 2) that respond to mechanical loading by increasing the vBMD. Our linkage analysis also identified loci on Chr 11 (69.9 cM), Chr 17 (39.3 cM), and Chr 18 (0 cM) that only influence bone size in response to mechanical loading. Furthermore, several novel loci regulating bone size on Chrs 3, 10, 11, 15, 16, 17, 18, and 19 were discovered using data from non-loaded bones. Based on these findings, it can be concluded that complex genetic mechanisms regulate variations in BMD and bone size in non-loaded and loaded bones. Another finding that provides substantial support for this concept of complex regulation of BMD and bone size is appearance of novel QTLs (Chr 5 and Chr 13) in the interaction study but not in the mainscan.

It is noteworthy that a previous study reported that a congenic strain in which a small fragment of C3H Chr 4 (40-80 cM) was introgressed in a B6 background showed increased

mechanosensitivity to loading. Our study, however, did not identify any QTL on Chr 4 for BMD and bone size. There are several possible explanations for why we did not find a QTL in chromosome 4: 1) The two models of loading used to study the bone anabolic responses are different. 2) The number of F2 mice used may not be adequate to identify all of the mechanical loading QTL; and 3) While many of the mechanical loading QTL may regulate anabolic response to four-point bending at multiple skeletal sites, there may be some QTL that are site specific i.e. regulate anabolic response in some but not other skeletal sites. In this regard, it is known that there are common BMD QTL that regulate BMD at multiple skeletal sites and site specific BMD QTL that regulate BMD at some sites but not at others [24]. Consistent with the previous study, we did observe that the BMD response to mechanical loading was higher for C3H alleles on Chr 8 QTL as compared to B6 alleles. Since C3H mice demonstrate poor adaptation to mechanical loading [22] as compared to the B6 mice, these findings of high response alleles in C3H were unexpected. It is possible that C3H alleles at these loci are phenotypically silent in the context of the C3H genome but increase BMD in response to four-point bending in the presence of one or more B6 alleles.

Although this first genome-wide research for mechanical loading QTL using C3H and B6 strains of mice has revealed evidence for the presence of multiple genetic loci regulating the skeletal response to loading, our findings should be viewed in the context of the following limitations. The use of growing mice rather than mature mice may have confounded the response. In this regard, we have recently found that four-point bending significantly increased bone density in B6 mice compared to C3H mice at 10-, 16- and 36-week [19], regardless of age. In addition, the non-loaded contralateral bone was used to

control for growth effects. Second, in our recent study, we observed that the amount of strain in C3H and B6 mice was similar at 9N force. However, the variable genetic background in each F2 mouse resulted in mice with variable cross-sectional area of tibia. With a fixed amount of force (9N), the amount of strain experienced by each mouse will depend on cross-sectional area (moment of inertia), suggesting that a mouse with a large cross-sectional area will experience lower strain and vice versa. This would generate a variable response to loading independent of genetic response to loading. However, absence of any significant correlation between skeletal response to loading and periosteal circumference of corresponding non-loaded bone suggests variation in loading strains was less important than variation in response due to genetics. Third, in the phenotype distribution, we found some of the F2 mice showed negative BMD response to mechanical loading. It remains unknown whether the negative BMD response is due to loading-induced changes in architecture/shape or due to rapid increase in poorly mineralized bone at the periosteum. Fourth, our study used a relatively low number of F2 mice (n=329) to perform the QTL analysis. This was mainly due to practical difficulties in performing four-point bending-based loading in a large number of mice. Therefore, the power to detect QTL was less than studies with 600-1000 animals. Thus, there are likely additional chromosomal regions that affect the bone response to loading which were undetected in this study. This was further evident by the loci interactions that showed only 11% variance. Finally, hormonal status is shown to significantly influence the response to loading, therefore the QTLs identified in this study could be specific to female mice. In this regard, mapping of each loci in the male mice will provide more definitive proof as to whether the same loci or closely linked loci underlie the QTLs mapped to overlapping chromosomal regions using only females.

In conclusion, mechanical loading has long been identified as a means to regulate bone architecture; however, the benefits of loading depend on genetic background. The results of this study provide an important first step in identifying the genetic factors that regulate the bone adaptive response to mechanical loading. Our results confirm that response to mechanical loading has a strong genetic component with several loci regulating loading induced bone modeling. The future discovery of genes at these loci could provide a basis for the observed variability in bone mass accretion and maintenance due to exercise in normal healthy individuals.

ACKNOWLEDGMENTS

This work was supported by the Army Assistance Award No. DAMD17-01-1-0074. The US Army Medical Research Acquisition Activity (Fort Detrick, MD) 21702-5014 is the awarding and administering acquisition office for the DAMD award. The information contained in this publication does not necessarily reflect the position or the policy of the Government, and no official endorsement should be inferred. All work was performed in facilities provided by the Department of Veterans Affairs. We would like to thank Mr. Jay Javier and Mr. Alex Cortez for their contribution in this project and Mr. Sean Belcher for his editorial assistance.

REFERENCES

1. Turner CH, Robling AG: Exercise as an anabolic stimulus for bone. Curr Pharm Des 2004;10:2629-2641.
2. Bailey DA, McCulloch RG: Bone tissue and physical activity. Can J Sport Sci 1990;15:229-239.
3. Warden SJ, Fuchs RK, Turner CH: Steps for targeting exercise towards the skeleton to increase bone strength. Eura Medicophys 2004;40:223-232.
4. Borer KT: Physical activity in the prevention and amelioration of osteoporosis in women: interaction of mechanical, hormonal and dietary factors. Sports Med 2005;35:779-830.
5. Gross TS, Srinivasan S, Liu CC, Clemens TL, Bain SD: Noninvasive loading of the murine tibia: an in vivo model for the study of mechanotransduction. J Bone Miner Res 2002;17:493-501.
6. Kodama Y, Umemura Y, Nagasawa S, Beamer WG, Donahue LR, Rosen CR, Baylink DJ, Farley JR: Exercise and mechanical loading increase periosteal bone formation and whole bone strength in C57BL/6J mice but not in C3H/Hej mice. Calcif Tissue Int 2000;66:298-306.
7. Mori T, Okimoto N, Sakai A, Okazaki Y, Nakura N, Notomi T, Nakamura T: Climbing exercise increases bone mass and trabecular bone turnover through transient regulation of marrow osteogenic and osteoclastogenic potentials in mice. J Bone Miner Res 2003;18:2002-2009.
8. Bikle DD, Halloran BP: The response of bone to unloading. J Bone Miner Metab 1999;17:233-244.
9. Bikle DD, Sakata T, Halloran BP: The impact of skeletal unloading on bone formation. Gravit Space Biol Bull 2003;16:45-54.
10. Umemura Y, Baylink DJ, Wergedal JE, Mohan S, Srivastava AK: A time course of bone response to jump exercise in C57BL/6J mice. J Bone Miner Metab 2002;20:209-215.
11. Rubin CT, Lanyon LE: Regulation of bone formation by applied dynamic loads. J Bone Joint Surg Am 1984;66:397-402.
12. Kodama Y, Dimai HP, Wergedal J, Sheng M, Malpe R, Kutilek S, Beamer W, Donahue LR, Rosen C, Baylink DJ, Farley J: Cortical tibial bone volume in two strains of mice: effects of sciatic neurectomy and genetic regulation of bone response to mechanical loading. Bone 1999;25:183-190.
13. Lecoq B, Potrel-Burgot C, Granier P, Sabatier JP, Marcelli C: Comparison of bone loss induced in female rats by hindlimb unloading, ovariectomy, or both. Joint Bone Spine 2005.
14. Suzuki Y, Akima H, Igawa S, Fukunaga T, Kawakub K, Goto S, Makita Y, Gunji A: Decrease of bone mineral density and muscle and/or strength in the leg during 20 days horizontal bed rest. J Gravit Physiol 1996;3:42-43.
15. Dalsky GP, Stocke KS, Ehsani AA, Slatopolsky E, Lee WC, Birge SJ, Jr.: Weight-bearing exercise training and lumbar bone mineral content in postmenopausal women. Ann Intern Med 1988;108:824-828.
16. Snow-Harter C, Bouxsein ML, Lewis BT, Carter DR, Marcus R: Effects of resistance and endurance exercise on bone mineral status of young women: a randomized exercise intervention trial. J Bone Miner Res 1992;7:761-769.

17. Tajima O, Ashizawa N, Ishii T, Amagai H, Mashimo T, Liu LJ, Saitoh S, Tokuyama K, Suzuki M: Interaction of the effects between vitamin D receptor polymorphism and exercise training on bone metabolism. J Appl Physiol 2000;88:1271-1276.
18. Dhamrait SS, James L, Brull DJ, Myerson S, Hawe E, Pennell DJ, World M, Humphries SE, Haddad F, Montgomery HE: Cortical bone resorption during exercise is interleukin-6 genotype-dependent. Eur J Appl Physiol 2003;89:21-25.
19. Kesavan C, Mohan S, Oberholtzer S, Wergedal JE, Baylink DJ: Mechanical loading induced gene expression and BMD changes are different in two inbred mouse strains. J Appl Physiol 2005.
20. Pedersen EA, Akhter MP, Cullen DM, Kimmel DB, Recker RR: Bone response to in vivo mechanical loading in C3H/HeJ mice. Calcif Tissue Int 1999;65:41-46.
21. Akhter MP, Cullen DM, Pedersen EA, Kimmel DB, Recker RR: Bone response to in vivo mechanical loading in two breeds of mice. Calcif Tissue Int 1998;63:442-449.
22. Robling AG, Li J, Shultz KL, Beamer WG, Turner CH: Evidence for a skeletal mechanosensitivity gene on mouse chromosome 4. Faseb J 2003;17:324-326.
23. Koller DL, Schriefer J, Sun Q, Shultz KL, Donahue LR, Rosen CJ, Foroud T, Beamer WG, Turner CH: Genetic effects for femoral biomechanics, structure, and density in C57BL/6J and C3H/HeJ inbred mouse strains. J Bone Miner Res 2003;18:1758-1765.
24. Beamer WG, Shultz KL, Donahue LR, Churchill GA, Sen S, Wergedal JR, Baylink DJ, Rosen CJ: Quantitative trait loci for femoral and lumbar vertebral bone mineral density in C57BL/6J and C3H/HeJ inbred strains of mice. J Bone Miner Res 2001;16:1195-1206.
25. Srivastava AK, Masinde G, Yu H, Baylink DJ, Mohan S: Mapping quantitative trait loci that influence blood levels of alkaline phosphatase in MRL/MpJ and SJL/J mice. Bone 2004;35:1086-1094.
26. Li X, Masinde G, Gu W, Wergedal J, Mohan S, Baylink DJ: Genetic dissection of femur breaking strength in a large population (MRL/MpJ x SJL/J) of F2 Mice: single QTL effects, epistasis, and pleiotropy. Genomics 2002;79:734-740.
27. Masinde GL, Wergedal J, Davidson H, Mohan S, Li R, Li X, Baylink DJ: Quantitative trait loci for periosteal circumference (PC): identification of single loci and epistatic effects in F2 MRL/SJL mice. Bone 2003;32:554-560.
28. Lumeng L, Crabb DW: Genetic aspects and risk factors in alcoholism and alcoholic liver disease. Gastroenterology 1994;107:572-578.
29. Wergedal JE, Sheng MH, Ackert-Bicknell CL, Beamer WG, Baylink DJ: Genetic variation in femur extrinsic strength in 29 different inbred strains of mice is dependent on variations in femur cross-sectional geometry and bone density. Bone 2005;36:111-122.
30. Churchill GA, Doerge RW: Empirical threshold values for quantitative trait mapping. Genetics 1994;138:963-971.
31. Sen S, Churchill GA: A statistical framework for quantitative trait mapping. Genetics 2001;159:371-387.

32. Turner CH, Sun Q, Schriefer J, Pitner N, Price R, Bouxsein ML, Rosen CJ, Donahue LR, Shultz KL, Beamer WG: Congenic mice reveal sex-specific genetic regulation of femoral structure and strength. Calcif Tissue Int 2003;73:297-303.
33. Shultz KL, Donahue LR, Bouxsein ML, Baylink DJ, Rosen CJ, Beamer WG: Congenic strains of mice for verification and genetic decomposition of quantitative trait loci for femoral bone mineral density. J Bone Miner Res 2003;18:175-185.
34. Bouxsein ML, Uchiyama T, Rosen CJ, Shultz KL, Donahue LR, Turner CH, Sen S, Churchill GA, Muller R, Beamer WG: Mapping quantitative trait loci for vertebral trabecular bone volume fraction and microarchitecture in mice. J Bone Miner Res 2004;19:587-599.
35. Turner CH, Forwood MR, Rho JY, Yoshikawa T: Mechanical loading thresholds for lamellar and woven bone formation. J Bone Miner Res 1994;9:87-97.
36. Raab-Cullen DM, Akhter MP, Kimmel DB, Recker RR: Bone response to alternate-day mechanical loading of the rat tibia. J Bone Miner Res 1994;9:203-211.
37. Turner CH, Akhter MP, Raab DM, Kimmel DB, Recker RR: A noninvasive, in vivo model for studying strain adaptive bone modeling. Bone 1991;12:73-79.
38. Specker B, Binkley T, Fahrenwald N: Increased periosteal circumference remains present 12 months after an exercise intervention in preschool children. Bone 2004;35:1383-1388.
39. Massett MP, Berk BC: Strain-dependent differences in responses to exercise training in inbred and hybrid mice. Am J Physiol Regul Integr Comp Physiol 2005;288:R1006-1013.
40. Simonen R, Levalahti E, Kaprio J, Videman T, Battie MC: Multivariate genetic analysis of lifetime exercise and environmental factors. Med Sci Sports Exerc 2004;36:1559-1566.
41. Volkman SK, Galecki AT, Burke DT, Miller RA, Goldstein SA: Quantitative trait loci that modulate femoral mechanical properties in a genetically heterogeneous mouse population. J Bone Miner Res 2004;19:1497-1505.
42. Lang DH, Sharkey NA, Mack HA, Vogler GP, Vandenbergh DJ, Blizard DA, Stout JT, McClearn GE: Quantitative trait loci analysis of structural and material skeletal phenotypes in C57BL/6J and DBA/2 second-generation and recombinant inbred mice. J Bone Miner Res 2005;20:88-99.
43. Li X, Masinde G, Gu W, Wergedal J, Hamilton-Ulland M, Xu S, Mohan S, Baylink DJ: Chromosomal regions harboring genes for the work to femur failure in mice. Funct Integr Genomics 2002;1:367-374.
44. Yershov Y, Baldini TH, Villagomez S, Young T, Martin ML, Bockman RS, Peterson MG, Blank RD: Bone strength and related traits in HcB/Dem recombinant congenic mice. J Bone Miner Res 2001;16:992-1003.

Table-1 Changes in the bone parameters in response to 12 days of sham-bending at 9N load in 10-week female B6 mice.

	Mean ± SD

Bone parameters	Non-loaded	Loaded	p-value
Total Area, mm^2	2.01 ± 0.11	2.07 ± 0.10	0.30
Total Mineral content, mg/mm	1.08 ± 0.04	1.10 ± 0.04	0.46
Periosteal. Circum, mm	5.02 ± 0.14	5.10 ± 0.12	0.29
Endosteal. Circum, mm	4.09 ± 0.15	4.17 ± 0.12	0.31
Total vBMD, mg/cm^3	649 ± 14.64	663.7 ± 19.7	0.15
Cortical vBMD, mg/cm^3	1031 ± 9.8	1038 ± 13.5	0.26

N=7

Table-2 Significant and suggestive QTLs for the mechanical load-induced phenotypes in the B6xC3H F2 female mice.

Phenotype	Chromosome	Locus	cM	LOD score	% Variation
Total vBMD	1	D1Mit113	91.8	3.4[a]	5.5
	8	D8Mit88	60.1	4.2[a]	8.5
	9	D9Mit336	33.9	2.5[c]	4.8
Cortical vBMD	1	D1Mit113	91.8	2.3[c]	3.6
	3	D3Mit320	50.3	3.6[a]	7.3
	9	D9Mit355	49.2	2.5[c]	3.4
Periosteal circumference	8	D8Mit49	68.9	3.0[b]	4.3
	9	D9Mit97	24	2.2[c]	3.3
	11	D11Mit333	69.9	2.1[c]	3.3
	18	D18Mit64	0	3.0[b]	4.4
Cortical thickness	8	D8Mit88	60.1	3.6[a]	5.7
	9	D9Mit2	13.1	3.0[b]	3.2
	11	D11Mit333	69.9	2.5[c]	4.2
	17	D17Mit93	39.3	3.0[b]	4.2

[a]The threshold for the highly significant LOD score is $p<0.01$
[b]The threshold for the significant LOD score is $p<0.05$
[c]The threshold for the suggestive LOD score is $p<0.1$
Variances explained are from the peak LOD score in each phenotype

Table-3 List of significant marker pairs showing interaction from genome-wide analysis of multiple phenotypes in B6xC3H F2 female mice.

Phenotype	Chr pairs	cM1	cM2	LOD Full	LOD Int	p-value (interaction)
Total vBMD	8 × 13	60	45	9.10	2.96	0.008
	1 × 13	90	45	7.57	2.65	0.01
Cortical vBMD	1 × 3	75	55	8.72	2.17	0.04
CT	5 × 8	80	10	7.41	4.50	0.004

For vBMD full LOD score threshold (effect of both markers in affecting the bone phenotype) significant was 7.68 ($p<0.05$) and for cortical vBMD full LOD score threshold significant was 7.95 ($p<0.05$). Suggestive threshold was 7.32 ($p<0.1$) for vBMD and 6.83 ($p<0.6$) for CT Full LOD score effect.

Table-4 Significant and suggestive QTLs for the non-loaded phenotypes in the B6xC3H F2 female mice.

Phenotypes	Chromosome	Locus	cM	LOD score	% Variation
Total vBMD	1	D1Mit380	37.1	3.8[a]	5.3
		D1Mit106	83.1	2.8[c]	3.9
	2	D2Mit1*	14.2	2.3[c]	4.6
	3	**D3Mit147**	**59.0**	**2.8[c]**	**3.9**
	4	D4Mit251	66.7	3.6[a]	5.4
	6	D6Mit209*	16.9	2.9[c]	4.8
	10	**D10Mit233**	**63.4**	**3.8[a]**	**5.3**
	12	D12Mit16*	44.5	3.3[a]	5.9
	16	D16Mit60	24.0	2.9[c]	4.0
	17	**D17Mit93**	**39.0**	**5.4[a]**	**7.4**
Cortical vBMD	1	D1Mit380	37.2	2.7[c]	3.8
	3	**D3Mit147**	**59.1**	**3.2[a]**	**4.6**
	10	**D10Mit95**	**50.3**	**3.0[b]**	**4.2**
	12	D12Mit16*	40.5	2.9[c]	5.7
	15	D15Mit107	41.5	3.0[b]	4.5
	16	D16Mit60	24.0	3.6[a]	4.9
	17	**D17Mit93**	**39.3**	**5.9[a]**	**8.0**
Periosteal circumference	**3**	**D3Mit320***	**46.4**	**4.0[a]**	**7.2**
	10	**D10Mit233***	**57.3**	**2.4[c]**	**3.9**
	11	**D11Mit285**	**49.2**	**4.3[a]**	**6**
	15	**D15Mit107**	**41.5**	**3.1[b]**	**4.7**
	16	**D16Mit60**	**24.0**	**3.1[b]**	**4.3**
	17	**D17Mit93**	**39.3**	**5.1[a]**	**7**
Cortical thickness	**1**	**D1Mit380**	**37.2**	**5.9[a]**	**8**
		D1Mit106	**83.1**	**5.4[a]**	**7.3**
	3	**D3Mit147***	**55.3**	**2.5[c]**	**4.2**
	10	**D10Mit233**	**63.4**	**3.7[a]**	**5.1**
	16	**D16Mit60**	**24.0**	**3.1[b]**	**4.2**
	17	**D17Mit93**	**39.3**	**4.7 [a]**	**6.5**
	18	**D18Mit12**	**9.8**	**2.7[c]**	**3.8**
	19	**D19Mit28***	**9.8**	**2.8[c]**	**6**

[a]The threshold for the highly significant LOD score is p<0.01
[b]The threshold for the significant LOD score is p<0.05
[c]The threshold for the suggestive LOD score is p<0.1
Novel QTLs are highlighted in bold
* Corresponds to marker closer to the peak LOD score

FIGURE LEGEND

Figure 1: Distribution of percentage changes for (A) Total vBMD, (B) Cortical vBMD, (C) PC, and (D) cortical thickness in the F2 population after two weeks of four-point bending. The x-axis represents the percentage change ('–'indicates reduction) and y-axis represents the number of observations (mice). Total vBMD, Total volumetric bone mineral density; cortical vBMD, cortical volumetric bone mineral density; Log PC, Periosteal circumference; and CTh, Cortical thickness. The solid line represents theoretical normal distribution. Based on kolmogorov-smirnov test, total vBMD, cortical vBMD, PC and CTh show normal distribution (n=329).

Figure 2: Genome-wide scan for percent change in (a) Total vBMD, (b) Cortical vBMD and (c) PC and (d) CTh induced by mechanical loading in the F2 population of B6xC3H intercross. The y-axis indicates LOD score and x-axis represent chromosomes. The solid line indicates genome-wide thresholds for significant QTL and broken links indicate thresholds for suggestive QTL.

Figure 3: Detailed map for chromosomes 8, 1 and 3 showing significant QTLs for total vBMD, cortical thickness and cortical vBMD. LOD scores between markers were determined using Pseudomarker MAINSCAN program with a default setting of 2.5cM between steps. The marker positions are highlighted as vertical lines in the x-axis. Posterior probability density (shown on right y-axis) plots allow best estimate of putative QTL position on the marker map.

Figure 4: Effect of B6 vs. C3H alleles at the major QTLs affecting total vBMD and bone size phenotypes on chromosome 1 and 8. Significant differences ($p<0.01$) are indicated by the lowercase letters, where “a” indicates the B6 or C3H allele is significantly different than mice with C3H or B6 allele and “b” indicates that the B6 or C3H allele differs from mice with B6C3H allele. The values shown here are mean ± SD. The y-axis represents percent change of vBMD and PC in the F2 population and x-axis represents mouse genotypes. The total number of mice was 329 but due to missing data the number of genotype marker data varied.

Figure 5: Genome-wide scan associated with non-loaded (a) Total vBMD, (b) Cortical vBMD, (c) PC and (d) CTh in the F2 population of B6-C3H intercross. The y-axis indicates LOD score and x-axis represents chromosomes. The solid line indicates genome-wide threshold for significant QTL and broken lines indicate thresholds for suggestive QTL.

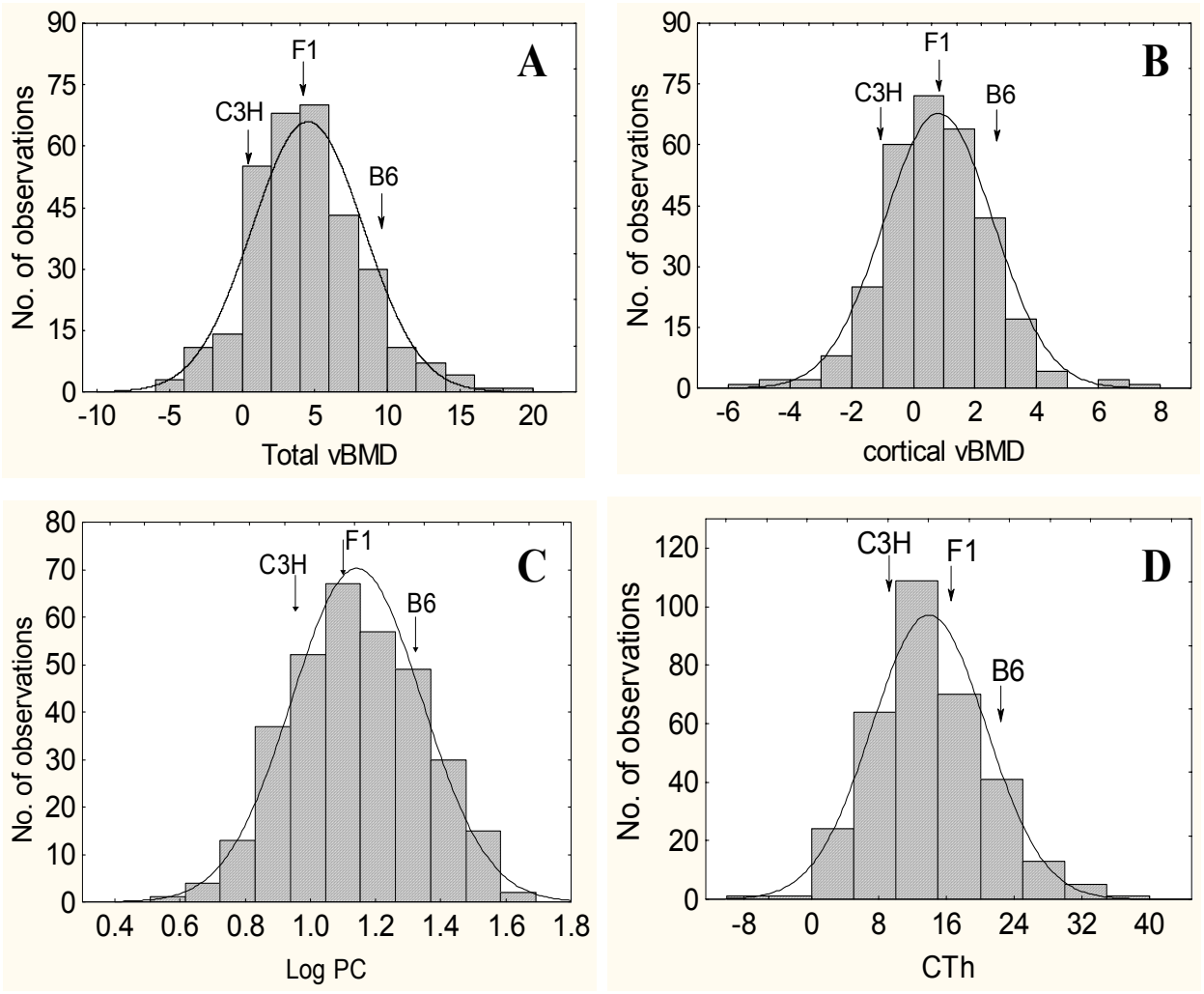
A
No. of observations
Total vBMD
C3H
F1
B6
B
cortical vBMD
C
Log PC
D
CTh

Figure 1

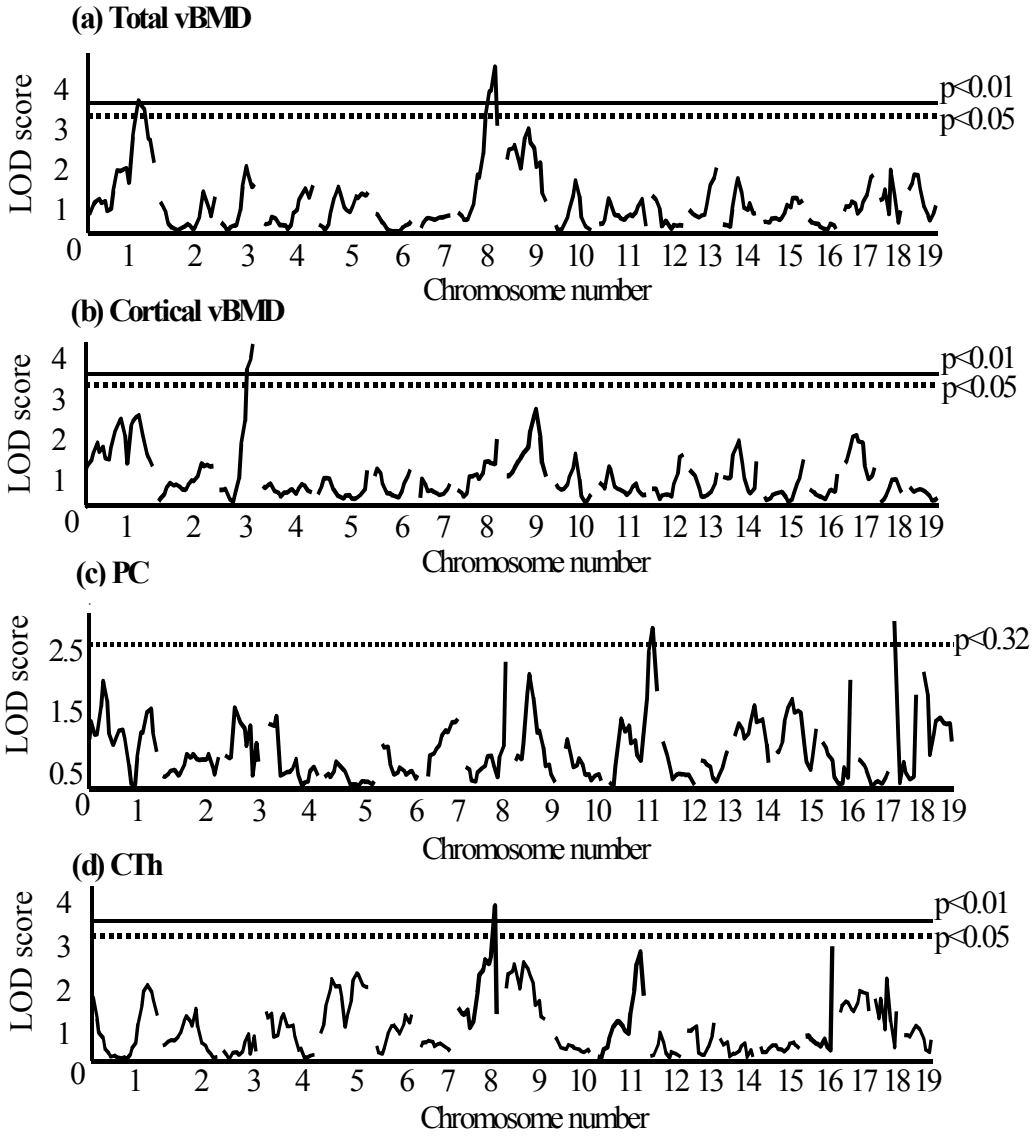
(a) Total vBMD
LOD score
p<0.01
p<0.05
Chromosome number
(b) Cortical vBMD
LOD score
p<0.01
p<0.05
Chromosome number
(c) PC
LOD score
p<0.32
Chromosome number
(d) CTh
LOD score
p<0.01
p<0.05
Chromosome number

Figure 2

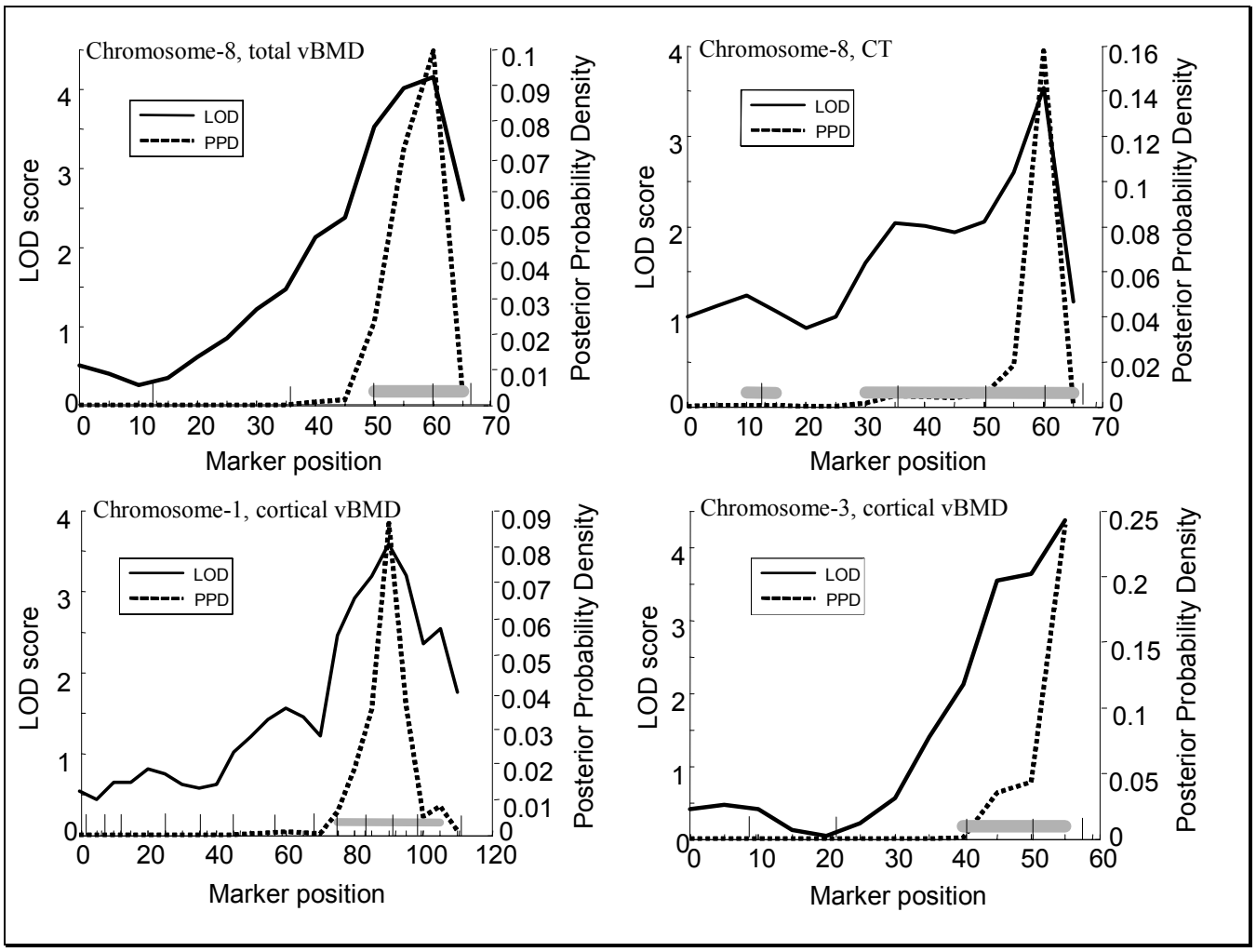
Chromosome-8, total vBMD
LOD
PPD
LOD score
Posterior Probability Density
Marker position
Chromosome-8, CT
LOD
PPD
LOD score
Posterior Probability Density
Marker position
Chromosome-1, cortical vBMD
LOD
PPD
LOD score
Posterior Probability Density
Marker position
Chromosome-3, cortical vBMD
LOD
PPD
LOD score
Posterior Probability Density
Marker position

Figure 3

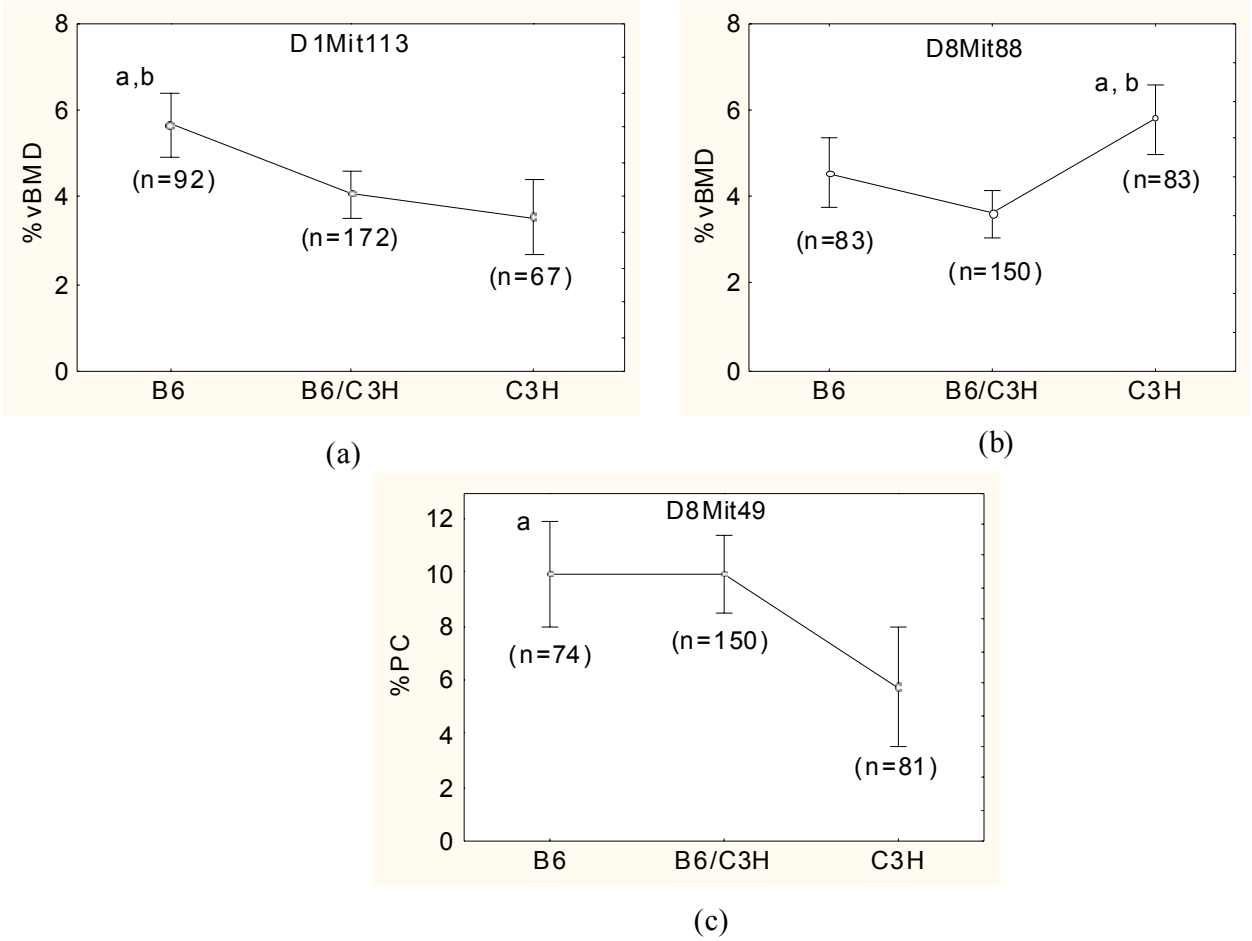
D1Mit113
a,b
(n=92)
(n=172)
(n=67)
%vBMD
B6
B6/C3H
C3H
(a)
D8Mit88
a, b
(n=83)
(n=150)
(n=83)
%vBMD
B6
B6/C3H
C3H
(b)
D8Mit49
a
(n=74)
(n=150)
(n=81)
%PC
B6
B6/C3H
C3H
(c)

Figure 4

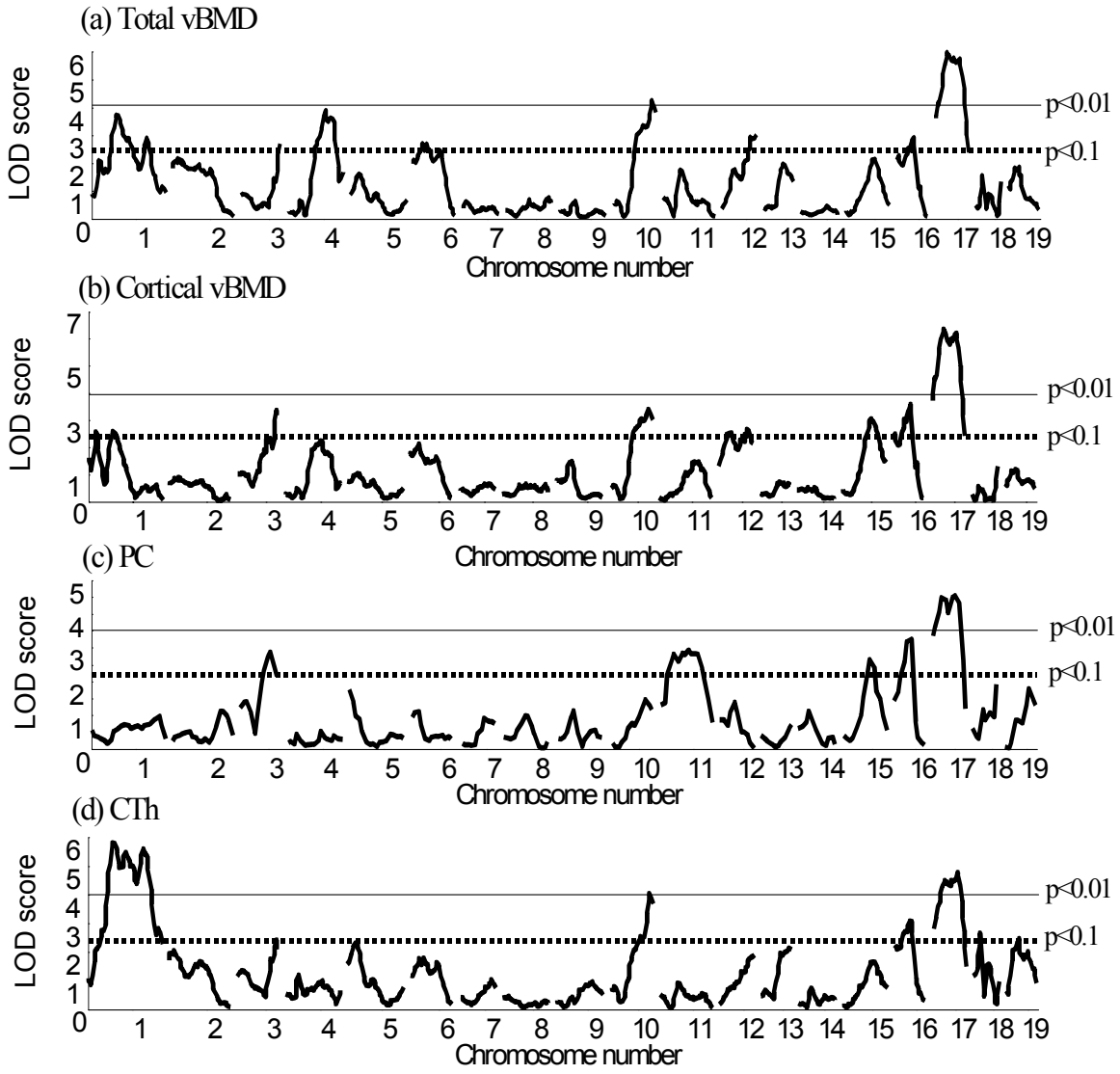
(a) Total vBMD
LOD score
p<0.01
p<0.1
Chromosome number
(b) Cortical vBMD
LOD score
p<0.01
p<0.1
Chromosome number
(c) PC
LOD score
p<0.01
p<0.1
Chromosome number
(d) CTh
LOD score
p<0.01
p<0.1
Chromosome number

Figure 5

Appendix-2

Novel Mechanoresponsive BMD and Bone Size QTL Identified in a Genome Wide Linkage Study Involving C57BL/6J-C3H/HeJ Intercross

Chandrasekhar Kesavan[1], Subburaman Mohan[1, 2], Hongrun Yu[1], Susanna Kapoor[1], Jon E Wergedal[1, 2] and David J Baylink[1, 2]

[1]Musculoskeletal Disease Center, VA Loma Linda Healthcare System, Loma Linda, CA.
[2]Department of Medicine, Loma Linda University, Loma Linda, CA.

Abstract

Previously, we demonstrated that 2 wks of 4-point bending caused a dramatic 15% increase in volumetric BMD (vBMD) in the tibia of C57BL/6J (B6), but not C3H/HeJ (C3H) mice. To identify the genetic loci that contribute to variation in BMD response to mechanical loading (ML), we performed a genome-wide linkage study in the B6-C3H mice intercross. The left tibias of 329 B6xC3H F2 female mice at 10 wks age were subjected to 9 N cyclic load at 2Hz for 36 cycles daily for 2 wks while right tibia was used as unloaded control. Two days after the last loading, vBMD and bone size (periosteal circ.) were measured by pQCT. ML-induced changes ([loaded-unloaded/unloaded] X 100) in vBMD (-5 to +15%) and bone size (-5 to +20%) in the B6-C3H F2 mice showed normal distributions consistent with the complex traits controlled by several genes. % change in BMD or bone size in the F2 mice of loaded bones did not correlate with body wt, suggesting that variation in bone anabolic response to ML is independent of body size. Genome-wide search using 111 microsatellite markers with 15 cM intervals in the F2 mice revealed the following ML QTLs for BMD and bone size phenotypes (% change in loaded vs unloaded bone) using MAPQTL program (a=p<0.01; b=p<0.05):

Phenotype	Locus	LOD Score	% Variation
vBMD	D1Mit113	3.4 [a]	4.7
vBMD	D8Mit88	4.2 [a]	5.8
vBMD	D9Mit336	2.5 [b]	3.5
Bone Size	D8Mit49	3.0 [b]	4.1
Bone Size	D9Mit97	2.8 [b]	3.9
Bone Size	D11Mit333	2.6 [b]	3.6
Bone Size	D18Mit64	2.8 [b]	3.5

We found that ML BMD QTL for Chr. 8 and 9 and bone size QTL for Chr. 8 and 18 could not be detected using phenotype data from unloaded bones, suggesting that these QTLs are unique to ML phenotypes. Furthermore, chromosome 8 BMD QTL has not been reported for BMD in any other inbred strain crosses. Conclusions: 1) Our study provides the first demonstration of chromosomal location of genetic loci affecting variation in skeletal anabolic response to ML in the B6-C3H intercross. 2) Only 15 % of the genetic variation was accounted for by the

identified ML QTL suggesting additional QTL or interactions exist. 3) Future identification of the genes responsible for the ML QTL should lead to improved understanding of molecular pathways for ML-induced skeletal anabolic response.

Appendix-3

Quantitative Trait loci for Tibia Periosteal Circumference in the C57BL/6J-C3H/HeJ mice intercross

Chandrasekhar. K, Baylink DJ, Susanna K, Wergedal JE, Hongrun Yu and Mohan S
[1]Musculoskeletal Disease Center, VA Loma Linda Healthcare System, Loma Linda, CA.
[2]Department of Medicine, Loma Linda University, Loma Linda, CA.

Bone size is an important determinant of bone strength and is a risk factor for osteoporotic fractures in humans. Bone size is highly variable and heritable, as evidenced by studies in humans. The present study was undertaken to test the hypotheses that: 1) bone size is a complex trait controlled by multiple genes; and 2) bone size that differs in different skeletal sites is regulated by common and bone specific QTL. We performed a genome-wide linkage study using B6 and C3H inbred strains of mice that have extreme differences in bone size. Previously, for a mechanical loading study, we generated 329 female F2 mice from the B6-C3H intercross. We used the non-loaded left tibia to identify bone size QTL. At 12-weeks, *in vivo* pQCT was performed and periosteal circumference (PC) was measured. A genome-wide scan was performed using 111 micro-satellite markers in DNA samples collected from the liver of the 329 F2 mice. The heritability response for the PC was 73%. The range of PC was 3.93 to 6.08 mm and after adjusting with body weight was 0.19 to 0.30 mm in F2 mice. There was a normal distribution of PC values in the F2 mice. Presence of a significant correlation between bone size and body weight suggested that some of the QTL obtained for PC are the same for body weight. After adjusting with body weight, interval mapping revealed that bone size was influenced by five significant loci and one suggestive loci, as shown below.

Trait	Chr	Marker	cM	LOD	Variance %	Alleles contributed by
Bone size	3	D3Mit320*	46.4	4.0[a]	7.2	C3H
	10	D10Mit233*	57.3	2.4[c]	3.9	C3H
	11	D11Mit285	49.2	4.3[a]	6	B6
	15	D15Mit107	41.5	3.1[b]	4.7	B6
	16	D16Mit60	24.0	3.1[b]	4.3	B6
	17	D17Mit93	39.3	5.1[a]	7	C3H

Highly [a] significant LOD score ($p<0.01$), [b] significant LOD score ($p<0.05$) and [c] suggestive LOD score ($p<0.1$), * Marker closest to the peak LOD score.

Chr 17 showed the highest significance after adjustment with bodyweight. Pairwise analysis showed the presence of several significant interactions between loci on Chrs 1, 2, 4, 12, and 14 for the bone size trait. In summary, novel Chr 3 QTL specific for tibia size regulation and known QTL (Chr 10, 11, 15, 16, and 17) have been identified for PC trait in B6-C3H F2 mice. The known QTL are also involved in regulating BMD, thus suggesting that the genes in these QTL may regulate multiple phenotypes. Chr 10 and Chr 11 have been identified in multiple strain crosses, thus suggesting the importance of this QTL in bone size regulation. In conclusion, QTL identified for bone size are the same as QTL previously identified for femur, suggesting that the same mechanisms are involved in the regulation of bone size in both femur and tibia.

Appendix-4

THE JOURNAL OF BIOLOGICAL CHEMISTRY VOL. 281, NO. 14, pp. 9576–9588, April 7, 2006
Printed in the U.S.A.

Up-regulation of the Wnt, Estrogen Receptor, Insulin-like Growth Factor-I, and Bone Morphogenetic Protein Pathways in C57BL/6J Osteoblasts as Opposed to C3H/HeJ Osteoblasts in Part Contributes to the Differential Anabolic Response to Fluid Shear*[S]

Received for publication, August 22, 2005, and in revised form, January 13, 2006 Published, JBC Papers in Press, February 3, 2006, DOI 10.1074/jbc.M509205200

Kin-Hing William Lau[1], **Sonia Kapur, Chandrasekhar Kesavan, and David J. Baylink**

From the Musculoskeletal Disease Center, Jerry L. Pettis Memorial Veterans Affairs Medical Center, and the Department of Medicine, Loma Linda University, Loma Linda, California 92357

C57BL/6J (B6), but not C3H/HeJ (C3H), mice responded to mechanical loading with an increase in bone formation. A 30-min steady fluid shear of 20 dynes/cm^2 increased [^{3}H]thymidine incorporation and alkaline phosphatase activity and up-regulated the expression of early mechanoresponsive genes (integrin β1 (*Igtb1*) and cyclooxygenase-2 (*Cox-2*)) in B6 but not C3H osteoblasts, indicating that the differential mechanosensitivity was intrinsic to osteoblasts. In-house microarray analysis with 5,500 gene fragments revealed that the expression of 669 genes in B6 osteoblasts and 474 genes in C3H osteoblasts was altered 4 h after the fluid shear. Several genes associated with the insulin-like growth factor (IGF)-I, the estrogen receptor (ER), the bone morphogenetic protein (BMP)/transforming growth factor-β, and Wnt pathways were differentially up-regulated in B6 osteoblasts. *In vitro* mechanical loading also led to up-regulation of these genes in the bones of B6 but not C3H mice. Pretreatment of B6 osteoblasts with inhibitors of the Wnt pathway (endostatin), the BMP pathway (Noggin), or the ER pathway (ICI182780) blocked the fluid shear-induced proliferation. Inhibition of integrin and Cox-2 activation by echistatin and indomethacin, respectively, each blocked the fluid shear-induced up-regulation of genes associated with these four pathways. In summary, up-regulation of the IGF-I, ER, BMP, and Wnt pathways is involved in mechanotransduction. These four pathways are downstream to the early mechanoresponsive genes, *i.e. Igtb1* and *Cox-2*. In conclusion, differential up-regulation of these anabolic pathways may in part contribute to the good and poor response, respectively, in the B6 and C3H mice to mechanical loading.

Mechanical loading is essential for maintenance of skeletal architectural integrity. Loading stimulates bone formation and suppresses bone resorption, leading to an overall increase in bone mass (1), whereas unloading results in an overall decrease in bone mass, because of an inhibition of formation along with an increase in resorption (2). Loading produces strains in the mineralized matrix of bone, which generates interstitial fluid flow through lacunar/canalicular spaces (3). This fluid flow exerts a shear stress at surfaces of osteoblasts and osteocytes lining these spaces, which generates biochemical signals to produce biological effects. Multiple interacting signaling pathways are involved in translating the fluid shear signals into biological effects in bone cells (4), and these pathways are collectively referred to as the mechanotransduction mechanism. Mechanical loading is a key regulatory process for bone mass and strength (5). Knowledge of the mechanotransduction mechanism would not only yield information about the mechanical stimulation of bone formation but would also provide insights into the pathophysiology of osteoporosis and other bone-wasting diseases.

There is increasing evidence that genetics play a major part in determining the bone response to mechanical loading. Studies from our group (6, 7) and others (8, 9) demonstrate that C57BL/6J (B6)[2] inbred mice responded to *in vivo* mechanical loading with an increased bone formation, but C3H/HeJ (C3H) mice showed no such response. We postulate that the differential osteogenic response to mechanical stress in B6 and C3H inbred strains of mice is intrinsic to bone cells and that comparative global gene expression profiling studies in osteoblasts derived from this pair of inbred mouse strains in response to fluid shear could provide information concerning potential signaling pathways involved in the mechanical stimulation of bone formation. This would also yield important information about the identity of mechanosensitivity genes that determine the good and poor mechanical response in bone formation, respectively, in B6 and C3H mice.

The objectives of this study were 4-fold and are as follows: 1) to confirm that the differential anabolic response to mechanical loading in B6 and C3H strains of mice is intrinsic to osteoblasts, using an *in vitro* fluid flow shear stress model as a surrogate of mechanical loading (4); 2) to perform in-house microarray analyses in isolated B6 and C3H osteoblasts to identify potential signaling pathways that in part contribute to the differential osteogenic response; 3) to confirm that the pathways-of-interest are essential for fluid shear-induced cell proliferation; and 4) to determine the relationship between the pathways-of-interest and the early mechanoresponsive gene products, such as integrins and cyclooxygenase-2 (*Cox-2*).

* This work was supported in part by a special appropriation to the Jerry L. Pettis Memorial Veterans Affairs Medical Center, Musculoskeletal Disease Center, and by a Merit Review provided by the Office of Research and Development, Medical Research Service, Department of Veteran Affairs, and in part by Assistance Award DAMD17-01-1-0744 provided by The United States Army Medical Research Acquisition Activity (Fort Detrick MD 21702-5014). The costs of publication of this article were defrayed in part by the payment of page charges. This article must therefore be hereby marked "*advertisement*" in accordance with 18 U.S.C. Section 1734 solely to indicate this fact.

[S] The on-line version of this article (available at http://www.jbc.org) contains supplemental Tables 1–3.

[1] To whom correspondence should be addressed: Musculoskeletal Disease Center (151), Jerry L. Pettis Memorial Veterans Affairs Medical Center, 11201 Benton St., Loma Linda, CA 92357. Tel.: 909-825-7084 (ext. 2836); Fax: 909-796-1680; E-mail: William.Lau@med.va.gov.

[2] The abbreviations used are: B6, C57BL/6J inbred mice; ALP, alkaline phosphatase; BMP, bone morphogenetic protein; C3H, C3H/HeJ inbred mice; Cox-2, cyclooxygenase-2; ER, estrogen receptor; Erk1/2, extracellular signal-regulated kinases 1/2; pErk1/2, phosphorylated Erk1/2; EST, expressed sequence tag; IGF-I, insulin-like growth factor-I; TGF-β, transforming growth factor-β; Wnt, wingless- and int-related protein.

Supplemental Material can be found at:
http://www.jbc.org/cgi/content/full/M509205200/DC1

EXPERIMENTAL PROCEDURES

Materials—Tissue culture plasticware was obtained from Falcon (Oxnard, CA). Dulbecco's modified Eagle's medium was from Mediatech, Inc. (Herndon, VA). Bovine calf serum was from HyClone (Logan, UT). Trypsin and EDTA were products of Irvine Scientific (Santa Ana, CA). [^{3}H]Thymidine (48 Ci/mmol) was obtained from Research Products International (Mount Prospect, IL). Anti-pErk1/2, anti-pan-Erk1/2, anti-β-catenin, anti-integrin β1, anti-Cox-2, and anti-actin antibodies were from Santa Cruz Biotechnology (Santa Cruz, CA), Upstate Biotechnology, Inc. (Lake Placid, NY), or BD Transduction Laboratories. Echistatin, endostatin, and indomethacin were products of Sigma. ICI182780 was purchased from Tocris (Ellisville, MO), and Noggin was obtained from R&D Systems (Minneapolis, MN). Other chemicals were of molecular biology grade and were from Fisher or Sigma.

Cell Culture and Fluid Shear Stress Experiments—Osteoblasts, isolated from calvarias or long bones of 8-week-old B6 and C3H mice by collagenase digestion as described previously for neonatal calvarial osteoblasts (10), were maintained in Dulbecco's modified Eagle's medium supplemented with 10% bovine calf serum. Pilot studies indicated that cell passage, up to passage 7, had no significant effects on the responsiveness of primary B6 mouse osteoblasts to fluid shear stress with respect to [^{3}H]thymidine incorporation, alkaline phosphatase (ALP) specific activity, and Erk1/2 phosphorylation. Accordingly, cells of passages 3–6 were used in this study.

50,000 cells were plated on each glass slide. At ~80% confluency, the cells were serum-deprived for 24 h and subjected to a steady fluid shear stress of 20 dynes/cm^2 for 30 min in the Cytodyne flow chamber as described previously (4). This dosage of fluid shear stress is believed to be within the physiologically relevant range of laminar shear stress produced by the circulation (11). Replicate glass slides of cells were placed in a parallel flow chamber but without the fluid shear stress as static controls in each experiment.

To test the potential involvement of a given signaling pathway-of-interest, cells were pretreated with a specific inhibitor of the pathway-of-interest (*i.e.* ICI182780 for the estrogen receptor (ER) pathway, endostatin for the canonical wingless- and int-related protein (Wnt) pathway, and Noggin for the bone morphogenetic protein (BMP) pathway), for 24 h prior to the fluid shear stress. To assess the role of integrin activation and Cox-2 on the up-regulation of these pathways, cells were pretreated with echistatin or indomethacin, respectively, for 2 h prior to the fluid shear stress.

[^{3}H]Thymidine Incorporation Assay—Cell proliferation was assessed by [^{3}H]thymidine incorporation during the final 6 h of the 24-h post-exposure to fluid shear as described previously (4, 12).

Cellular ALP Specific Activity Assay—Osteoblast differentiation was measured by the increase in the specific activity of ALP 24 h post-exposure to the shear stress as described previously (4, 13). The ALP-specific activity (*i.e.* normalized against cellular protein content) was reported to adjust for the difference in the cell number because of the increase in cell proliferation in response to fluid shear.

Western Immunoblot Assays—Cellular integrin β1, Cox-2, and β-catenin were determined by Western immunoblot assays were performed as described previously (4) using respective commercial polyclonal antibodies and normalized against each corresponding cellular actin level. The relative cellular phosphorylated Erk1/2 (pErk1/2) level (an index of Erk1/2 activation) was determined with the phospho-specific antibody against pErk1/2 and normalized against corresponding total Erk1/2 level, determined with anti-pan-Erk1/2 polyclonal antibody.

RNA Purification—Total RNA of cells on each slide was extracted with Qiagen mini RNA kit (Qiagen, Valencia, CA). The purity and integrity of each RNA sample was confirmed with Bio-analyzer (Agilent, Palo Alto, CA). Only undegraded RNA samples were used in this study.

In-house Microarray Hybridization and Data Analysis—For the preparation of our in-house microarray chips, cDNA inserts of 5,500 cDNA clones of mouse, rat, human, or monkey genes or ESTs (largely mouse and human genes) were isolated, purified, and evaluated with agarose gel electrophoresis. The microarrays were printed on aminosilane-coated microscope slides (Corning, NY) with a GMS 417 Arrayer (Genetic MicroSystems, Santa Clara, CA). Six replicates of each clone were printed on each slide. DNA was fixed to the slides by baking at 80 °C for 2 h.

The experimental strategy and analyses of the microarray experiment are described briefly as follows. Primary osteoblasts isolated from B6 or C3H inbred strain of mice were plated on glass slides and subjected to a 30-min steady shear stress as described above. Replicate plates of B6 or C3H osteoblasts were placed in the flow chamber without the fluid shear as the static control. Four hours after the fluid shear, total RNA was isolated. cDNA synthesized from 1 μg of total RNA of cells received the fluid shear, and corresponding static control cells were each fluorescently labeled with Cy5 and Cy3, respectively, as previously described (14). The microarray hybridization was performed as described previously (14). The slide was scanned using a ScanArray 4000 scanner (GSI Lumonics, San Jose, CA). The fluorescent images were acquired using ScanArray software (version 2.1; GSI Lumonics), and data were analyzed using GeneSpring Image Analysis program (Silicon Genetics, San Jose, CA). Each array spot was individually inspected using the GeneSpring Image Analysis program. The microarray analysis was repeated in osteoblasts of four pairs of B6/C3H mice. Statistically significant differences in gene expression between each pair of stressed and corresponding static control samples was analyzed using Lowess Normalization and paired t test. Differences of $p < 0.05$ were considered significant. Only known mouse genes were analyzed further. Because the gene annotation or accession numbers of many of the known mouse genes on our array were missing, the computer-based gene ontology and pathway analyses were not performed. Tentative classification of gene functions was determined manually based on information available on the PubMed data base.

Real Time PCR Analyses—Real time PCR was carried out with the SYBR Green method on the MJ Research DNA Engine Opticon® 2 System (Waltham, MA). The purified total RNA was used to synthesize cDNA by reverse transcription using random hexamer primers and Superscript II reverse transcriptase (Invitrogen). The cDNA was then subjected to real time PCR amplification using the gene-specific primers listed in Table 1. The primers were designed with the IDT Vector NTI software (Coralville, IA). An aliquot (25 μl) of reaction volume (consisted of 2× (12.5 μl) QuantiTect SYBR Green PCR master mix, which contained the Hot Start *Taq* polymerase (Qiagen), 0.5 μM of primers, and 1–5 μl of cDNA template) was used in each assay. The PCR conditions consisted of an initial 10-min hot start at 95 °C, followed by 40 cycles of denaturation at 95 °C for 30 s, annealing, and extension at appropriate temperature (50–72 °C) (see Table 1) for 30 s, and a final step of melting curve analysis from 60 to 95 °C. Each reaction was performed in triplicate. The data were analyzed using Opticon® Monitor Software 2.0. Data normalization was performed against β-actin, and the normalized values were used to calculate the relative fold change between the control and the experiment groups by the threshold cycle method.

In Vivo Mechanical Loading Model—We adapted the four-point bending exercise regimen, originally developed by Akhter *et al.* (15) on rat tibia, as the *in vivo* mechanical loading model for mouse tibia as

TABLE 1
List of primer sets used in the real-time PCR amplification reactions

Gene	Primer sequences	Annealing temperature	Extension temperature
		°C	
β-Actin	Forward primer, 5′-CAG GCA TTG CTG ACA GGA TG-3′ Reverse primer, 5′-TGC TGA TCC ACA TCT GCT GG-3′	56	72
Tgfb1	Forward primer, 5′-CGG CAG CTG TAC ATT GAC TT-3′ Reverse primer, 5′-TGT GTT GGT TGT AGA GGG CA-3′	53	72
Ctnnb1	Forward primer, 5′-GAC TCA CGC AGT GAA GAA TG-3′ Reverse primer, 5′-GCT GTA GCA GGT TCA CTA GA-3′	50	72
Bmpr1	Forward primer, 5′-GCT TAT TCT GCT GCT TGT GGG-3′ Reverse primer, 5′-ATT TAA CAG CTA GGC CCA GG-3′	53	72
Igf1r	Forward primer, 5′-GCC AAC AAG TTC GTC CAC AG-3′ Reverse primer, 5′-CCG AAG GAC CAG ACA TCA GA-3′	56	72
Wnt1	Forward primer, 5′-GGT GTT GCG GTT CCT GAT GT-3′ Reverse primer, 5′-TCC GAG GCA GAG ACA AGG AG-3′	54	72
Wnt3a	Forward primer, 5′-ATA GCC TGC ATC CGC TCT GA-3′ Reverse primer, 5′-TGG TGA CCA TTG CCT CAA CA-3′	54	72
Wnt5a	Forward primer, 5′-AAC TGC AGC ACA GTG GAC AA-3′ Reverse primer, 5′-TAG TCG ATG TTG TCT CCG CA-3′	54	72
Axin	Forward primer, 5′-TCT GGA TAC CTG CCC ACT TT-3′ Reverse primer, 5′-TGC CTT CGT TGT ACC GTC TA-3′	54	72
Lef1	Forward primer, 5′-ACG GAC AGT GAC CTA ATG CA-3′ Reverse primer, 5′-TCT CCT TTA GCG TGC ACT CA-3′	54	72
Lrp5	Forward primer, 5′-ACA CTA TAT CCG CCG ATC CT-3′ Reverse primer, 5′-GAC TGG TGC TGT AGT CAC TG-3′	53	72
Esr1	Forward primer, 5′-ATG TGC AGG AGG CAG ACA TT-3′ Reverse primer, 5′-TGG AGC CTG CTT GGA GTT AT-3′	56	72
Ncoa1	Forward primer, 5′-GCA CAG CCA GGA GTG TAC AA-3′ Reverse primer, 5′-GAC GAG AGC TGG TTG CAG TA-3′	56	72
Dlx1	Forward primer, 5′-GGA CCG GAC CAG ACT CTC AT-3′ Reverse primer, 5′-GTG GCT CAG ACC TGG TGA CT-3′	56	72
c-*Fos*	Forward primer, 5′-CCT GAG GTC TTT CGA CAT GTG GAA-3′ Reverse primer, 5′-AAG AGA GCA AGA AGG TGG TCG CAT-3′	56	72

described previously (16). Briefly, the four-point bending device (Instron, Canton, MA) consisted of two upper vertically movable points covered with rubber pads (4-mm apart), and two 12-mm lower non-movable points covered with rubber pads. During the bending exercise, the two upper pads touched the lateral surface of the tibia through overlying muscle and soft tissue, whereas the lower pads touched the medial surface of the proximal and distal parts of the tibia. The loading protocol consisted of a 9-newton load at a frequency of 2 Hz for 36 cycles, and the exercise was performed once daily. The right tibia was subjected to the loading exercise, and the left tibia was used as an internal unloaded control. Upon anesthesia with halothane, the ankle of the tibia was positioned on the second lower immobile points of the Instron equipment, such that the region of the tibia loaded did not vary from mouse to mouse. The loading was applied for 6 days/week with 1 day of rest for 2 weeks. Forty eight h after the final loading, mice were sacrificed. The marrow-flushed tibias were stored at −80 °C until RNA extraction. The animal protocol was approved by the Institutional Animal Care and Use Committee of the J. L. Pettis Memorial Veterans Affairs Medical Center.

One of the potential limitations of this model is that force applied over the soft tissues may have local bruising effects that could result in inflammation. Accordingly, extra efforts were taken to minimize the bruising effect of loading on soft and hard tissues by changing the rubber pads frequently. We also looked for histological evidence for inflammation (*i.e.* presence of inflammatory cells and/or blood clots) in the loaded muscles and bones after the loading regimen in several mice in preliminary experiments, and we found no evidence for the presence of lymphocytes or other inflammatory cells in the muscle and bone tissues at the loading sites in all samples examined. We also found no evidence of blood clotting at the loading limb.

RNA Extraction from Bones—Briefly, bones were pulverized in liquid nitrogen. Total RNA was purified with Trizol reagent (Invitrogen), followed by RNeasy columns (Qiagen). The quality and quantity of RNA were analyzed using Bio-analyzer and Nano-drop instrumentation, respectively. Only good quality RNAs were used for subsequent real time PCR analyses.

Bone Histomorphometry—Both the loaded and unloaded (control) tibiae of B6 and C3H mice were removed, after euthanasia, and fixed with 10% cold neutral buffered formalin on ice. The fixed bones were then rinsed free of formalin, defleshed, and embedded in methyl methacrylate (17). Thick (0.5 mm) cross-sections were cut from the mid-diaphysis of the tibia with a wire saw (Delaware Diamond Knives), lightly ground, and stained with Goldner's trichrome stain for mineralized bone. The stained bone slices were mounted in Fluoromount-G (Fisher) and examined under an Olympus BH-2 fluorescence/bright field microscope.

Statistical Analysis—Results are shown as mean ± S.D. with 3–6 replicates or repeat measurements. Statistical significance was determined with two-tailed Student's *t* test, and the difference was significant at $p < 0.05$.

RESULTS

Effects of Fluid Shear Stress on the Proliferation, Differentiation, and Expression of Early Mechanoresponsive Genes in Primary Osteoblasts of B6 and C3H Inbred Strains of Mice—The 30-min steady fluid shear stress of 20 dynes/cm^2 significantly increased (~2-fold each) the [^{3}H]thymidine incorporation (Fig. 1*A*) (an index of cell proliferation) and ALP-specific activity (Fig. 1*B*) (a marker of osteoblast differentiation) of B6 osteoblasts. No such response was seen in C3H osteoblasts.

Mechanical stimulation, including fluid shear stress, has been shown to up-regulate several early mechanoresponsive genes, such as integrins and Cox-2, within minutes in bone cells (18). Thus, we evaluated whether there was also a differential response to fluid shear in the expression of integrin β1 (*Igtb1*) and *Cox-2* in C3H and B6 osteoblasts. Fig. 1*C* shows that while the 30-min steady fluid shear stress significantly increased the cellular integrin β1 protein level in B6 osteoblasts

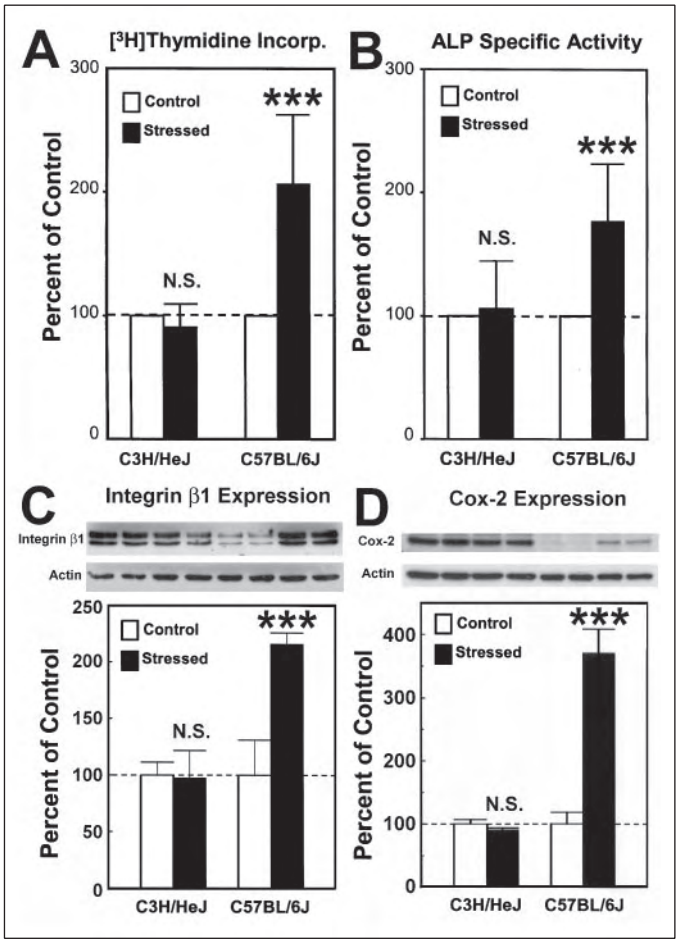

FIGURE 1. **Effects of fluid shear on cell proliferation, differentiation, and early mechanoresponsive gene expression of B6 and C3H osteoblasts.** *A,* cell proliferation was measured by [^{3}H]thymidine incorporation 24 h after a 30-min steady fluid shear at 20 dynes/cm^2. *B,* osteoblast differentiation was monitored by an increase in the specific activity of ALP 48 h after the fluid shear. *C* and *D,* cellular integrin β1 protein level (*C*) and Cox-2 protein level (*D*), normalized against each cellular actin protein level, was determined by Western immunoblot assay. Results are shown as mean ± S.D. ($n = 6$). ***, $p < 0.001$. *N.S.*, not significant.

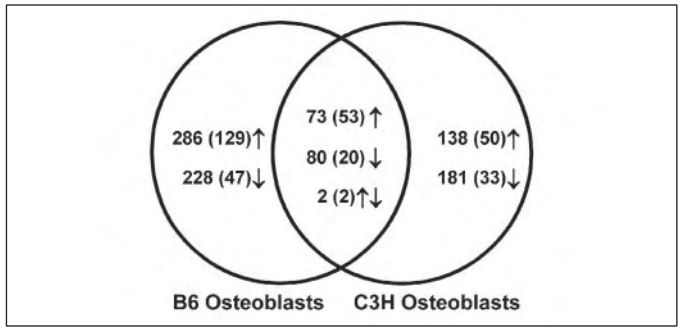

FIGURE 2. **Schematic summary of the number of genes whose expression was altered at 4 h after the 30-min steady fluid shear at 20 dynes/cm^2 in osteoblasts derived from B6 or C3H inbred strain of mice.** The *up arrows* represent up-regulated genes, and the *down arrows* represent down-regulated genes. The *numbers* indicate the total number of all genes and ESTs. The *numbers within parentheses* are the number of known mouse genes.

by ~2-fold 10 min after the stress, the same stress had no effect in C3H osteoblasts. Similarly, the fluid shear significantly increased Cox-2 protein expression by >2-fold in B6 osteoblasts but not in C3H osteoblasts (Fig. 1*D*). Fig. 1, *C* and *D*, also shows that the basal cellular integrin β1 and Cox-2 protein levels in C3H osteoblasts were severalfold higher than those in B6 osteoblasts. The significance of the higher basal expression of these two early mechanoresponsive genes in C3H osteoblasts is unclear. Nevertheless, these results clearly indicate that the osteogenic response to mechanical loading in this pair of inbred strains of mice is intrinsic to osteoblasts.

In-house Microarray Analysis of Shear Stress-mediated Changes in Gene Expression in Primary Osteoblasts of B6 and C3H Mice—Microarray analysis was performed with RNAs isolated from primary B6 or C3H osteoblasts 4 h after the 30-min fluid shear, using the in-house chips, which contained 5,500 genes or ESTs of mouse, human, and several other species. As schematically summarized in Fig. 2, of the 5,500 genes or ESTs on the microarray chip, the expression of 669 genes or ESTs in B6 osteoblasts (360 up-regulated and 309 down-regulated) and that of 474 genes or ESTs in C3H osteoblasts (212 up-regulated and 262 down-regulated) was significantly ($p < 0.05$) affected by the shear stress. Among the affected gene fragments, 286 were up-regulated and 228 down-regulated in B6 osteoblasts only, and 138 of them were up-regulated and 181 were down-regulated in C3H osteoblasts only. Seventy three genes or ESTs were up-regulated and 80 were down-regulated in both B6 and C3H osteoblasts. The fibronectin (*Fn1*) gene was up-regulated in B6 osteoblasts but down-regulated in C3H osteoblasts. Conversely, the solute carrier family 34 (sodium phosphate), member 2 (*Slc34a2*) gene was down-regulated in B6 osteoblasts but up-regulated in C3H osteoblasts. Although the relative changes in the expression level of these genes were mostly <3-fold, all of the changes were statistically significant ($p < 0.05$).

Because we sought to identify potential signaling pathways that might contribute to the differential osteogenic response in this pair of mouse strains, subsequent analyses were focused on the known mouse genes whose expression was affected differentially in B6 osteoblasts, with an emphasis on the up-regulating genes. Accordingly, 53 known mouse genes were up-regulated and 20 known genes were down-regulated in both B6 and C3H osteoblasts (supplemental Table 1). The up-regulated genes included a number of key regulator genes of cell proliferation and differentiation in both B6 and C3H osteoblasts, including several growth factor genes (*i.e. Tgfb1*, *Vegfd*, *Igf2*, *Pdgfa*, *Fgf1*, and *Op2*/*Bmp8b*), receptor genes (*Thr*, *Bmpr1a*, *Pthr*, *Esr2*, *Rarg*, *Fnrb*, *Osmr*, *Ifngr*, and *Tnfr*), vitamin D metabolism genes (*i.e. Cyp27b1*), small G-protein genes (*i.e. Ran* and *Era1*), and several inhibitory transcription factor genes of osteoblast differentiation (*i.e. M-twist*, *Id-2*, and *Dermo-1*). Because these genes were up-regulated in both C3H and B6 osteoblasts, these mechanoresponsive genes were likely to be upstream to the mechanosensitivity genes responsible for the differential anabolic response to fluid shear between B6 and C3H osteoblasts.

The expression of 88 known mouse genes (50 up-regulated and 33 down-regulated) was altered only in C3H osteoblasts (supplemental Table 2). Some of the up-regulated genes were growth factor and receptor genes (*Csf1*, *Tgfbr1*, *Igfbp2*, and *Fgfr*), transcription factor genes (*Hox8.1*/*Msx2*, and c-*Myc*), signal transduction genes (*Pld*, *Hic5*, *Itgb4bp*, and *Emk2*), and intracellular transport and trafficking genes (*Gs15*, *Cacnb3*, *Snx3*, and *Atp6d*). The shear stress also up-regulated *Pges* and *Bcl* genes in C3H osteoblasts but not in B6 osteoblasts. Because C3H osteoblasts did not respond anabolically to fluid shear, these genes were not analyzed further.

The expression of 129 known mouse genes was up-regulated in B6 osteoblasts only (supplemental Table 3). Consistent with an anabolic response to the fluid shear in B6 osteoblasts and not C3H osteoblasts, the fluid shear differentially up-regulated in B6 osteoblasts a number of genes associated with osteoblast proliferation and differentiation. These genes include, but are not limited to, bone growth factor, receptor, and associated genes (*i.e. Tgfb2*, *Bmp4*, *Fgf6*, *Kgf/Fgf7*, *Pdgfc*, *Igf1r*, *Ghr*,

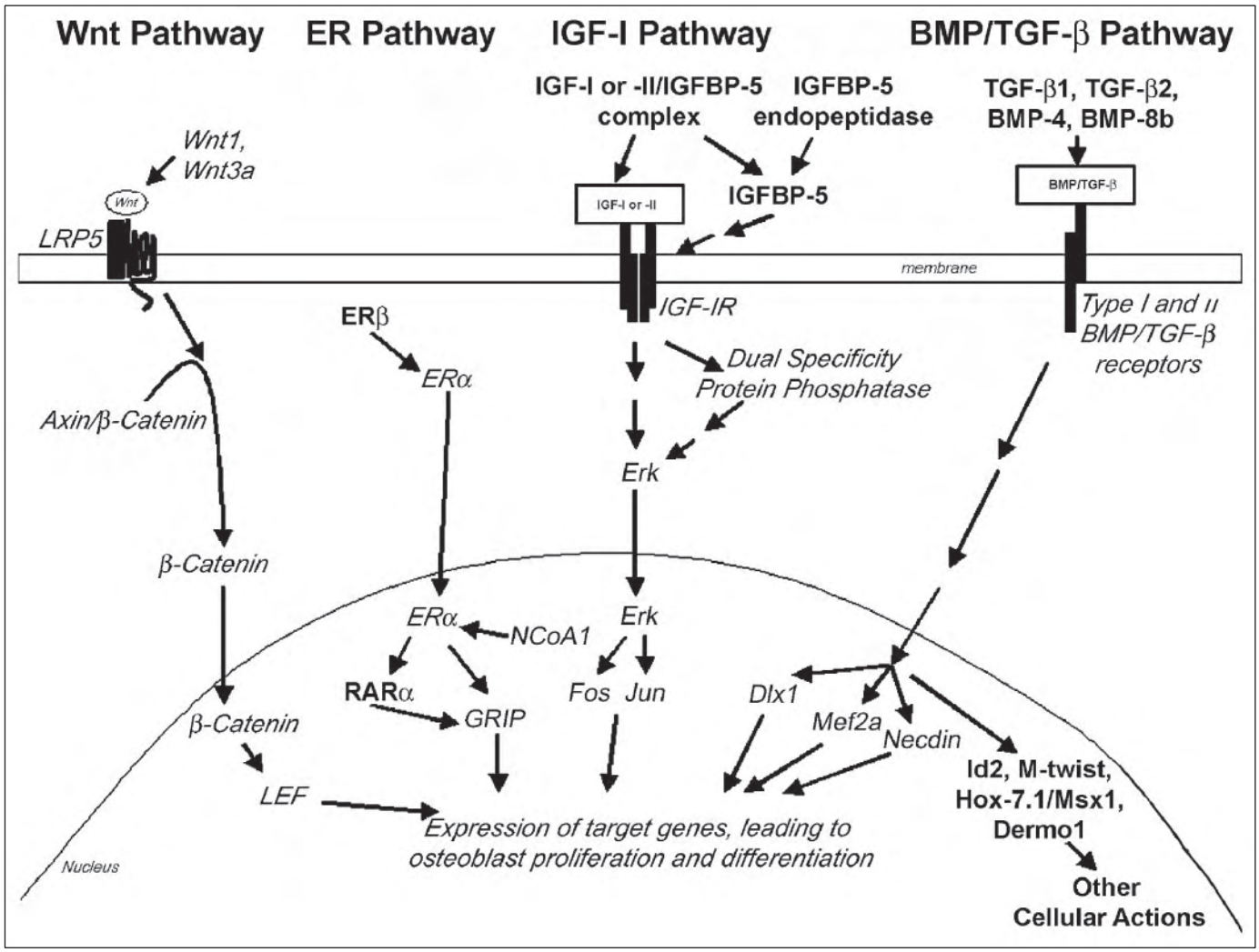

FIGURE 3. **Schematic summary of the genes associated with the Wnt, the ER, the IGF-I, and the BMP/TGF-β pathways, whose expression was up-regulated 4 h after the 30-min steady fluid shear stress of 20 dynes/cm^2.** Genes whose expression was up-regulated in both C3H and B6 osteoblasts are shown in *boldface letters*, and genes whose expression was up-regulated in B6 osteoblasts only are shown in *italic letters*.

Bmpr2, *Igfbp5*, and *Wnt5a*), cytokines, and receptor genes (*i.e. Osm*, *Il4*, *Il6*, *Il8*, and *Il6r*), *Esr1*, genes involved in protein and RNA synthesis, DNA synthesis, as well as cell proliferation. A number of energy and cell metabolism genes, intracellular transport and trafficking genes, as well as oxidative stress-responsive genes, such as *Hsc70*, *Osp94*, and p47^{Phox}, were also up-regulated in B6 but not C3H osteoblasts. Similarly, a large number of transcription factors and signal transduction molecules were differentially up-regulated in B6 osteoblasts.

Up-regulation of the Expression of Genes of Four Anabolic Signal Transduction Pathways in B6 Osteoblasts in Response to the Fluid Shear—A manual pathway analysis of the known mouse genes whose expression was up-regulated in B6 osteoblasts revealed that a number of genes associated with four anabolic signaling transduction pathways were differentially up-regulated in response to the fluid shear (Fig. 3). These pathways are as follows: the Wnt pathway, the BMP/transforming growth factor(TGF)-β pathway, the ER pathway, and the growth hormone/insulin-like growth factor(IGF)-I pathway. However, some of the upstream effector genes of these signaling pathways (with the exception of the Wnt pathway) and several downstream negative regulatory transcription factor genes of osteoblast differentiation of the BMP/TGF-β pathway (*i.e. Id-2*, *Dermo-1*, and *Hox-7.1/Msx1*) were also up-regulated in C3H osteoblasts, suggesting that these genes are unrelated to the mechanosensitivity genes responsible for the differential osteogenic response to mechanical stimulation in this pair of inbred strains of mice.

To confirm the microarray data, real time PCR analyses were performed on the expression levels of several genes of each of these four signaling pathways in B6 and C3H osteoblasts 4 h after the 30-min steady fluid shear. Because the in-house microarray chips contained only a limited number of known mouse genes, particularly those of the canonical Wnt signaling pathway, additional genes of the canonical Wnt pathway (*i.e. Wnt1*, *Wnt3a*, and *Lrp5*) were included in the real time PCR analysis. Table 2, which summarizes and compares the real time PCR and microarray results, confirms that the expression of several key genes of the Wnt signaling pathway (*i.e. Wnt1*, *Wnt3a*, *Wnt5a*, *Lrp5*, *Ctnnb1*, *Lef1*, and *Axin*), IGF-I pathway (*i.e. Igf1* and c-*Fos*), ER pathway (*i.e. Esr1* and *Ncoa1*), BMP/TGF-β pathway (*i.e. Tgfb1* and *Bmpr1*) were differentially up-regulated by the fluid shear in B6 osteoblasts and not in C3H osteoblasts.

Evidence That in Vivo Mechanical Loading Up-regulated Genes Associated with the Wnt, IGF-I, ER, and BMP/TGF-β Signaling Pathways—To determine whether up-regulation of genes of these four anabolic signaling pathways in response to loading also occurred in bone *in vivo*, we determined the effects of this 2-week loading regimen in the form of a four-point bending exercise on the expression of genes associated

TABLE 2

Microarray and real time PCR analyses of gene expression of the Wnt, BMP/TGF-β, IGF-I, and ER signaling pathways in response to the fluid shear in B6 osteoblasts as opposed to that in C3H osteoblasts

Gene	B6 osteoblasts		C3H osteoblasts	
	Microarray, fold changes, mean ± S.D. ($n = 4$)	Real time PCR, fold changes, mean ± S.D. ($n = 6$)	Microarray, fold changes, mean ± S.D. ($n = 4$)	Real time PCR, fold changes, mean ± S.D. ($n = 6$)
The Wnt signaling pathway genes				
Wnt1	NP[a]	2.32 ± 0.15[b]	NP	0.85 ± 0.12
Wnt3a	NP	3.28 ± 0.86[b]	NP	0.92 ± 0.15
Wnt5a	1.86 ± 0.49[b]	1.85 ± 0.02[b]	1.72 ± 1.23	0.14 ± 0.06
Lrp5	NP	3.23 ± 1.42[b]	NP	0.67 ± 0.45
Ctnnb1	2.35 ± 0.35[b]	3.36 ± 0.59[b]	1.33 ± 0.22	0.84 ± 0.56
Axin	1.70 ± 0.51[b]	3.48 ± 0.82[b]	1.26 ± 0.22	0.22 ± 0.10
Lef1	1.63 ± 0.44[b]	2.79 ± 0.49[b]	1.52 ± 0.91	0.49 ± 0.15
The BMP/TGF-β signaling pathway genes				
Tgfb1	1.99 ± 0.54[b]	2.44 ± 0.71[b]	1.99 ± 0.86[b]	0.95 ± 0.10
Bmp8b	1.83 ± 0.22[b]	ND[c]	2.19 ± 0.61[b]	ND
Tgfb2	1.71 ± 0.52[b]	ND	1.88 ± 0.85	ND
Bmp4	1.67 ± 0.49[b]	ND	1.58 ± 0.61	ND
Bmpr1	1.92 ± 0.55[b]	3.64 ± 0.41[b]	2.24 ± 1.01[b]	0.81 ± 0.27
Bmpr2	1.62 ± 0.38[b]	ND	1.78 ± 0.76	ND
Id2	2.06 ± 0.53[b]	ND	2.64 ± 1.12[b]	ND
M-twist	1.97 ± 0.21[b]	ND	2.67 ± 0.94[b]	ND
Hox-7.1/Msx1	1.74 ± 0.61[b]	ND	1.76 ± 0.83	ND
Dermo-1	1.70 ± 0.56[b]	ND	1.90 ± 0.53[b]	ND
Dlx1	1.56 ± 0.36[b]	1.70 ± 0.38[b]	1.29 ± 0.52	1.05 ± 0.36
Necdin	1.37 ± 0.19[b]	ND	1.18 ± 0.29	ND
Mef2a	1.22 ± 0.12[b]	ND	0.98 ± 0.13	ND
The IGF-I signaling pathway genes				
Igf2	1.64 ± 0.27[b]	ND	1.69 ± 0.53[b]	ND
Htra1	1.93 ± 0.43[b]	ND	2.25 ± 0.94[b]	ND
Igfbp5	2.55 ± 1.59[b]	ND	1.28 ± 1.37	ND
Igf1r	1.77 ± 0.35[b]	2.28 ± 0.39[b]	2.24 ± 1.42	1.15 ± 0.30
Mapk7	1.76 ± 0.61[b]	ND	2.04 ± 1.29	ND
Dusp10	1.49 ± 0.29[b]	ND	0.61 ± 1.41	ND
c-*Fos*	2.09 ± 0.57[b]	ND	1.75 ± 0.81	ND
c-*Jun*	1.34 ± 0.22[b]	ND	1.39 ± 0.48	ND
The ER signaling pathway genes				
Esr2	1.93 ± 0.49[b]	ND	1.64 ± 0.33[b]	ND
Esr1	2.04 ± 0.60[b]	2.24 ± 0.57[b]	1.82 ± 1.21	1.14 ± 0.05
Ncoa1	1.60 ± 0.25[b]	2.76 ± 0.81[b]	1.09 ± 0.57	1.25 ± 0.38
Rarg	2.15 ± 0.95[b]	ND	1.75 ± 0.16[b]	ND
Grip	1.73 ± 0.56[b]	ND	1.87 ± 0.83	ND

[a] NP indicates not present in the array chip.
[b] $p < 0.05$.
[c] ND indicates not determined.

with these four pathways in the loaded tibia of B6 and C3H mice by real time PCR. We have shown previously with peripheral quantitative computed tomography, serum biochemical markers, and gene expression evidence that the 2-week four-point bending loading regimen significantly increased bone formation and bone mass in B6 mice but not in C3H mice *in vivo* (18). In this study, we showed that this 2-week loading regimen also caused massive increase in cancellous bone formation (stained in blue by the Goldner's stain) at the periosteum of the loaded tibia of B6 mice, but not in the loaded tibia of C3H mice (Fig. 4), confirming that *in vivo* mechanical loading increased periosteal bone formation in B6 but not C3H mice (8, 9). Table 3 shows that the 2-week four-point bending exercise regimen significantly enhanced the expression of genes associated with the four anabolic signaling pathways-of-interest in the loaded tibia of B6 mice, but not in loaded tibia of C3H mice, confirming that *in vivo* mechanical loading also led to differential up-regulation of genes associated with these four anabolic pathways in bones of B6 and not of C3H mice.

Involvement of the ER Signaling Pathway in the Fluid Shear-induced Bone Cell Proliferation—To confirm the involvement of the ER signaling pathway in the fluid shear-induced osteoblast proliferation, B6 osteoblasts were pretreated with 200 nM of ICI182780, a pure antagonist of ER (19), for 24 h prior to the 30-min fluid shear, and the effect of this inhibitor on the fluid shear-induced proliferation in B6 osteoblasts was then determined. Because Erk1/2 activation is required for the fluid shear-induced bone cell proliferation (20), the effect of the inhibitor on Erk1/2 activation (assessed by Erk1/2 phosphorylation) was also evaluated. The ICI182780 pretreatment slightly, but not significantly, enhanced basal [^{3}H]thymidine incorporation (Fig. 5*A*) and Erk1/2 phos-

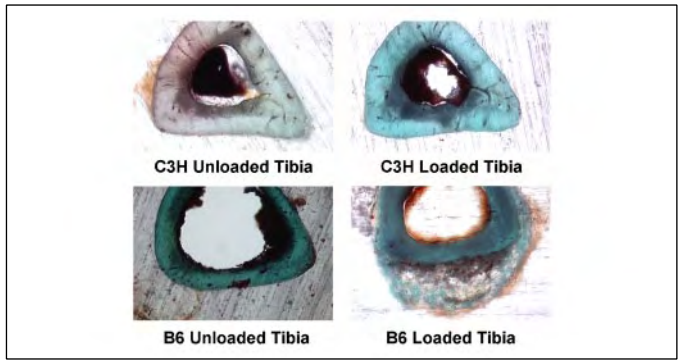

FIGURE 4. **Evidence that the 2-week four-point bending exercise regimen stimulates periosteal bone formation of the loaded tibia of 10-week female B6 mice but not of 10-week female C3H mice.** This figure shows the cross-sectional area of the nonloaded tibia (*left photomicrographs*) and the loaded tibia (*right photomicrographs*) of 10-week female C3H (the top photomicrographs) and B6 (*bottom photomicrographs*) mice. The sections were each stained with the Goldner's stain, which would stain bone tissues in *blue color*. This figure shows that the loading regimen caused a massive increase in cancellous bone formation at the periosteum of the loaded tibia of B6 mice but not of C3H mice.

phorylation (Fig. 5*B*). However, this pretreatment completely abolished the fluid shear-induced cell proliferation and Erk1/2 activation, confirming that the ER pathway is essential for the bone cell mitogenic action of fluid shear.

Involvement of the Canonical Wnt Signaling Pathway in the Fluid Shear-induced Bone Cell Proliferation—There are two major Wnt signaling pathways as follows: the canonical pathway that involves β-catenin stabilization and activation, and the noncanonical pathway that involves G-protein-dependent intracellular Ca^{2+} release (21). We focused on the canonical pathway because this pathway plays an important role in osteoblast functions and bone formation (22). Because activation of the canonical Wnt pathway blocks the glycogen synthase kinase-3β-mediated β-catenin phosphorylation, which then prevents the subsequent ubiquitination and degradation of hyperphosphorylated β-catenin, the increase in cellular β-catenin protein can be an index of activation of the canonical Wnt pathway. In this regard, the 30-min steady fluid shear yielded a significant 2-fold increase in total β-catenin protein levels in B6 osteoblasts, although it had no significant effect in C3H osteoblasts (Fig. 6), supporting the premise that fluid shear up-regulated the canonical Wnt pathway in B6 osteoblasts but not in C3H osteoblasts. Because the degradation (or "destabilization") of β-catenin is mediated by phosphorylation, we had also attempted to measure the cellular levels of phosphorylated β-catenin in this study. Unfortunately, we were unable to detect any significant levels of phosphorylated β-catenin in the stressed or control osteoblasts with any of the currently commercial phospho-specific polyclonal antibodies against β-catenin (Santa Cruz Biotechnologies).

To determine the role of the canonical Wnt pathway in the fluid shear-induced osteoblast proliferation, B6 osteoblasts were pretreated with 10 μg/ml of endostatin, a potent inhibitor of the canonical Wnt pathway (23), for 24 h prior to the 30-min fluid shear, and the effect of this inhibitor on fluid shear-induced cell proliferation and Erk1/2 activation was then determined. Although the endostatin pretreatment had no effect on basal [^{3}H]thymidine incorporation and Erk1/2 phosphorylation, this pretreatment partially, but significantly, reduced the fluid shear-induced cell proliferation (Fig. 7*A*) and Erk1/2 activation (Fig. 7*B*). Although the primary inhibitory action of endostatin on the canonical Wnt pathway is mediated through an increase in β-catenin degradation, there is also evidence that endostatin suppressed β-catenin (*Ctnnb1*) gene expression (23). Thus, measurements of β-catenin mRNA transcript level may be used to assess the effect of endostatin on β-catenin activation. Accordingly, our findings that this dose of endostatin completely blocked the fluid shear-induced up-regulation of β-catenin mRNA (Fig. 7*C*) and protein levels (Fig. 7*D*) in B6 osteoblasts suggest that the partial inhibition of fluid shear-mediated cell proliferation was not due to an insufficient amount of endostatin.

Involvement of the BMP Signaling Pathway in the Fluid Shear-induced Bone Cell Proliferation—To assess whether the BMP signaling pathway has an essential role in the fluid shear-induced osteoblast proliferation, B6 osteoblasts were pretreated with 300 ng/ml of Noggin, an inhibitor of the BMP signaling pathway (24), for 24 h prior to the fluid shear. The Noggin pretreatment did not affect the basal cell proliferation and Erk1/2 activation but completely abolished the fluid shear-induced cell proliferation (Fig. 8*A*) and Erk1/2 activation (Fig. 8*B*) in B6 osteoblasts.

The role of the IGF-I signaling pathway in fluid shear-induced osteoblast proliferation was not evaluated in this study, because we and others have previously provided compelling evidence for the involvement

TABLE 3

Real time PCR analyses of in vivo gene expression of the Wnt, BMP/TGF-β, IGF-I, and ER signaling pathways in response to the four-point bending exercise regimen in tibia of B6 inbred strain of mice as opposed to that of C3H inbred strain of mice (mean ± S.D., *n* = 6 for each mouse strain)

None of the changes in the expression of the test genes in C3H mice was statistically significant.

Gene	B6 mice, fold changes	C3H mice, fold changes
The canonical Wnt signaling pathway genes		
Wnt1	1.81 ± 0.68[a]	0.74 ± 0.45
Wnt3a	4.25 ± 2.12[b]	3.10 ± 2.26
Lrp5	9.08 ± 2.76[b]	3.22 ± 1.59
Ctnnb1	5.51 ± 2.62[b]	1.29 ± 0.37
The BMP/TGF-β signaling pathway genes		
Tgfb1	2.10 ± 0.80[b]	0.53 ± 0.34
Bmpr1	3.23 ± 0.96[b]	1.64 ± 0.78
Dlx1	3.06 ± 1.21[a]	Not detectable
The IGF-I signaling pathway genes		
Igfr1	2.74 ± 1.22[a]	1.51 ± 1.08
c-Fos	3.73 ± 1.65[b]	0.98 ± 0.65
The ER signaling pathway genes		
Esr1	3.17 ± 1.27[b]	1.55 ± 0.53
Ncoa1	2.05 ± 0.61[b]	1.56 ± 0.85

[a] $p < 0.05$.
[b] $p < 0.01$.

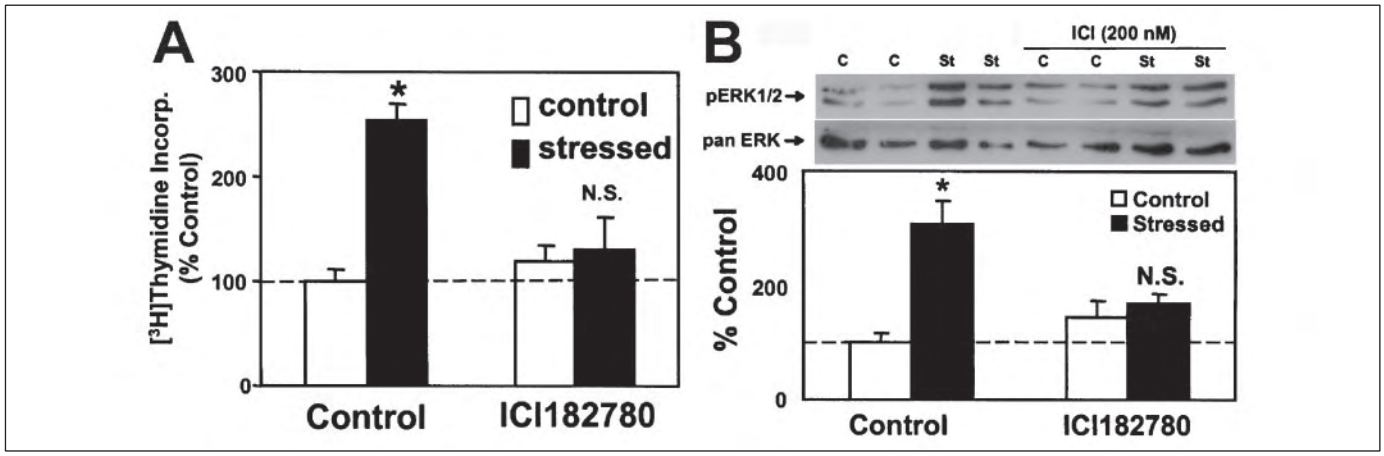

FIGURE 5. **Effects of ICI182780 pretreatment on the fluid shear-induced proliferation and Erk1/2 activation in B6 osteoblasts.** B6 osteoblasts were pretreated with 200 nM ICI182780 for 24 h prior to the fluid shear stress. Cell proliferation was measured by [^{3}H]thymidine incorporation, and Erk1/2 activation was assessed by the pErk1/2 level. *A* shows the results on [^{3}H]thymidine incorporation. Results are shown as mean ± S.D. of six replicate each. *B* shows the representative Western blots of pErk1/2 and the pan-Erk bands and the summarized results of three separate experiments on the relative levels of pErk1/2 normalized against the total Erk1/2 (pan-Erk) protein level. The results are shown as percentage of the corresponding static control. The *dashed lines* represent 100% of the corresponding static control value. *, $p < 0.05$. *N.S.*, not significant.

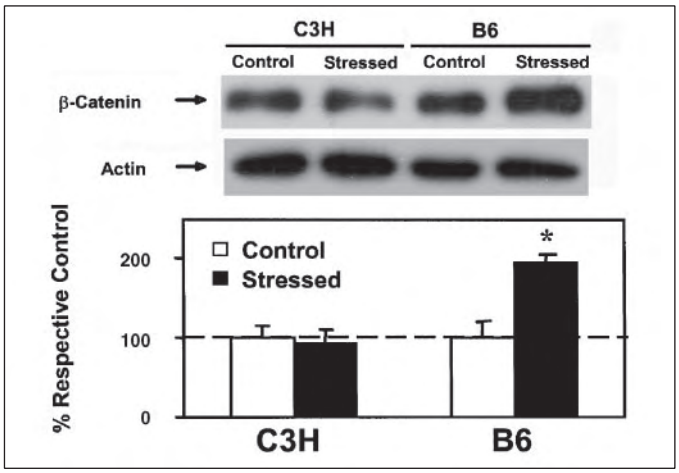

FIGURE 6. **Effects of fluid shear on the cellular β-catenin protein level in C3H and B6 osteoblasts.** *Top panel* shows the representative Western blots of β-catenin and actin protein bands. *Bottom panel* summarizes the results of three separate experiments on the relative levels of β-catenin normalized against the actin level. The results are shown as percentage of the corresponding static control. The *dashed lines* represent 100% of the corresponding static control value. *, $p < 0.05$.

of the IGF-I signaling pathway in mechanotransduction in osteoblasts (25–28).

Evidence that the Four Signaling Pathways-of-Interest Were Downstream to Integrin Activation and Cox-2 Expression—To evaluate the relationship between the early mechanoresponsive events (*i.e.* integrin and/or Cox-2 activation) and up-regulation of gene expression associated with the four anabolic pathways-of-interest, we examined the effects of the inhibition of integrin activation and Cox-2 expression with a 2-h pretreatment of B6 osteoblasts with 100 nM echistatin and 1 μM indomethacin, respectively, prior to the 30-min fluid shear stress. Gene expression associated with the four pathways-of-interest was then measured at 4 h after the shear stress by real time PCR. The test dosage of these inhibitors has each been shown to completely abolish the fluid shear-induced bone cell proliferation (4, 28). Table 4 shows that the 2-h echistatin or indomethacin pretreatment each blocked the shear stress-induced up-regulation of expression of genes associated with the four pathways-of-interest in B6 osteoblasts, indicating that the up-regulation of gene expression associated with these pathways-of-interest are downstream to integrin activation and *Cox-2* expression.

DISCUSSION

Previous studies in the B6-C3H pair of inbred strain of mice have demonstrated that genetics is an important determining factor of the bone formation response to mechanical loading (6–9, 16). In this regard, recent genetic studies with the quantitative trait linkage (29) and *N*-ethylnitrosourea mutagenesis (30) approaches on this pair of inbred mice have identified one or more quantitative trait loci on mouse chromosome 4 that are associated with mechanosensitivity in bone. However, the identity of the mechanosensitivity gene(s) or its underlying mechanism remains unknown. In this study, we showed that although primary osteoblasts isolated from B6 mice responded to a 30-min steady fluid shear stress of 20 dynes/cm^2 with an increase in cell proliferation and ALP activity *in vitro*, the same fluid shear did not produce similar anabolic effects in primary osteoblasts of C3H mice. Thus, it appears that the genetic component determining the mechanosensitivity of bone (at least in term of response to fluid shear) in this pair of inbred strain of mice is intrinsic to osteoblasts. Therefore, we conclude that primary osteoblasts of this pair of mouse strains can be used *in vitro* to investigate the identity and the underlying mechanism of the mechanosensitivity genes.

Global gene expression profiling by microarray analysis is a useful and complementary approach to genetic studies in the identification of genes and corresponding pathways contributing to a given phenotype (31). In this study, we have performed a microarray analysis with our in-house microarray chips on B6 osteoblasts that show good response to mechanical stimulation and C3H osteoblasts that show poor response. However, the relatively limited number of mouse gene fragments on our microarray chips precluded an extensive genome-wide assessment of the gene expression profile, and the incomplete annotation number of the gene fragments also did not permit computer-based analyses of the data. On the other hand, in contrast to previous microarray studies in chondrosarcoma cells (32) and in early osteochondroprogenitor cells (33), our study is unique in that we determined and compared a gene expression profile of B6 osteoblasts with that of C3H osteoblasts after a 30-min steady fluid shear stress. Because B6 osteoblasts, and not C3H osteoblasts, responded to fluid shear with an increase in cell proliferation and differentiation, an analysis of the genes whose expression is differentially regulated in B6 osteoblasts in response to the fluid shear could yield information about potential signal transduction pathways in the mechanotransduction mechanism, and this may help to identify potential candidate mechanosensitivity genes. Accordingly, the objective of this microarray study was not to obtain global gene expression profiling information but, rather, was to evaluate differential gene expression in B6 osteoblasts as opposed to C3H osteoblasts in response to the fluid shear to identify potential signaling pathways involved in the fluid shear-induced osteoblast proliferation. We hope to use this information to gain insights into the identity of mechanosensitivity genes that are responsible for the different bone formation response to loading in B6 and C3H mice.

Three observations of our microarray data were noteworthy. First, our study reveals that the expression of ~12% (*i.e.* 669 of 5,500) of the gene fragments on our in-house microarray chip was significantly affected (with more than half of them up-regulated) 4 h after the 30-min fluid shear in B6 osteoblasts. This relatively large number of mechanoresponsive genes in the good responding B6 osteoblasts underscores the complexity of mechanical stimulation in osteoblasts (4, 34). Of the 669 gene fragments whose expression was significantly altered by fluid shear, 514 (or 77%) were regulated differentially in B6 osteoblasts. This led us to postulate that the mechanosensitivity genes contributing to the different bone formation response in B6 and C3H mice may act on an upstream event of the mechanotransduction mechanism, leading to the subsequent changes in expression of up to 77% of the mechanoresponsive genes in B6 osteoblasts. Because there was also a differential up-regulation of at least two early mechanoresponsive genes, *i.e. Igtb1* and *Cox-2,* in B6 osteoblasts as opposed to C3H osteoblasts, the mechanosensitivity genes in this pair of inbred mice are also upstream to these two early mechanoresponsive genes.

The second noteworthy observation is that a large number of the known mouse genes that were up-regulated differentially in B6 osteoblasts are associated with various anabolic cellular processes, such as cell proliferation, protein and RNA syntheses, energy metabolism, and intracellular transport and trafficking mechanisms. These findings support an anabolic action of the fluid shear in B6 osteoblasts but not in C3H osteoblasts. Also consistent with the previous findings that mechanical loading (or fluid shear) stimulated the local production of bone growth factors, such as IGF-I (35), IGF-II (36), and TGF-β1 (37, 38), we found that the fluid shear significantly up-regulated the expression of these growth factor genes as well as several other bone growth factor genes, such as *Pdgf*, *Fgf*, and *Bmp*, in mouse osteoblasts. The fact

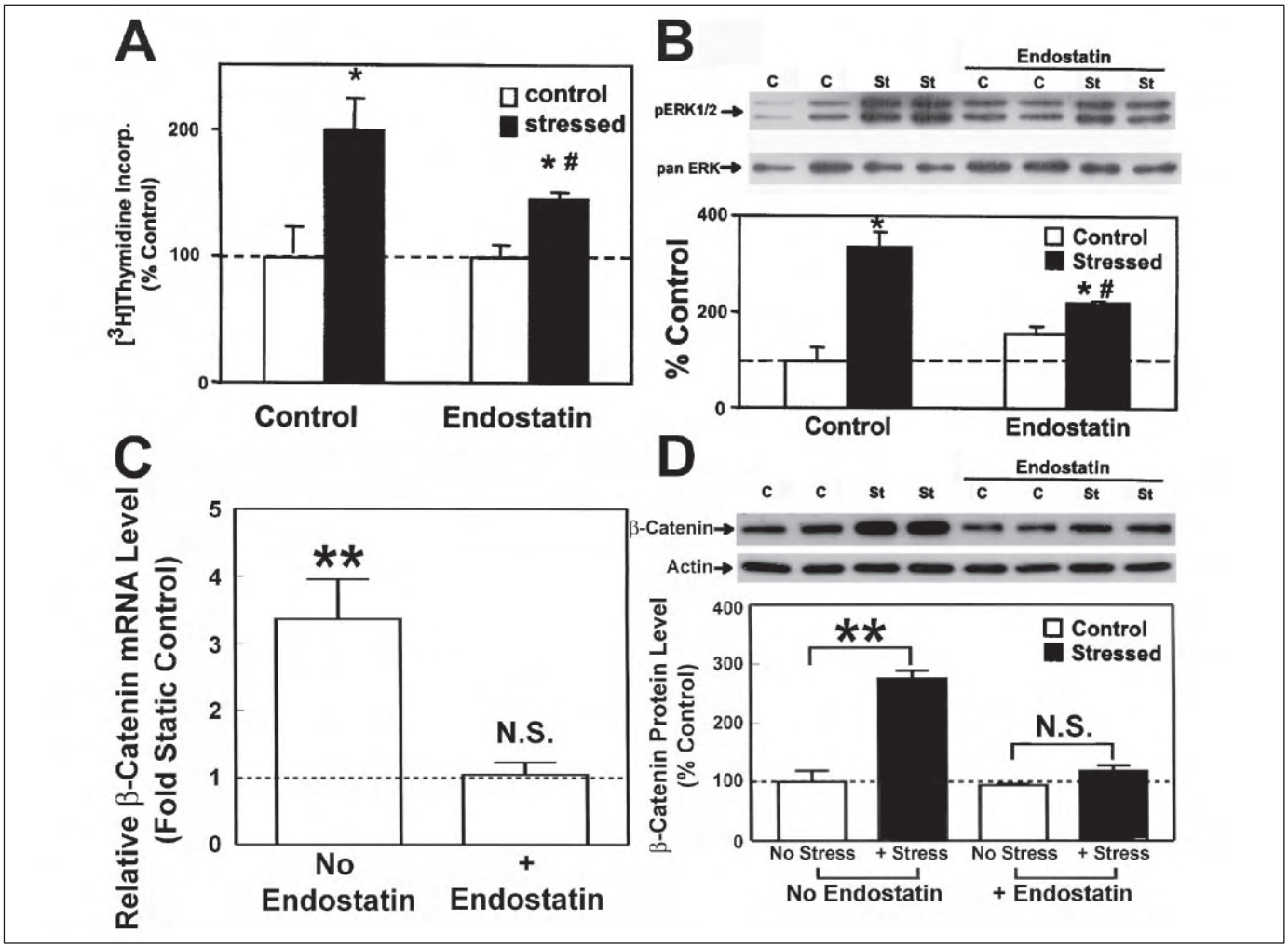

FIGURE 7. **Effects of endostatin pretreatment on the fluid shear-induced proliferation, Erk1/2, and β-catenin expression in B6 osteoblasts.** B6 osteoblasts were pretreated with 10 μg/ml endostatin for 24 h prior to the fluid shear stress. Cell proliferation was measured by [^{3}H]thymidine incorporation, and Erk1/2 activation was assessed by the pErk1/2 level. *A* shows the results on [^{3}H]thymidine incorporation. Results are shown as mean ± S.D. of six replicate each. *B* shows the representative Western blots of pErk1/2 and the pan-Erk bands and the summarized results of three separate experiments on the relative levels of pErk1/2 normalized against the total Erk1/2 (pan-Erk) protein level. The results are shown as percentage of the corresponding static control. The *dashed lines* represent 100% of the corresponding static control value. #, $p < 0.05$ compared to corresponding static controls with the endostatin treatment; *, $p < 0.05$ compared to corresponding static controls without endostatin. *C*, the relative β-catenin mRNA level at 4 h after the fluid shear stress was determined with real time PCR. Results are shown as relative fold of static control (mean ± S.D. of three replicate measurements). *, $p < 0.01$. *D* shows the effects of the endostatin pretreatment on the β-catenin protein level at 4 h after the fluid shear. *Top panel* shows the representative Western blots of β-catenin and actin protein bands. *Bottom panel* summarizes the results of three separate experiments on the relative levels of β-catenin normalized against the actin level. The results are shown as percentage of the corresponding static control. The *dashed lines* represent 100% of the corresponding static control value. **, $p < 0.01$. *N.S.*, not significant; *C*, control; *St*, stressed cells.

that fluid shear stress also up-regulated several bone growth factor receptor genes (*i.e. Igfr1*, *Pthr1*, and *Bmpr1*) suggests that the molecular mechanism whereby mechanical loading (or fluid shear) stimulates osteoblast proliferation may in part involve paracrine/autocrine actions of bone growth factors. On the other hand, because several of these growth factor (*Igf2*, *Pdgfa*, *Vegfd*, *Fgf1*, *Tgfb1*, and *Bmp8b*/*Op2*) and receptor (*Bmpr1* and *Pthr1*) genes were also up-regulated in C3H osteoblasts in response to fluid shear, these growth factor and receptor genes are either unrelated to or upstream to the mechanosensitivity genes in the overall mechanotransduction mechanism in osteoblasts. We favor the latter possibility because there is strong circumstantial evidence that at least IGF-II (36) and TGF-β1 (39–41) are involved in the mechanical stimulation of bone formation.

The third and the more important observation of our microarray analysis is the finding that a number of genes associated with the four anabolic signaling pathways, namely the IGF-I, the ER, the canonical Wnt, and the BMP/TGF-β signaling pathways, were up-regulated in B6 osteoblasts and not in C3H osteoblasts in response to the fluid shear stress. The differential up-regulation of gene expression of these four signaling pathways in B6 osteoblasts was confirmed by real time PCR analyses. These findings raise the following interesting possibilities: (*a*) up-regulation of these four anabolic pathways is involved in the fluid shear-induced osteoblast proliferation; (*b*) these four signaling pathways are downstream to the mechanosensitivity genes in the overall mechanotransduction mechanism in osteoblasts. The latter possibility is consistent with our observation that the mechanosensitivity genes contributing to the different bone formation response in B6 and C3H mice may act on an upstream event of the mechanotransduction mechanism, leading to the subsequent changes of a large number of downstream mechanoresponsive genes, including genes associated with these four anabolic signaling pathways. Although our supporting data for the conclusion that each of these four pathways plays an essential role in the fluid shear-induced osteoblast proliferation were based on RNA expression data and not protein production data (with the exception of β-catenin), this conclusion was supported by the findings that a specific inhibitor of the

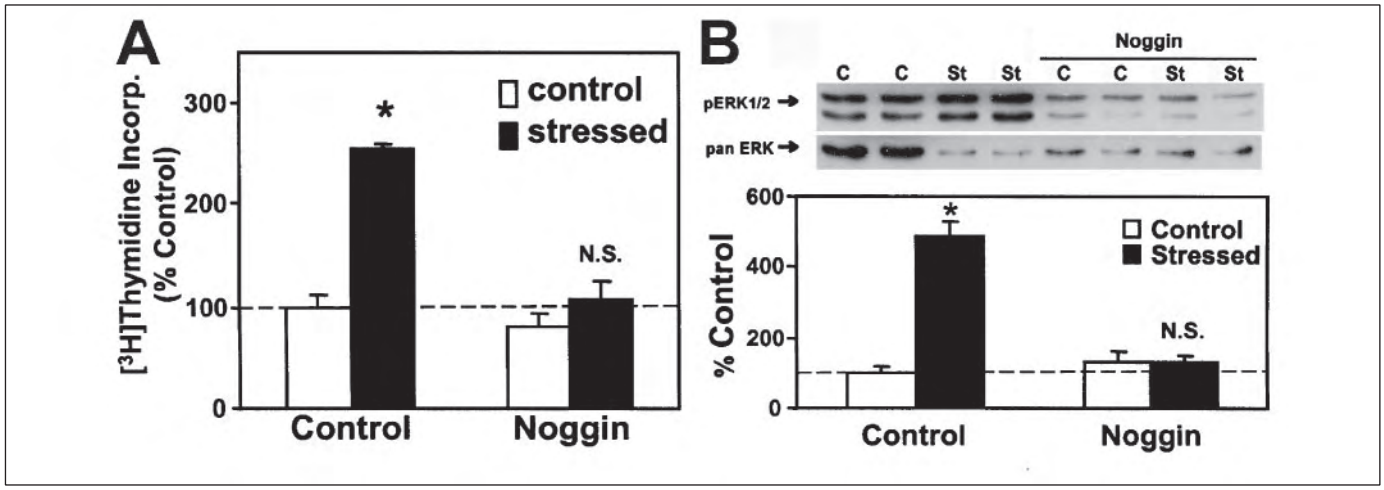

FIGURE 8. **Effects of Noggin pretreatment on the fluid shear-induced proliferation and Erk1/2 activation in B6 osteoblasts.** B6 osteoblasts were pretreated with 300 ng/ml Noggin for 24 h prior to the fluid shear stress. Cell proliferation was measured by [^{3}H]thymidine incorporation, and Erk1/2 activation was assessed by the pErk1/2 level. *A* shows the results on [^{3}H]thymidine incorporation. Results are shown as mean ± S.D. of six replicates each. *B* shows the representative Western blots of pErk1/2 and the pan-Erk bands and the summarized results of three separate experiments on the relative levels of pErk1/2 normalized against the total Erk1/2 (pan-Erk) protein level. The results are shown as percentage of the corresponding static control. The *dashed lines* represent 100% of the corresponding static control value. *, $p < 0.05$. *N.S.*, not significant; *C*, control; *St*, stressed cells.

TABLE 4

Effects of inhibition of integrin activation and/or Cox-2 activity on the fluid shear-mediated up-regulation of gene expression of genes associated with the Wnt, BMP/TGF-β, IGF-I, and ER signaling pathways in B6 osteoblasts (mean ± S.D., n = 6)

Up-regulation of gene expression was determined by real time PCR.

Gene	Inhibition of integrin activation (fold changes)		Inhibition of Cox-2 activity (fold changes)	
	No echistatin	+100 nM echistatin	No indomethacin	+1 μM indomethacin
The Wnt signaling pathway genes				
Wnt1	2.51 ± 0.87[a]	0.87 ± 0.15	2.59 ± 0.87[a]	0.95 ± 0.35
Wnt3a	3.18 ± 0.68[b]	1.19 ± 0.49	2.97 ± 1.00[a]	1.35 ± 0.23
Ctnnb1	2.26 ± 0.53[a]	1.27 ± 0.94	3.68 ± 1.13[a]	0.76 ± 0.26
The BMP/TGF-β signaling pathway genes				
Tgfb1	2.99 ± 1.31[a]	1.28 ± 0.63	2.47 ± 0.50[b]	0.71 ± 0.09[b]
Bmpr1	3.68 ± 1.49[a]	0.94 ± 0.55	3.01 ± 0.17[b]	0.73 ± 0.26
Dlx1	2.41 ± 0.63[a]	0.93 ± 0.48	2.77 ± 0.95[a]	1.04 ± 0.35
The IGF-I signaling pathway genes				
Igf1r	4.33 ± 1.98[a]	0.77 ± 0.38	3.38 ± 1.16[a]	0.97 ± 0.01[a]
c-Fos	ND[c]	ND	2.83 ± 0.89[a]	1.43 ± 0.49
The ER signaling pathway genes				
Esr1	3.74 ± 0.64[b]	0.97 ± 0.60	3.69 ± 0.97[b]	1.39 ± 0.44
Ncoa1	4.25 ± 2.03[a]	0.79 ± 0.45	3.01 ± 0.39[b]	0.92 ± 0.26

[a] $p < 0.05$.
[b] $p < 0.01$.
[c] ND indicates not determined.

ER signaling pathway (ICI182780), the canonical Wnt signaling pathway (endostatin), and the BMP signaling pathway (Noggin) each either completely abolished or markedly suppressed the fluid shear-induced cell proliferation in B6 osteoblasts.

We should emphasize that the *in vivo* application of mechanical loading through the 2-week four-point bending exercise regimen also led to up-regulation of expression of genes associated with the IGF-I, the ER, the canonical Wnt, and the BMP/TGF-β signaling pathways in the loaded tibia of B6 mice. Accordingly, inasmuch as there is a general belief that osteocytes, and not osteoblasts, are most likely the primary sensors of mechanical loading in bone (42), we conclude that our *in vitro* findings with the primary mouse osteoblasts are probably physiologically relevant, even though the issue as to whether osteoblasts indeed have a functional role in translating the mechanical signal into biochemical signals in bone remains controversial.

There is compelling evidence for the involvement of the IGF-I, ER, and canonical Wnt signaling pathways in mechanotransduction in bone. With respect to the IGF-I signaling pathway, it has been reported that the bone cell mitogenic response to mechanical strain is mediated through activation of the IGF-I receptor (25). We recently showed that fluid shear stress synergizes with IGF-I to stimulate Erk1/2 activation and osteoblast proliferation through integrin-dependent activation of the IGF-I signaling pathway (28), confirming a functional role of the IGF-I signaling pathway in the mechanical stimulation of osteoblast proliferation. Bikle and co-workers (26, 27) have also demonstrated that skeletal unloading induces resistance to IGF-I to induce bone formation, which is caused by inhibition of the IGF-I signaling pathway through down-regulation of the integrin pathway. Regarding the ER signaling pathway, Lanyon and co-workers (25, 43–46) have provided compelling evidence that ER, especially ERα, is essential for mechanical stimulation of bone formation. Specifically, they showed that knocking out the ERα (*Esr1*) expression in mice completely abolished the osteogenic response to mechanical loading *in vivo* (45) and *in vitro* (46). Their recent data suggested that ERβ may also have a certain role in mediating the mechanical signal to stimulate bone formation, because knocking out ERβ (*Esr2*) expression in female mice also blocked the mechanical stimulation of bone formation (47). In support of a role of the canonical Wnt pathway in mechanotransduction, it has been reported recently

that activation of the canonical Wnt signaling pathway by the G171V mutation of the low density LRP5 led to an enhanced response in the mechanical stimulation of bone formation (48) and that mechanical loading activated the canonical Wnt signaling pathway in TOPGAL mice, which are transgenic mice expressing a β-galactosidase reporter gene driven by a T cell factor β-catenin-responsive promoter (49). There is also evidence for a role of the TGF-β signaling pathway in mechanotransduction in bone, although the evidence is less compelling. Accordingly, mechanical loading or fluid shear significantly up-regulated the expression and secretion of TGF-β1 in bone cells, whereas mechanical unloading markedly suppressed *Tgfb1* expression in bone (37–41). Consequently, our findings that the IGF-I, the ER, the canonical Wnt, and even the TGF-β signaling pathways are involved in the mechanotransduction mechanism in B6 osteoblasts are not entirely surprising.

What was surprising to us is the finding that blocking the BMP signaling pathway in B6 osteoblasts by Noggin led to the complete abolition of the fluid shear-induced osteoblast proliferation. In this regard, although it is well known that BMPs are potent osteoblast differentiation agents, which stimulated bone formation primarily through its ability to promote osteoblast differentiation (50), there has been little evidence that BMPs can directly stimulate osteoblast proliferation. Consequently, the mechanism whereby inhibition of the BMP signaling pathway by Noggin blocked the fluid shear-induced cell proliferation and Erk1/2 activation in B6 osteoblasts is unclear. However, it has been demonstrated that there are significant cross-talks among the various signaling pathways involved in mechanotransduction (4, 34). Specifically, there is evidence in other cell types that the BMP signaling pathway can cross-talk with other signaling pathways, including the canonical and noncanonical Wnt pathways (51), and the ER pathway (52). Because we have recent preliminary data that inhibition of the BMP pathway with Noggin could completely block the fluid shear-induced up-regulation of the expression of genes associated with the canonical Wnt pathway in B6 osteoblasts (53), we tentatively conclude that the canonical Wnt pathway is downstream to the BMP signaling pathway in fluid shear stress-induced osteoblast proliferation. Accordingly, we suggest that the mechanism whereby the BMP signaling pathway mediates the fluid shear-induced osteoblast proliferation involves the subsequent activation of the canonical Wnt signaling pathway.

It is also foreseeable that there would be cross-talks among these four anabolic pathways, as there is evidence that the BMP signaling pathway can cross-talk with the ER pathway in other cell types (52) and that the IGF-I signaling pathway interacts with the ER pathway in the proliferative response of osteoblasts to mechanical strain (25). Consequently, it may be speculated that these potential cross-talks may explain why inhibition of a single signaling pathway (*e.g.* the ER or the BMP pathway) could lead to complete abrogation of the fluid shear-induced cell proliferation and Erk1/2 activation in B6 osteoblasts.

It is also intriguing to note that endostatin was only able to partially block the fluid shear-induced Erk1/2 activation and cell proliferation, suggesting that the canonical Wnt signaling pathway is only partially involved in mechanotransduction in osteoblasts. On the other hand, fluid shear stress appeared to also up-regulate the noncanonical Wnt signaling pathway, as the expression of *Wnt5a* was also up-regulated in response to the fluid shear stress in B6 osteoblasts. Thus, it is possible that the mechanical stimulation of osteoblast proliferation may involve up-regulation of both canonical and noncanonical Wnt pathways. Thus, blocking the canonical Wnt pathway alone is insufficient to block completely the fluid shear-induced osteoblast proliferation.

The exact molecular mechanism as to how each of these four anabolic signaling pathways mediate the fluid shear-induced osteoblast proliferation remains to be defined. However, we (20) and others (54) have demonstrated that Erk1/2 activation is required and essential for the mechanical stimulation of osteoblast proliferation. Accordingly, because blocking each of these pathways by a specific inhibitor completely blocked the fluid shear-induced cell proliferation and Erk1/2 activation in osteoblasts (this study and see Ref. 28), we believe that the molecular mechanism whereby each of these four anabolic signaling pathways mediates the mechanical stimulation of osteoblast proliferation involves Erk1/2 activation or converges to steps leading to Erk1/2 activation.

The role of early mechanoresponsive genes, such as integrins and *Cox-2*, in the mechanical stimulation of osteoblast proliferation has been documented (4, 18, 34). This study confirms that the fluid shear up-regulated the expression of at least two early mechanoresponsive genes, *i.e. Igtb1* and *Cox-2*, in B6 osteoblasts. This study also demonstrates for the first time that the up-regulation of these early mechanoresponsive genes was seen only in B6 osteoblasts and not in C3H osteoblasts, indicating that these two early mechanoresponsive genes are downstream effectors to the mechanosensitivity genes contributing to the differential osteogenic responses to mechanical loading in C3H-B6 pair of mice. More importantly, this study shows that blocking the fluid shear-induced stimulation of integrins (with echistatin) and Cox-2 (with indomethacin) each prevented the up-regulation of gene expression associated with the four signaling pathways (*i.e.* the IGF-I, ER, BMP/TGF-β, and canonical Wnt pathways) in B6 osteoblasts. Consequently, we conclude that these four signaling pathways are downstream to these two early mechanoresponsive genes in the mechanotransduction mechanism.

On the basis of our findings, we have advanced a model for the molecular mechanism of mechanotransduction in osteoblasts (Fig. 9). In this model, we postulate that the fluid shear (or mechanical strain or stress) on osteoblasts would lead to up-regulation of the expression of integrins and their signaling pathways through the putative mechanosensors and yet-to-be-defined mechanisms. Up-regulation of the integrin signaling pathway would result in the induction of *Cox-2* expression (55) as well as other early mechanoresponsive genes, such as c-*Fos* (18). One of the consequences of the activation of these early mechanoresponsive genes is the up-regulation of local growth factor production, such as IGF-I, BMPs, and TGF-βs as well as ERs. The increased production of these growth factors would act as paracrine/autocrine effectors to activate their respective signaling pathways. We further postulate that the activation of the BMP/TGF-β pathway would lead to up-regulation of local production of Wnts, which then activate both the canonical and noncanonical Wnt signaling pathways. Activation of each of these four pathways would each lead to Erk1/2 activation, which then subsequently would result in stimulation of osteoblast proliferation and/or differentiation. Because there is strong evidence that the integrin signaling pathway could cross-talk with the IGF-I signaling pathway through recruitment of Src homology protein phosphatase-1 (SHP-1) between integrins and IGF-I receptor (28, 56), the ER signaling pathway through activation of c-Src (57), the Wnt signaling pathway through activation of integrin-linked kinase (58), and the BMP/TGF-β pathway (59), presumably also through c-Src activation (60), we further postulate that the cross-talks between the integrin signaling pathway and the four other pathways-of-interest further enhance up-regulation of these signaling pathways. This model is the current focus of investigations in our laboratory.

Finally, perhaps the most important information derived from this study is the finding that the mechanosensitivity genes contributing to the good and poor bone formation response, respectively, in B6 and

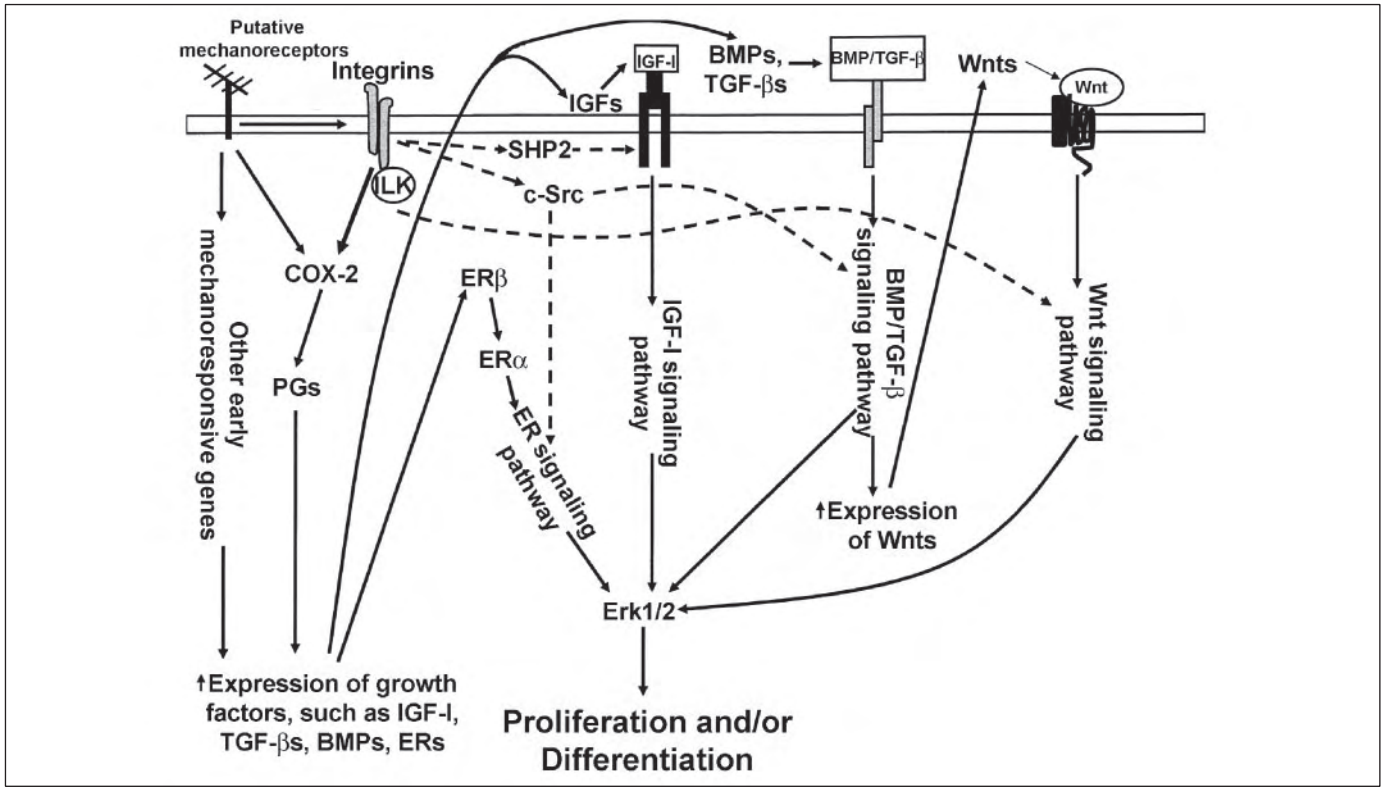

FIGURE 9. **A proposed model of the molecular mechanism whereby mechanical stimulation up-regulates expression of genes associated with the IGF-I, the ER, the BMP/TGF-β, and the Wnt pathways.** Please see "Discussion" for detailed description of the model.

C3H inbred strain of mice are upstream to the IGF-I, the ER, the Wnt, and the BMP/TGF-β signaling pathways. In this regard, we believe that the mechanosensitivity may act on an upstream event between the putative mechanosensors and the activation of integrin signaling pathway (Fig. 9). This information should be very useful in our continuing efforts to search for the identity and underlying mechanism of the mechanosensitivity genes that are responsible for the different bone formation response in this pair of inbred mice. Accordingly, we believe that the ability of a candidate gene to up-regulate the expression of genes associated with all of these four signaling pathways in response to mechanical stimulation can be a useful functional screen assay for candidate genes of mechanosensitivity. Moreover, because the mechanosensitivity genes appear to be upstream regulators, this information may allow us to narrow our search of candidate genes to upstream regulators. In this regard, the quantitative trait locus for mechanosensitivity in mouse chromosome 4 identified by Robling *et al.* (29) is a large 40–80-centimorgan region and contains several hundreds of genes, including a number of upstream signal transduction regulator genes. These include receptor genes (such as *Lepr*, *Il22ra1*, *Ptafr*, *Oprd1*, *Htr1D*, and *Htr6*, *Epha1*, and *Ephb2*, and *Tnfr*), several receptor tyrosine kinases, *Ptpru*, ion channel genes (*Gjb3*), and several other candidate genes. In order for any of these or other candidate genes to be the mechanosensitivity gene, the candidate gene must be able to up-regulate these four aforementioned anabolic signaling pathways in response to mechanical stimulation. Two genes (*Bmp8*/*Op2* and *Jun*) whose expression was up-regulated by the fluid shear in osteoblasts were located within this quantitative trait locus. However, because the expression of *Bmp8*/*Op2* was up-regulated by fluid shear in both B6 and C3H osteoblasts, and because Jun is a downstream effector of the signaling pathways-of-interest, neither of these two genes would likely be the mechanosensitivity gene(s) that contributes to the different bone formation response to mechanical loading in B6 and C3H inbred strain of mice.

In conclusion, we have demonstrated that fluid shear induced an anabolic response in B6 osteoblasts but not in C3H osteoblasts, indicating that the differential osteogenic response to mechanical stimulation in this pair of inbred strain of mice is intrinsic to osteoblasts. More importantly, we showed for the first time that fluid shear differentially up-regulated the expression of genes associated with four anabolic signaling pathways (*i.e.* the IGF-I, the ER, the Wnt, and the BMP/TGF-β pathways) in the good responder, B6 osteoblasts, and not in the poor responder, C3H osteoblasts. An important implication of these findings is that the mechanosensitivity genes contributing to the different bone formation response in B6 and C3H inbred strain of mice are upstream to these four anabolic signaling pathways. This information should be very helpful in our search of the identity and/or the underlying mechanism of mechanosensitivity genes.

REFERENCES

1. Hillam, R. A., and Skerry, T. M. (1995) *J. Bone Miner. Res.* **10,** 683–689
2. Bikle, D. D., and Halloran, B. P. (1999) *J. Bone Miner. Metab.* **17,** 233–244
3. Hillsley, M. V., and Frangos, J. A. (1994) *Biotechnol. Bioeng.* **43,** 573–581
4. Kapur, S., Baylink, D. J., and Lau, K.-H. W. (2003) *Bone* (*NY*) **32,** 241–251
5. Frost, H. M. (1982) *Metab. Bone Dis. and Relat. Res.* **4,** 217–229
6. Kodama, Y., Umemura, Y., Nagasawa, S., Beamer, W. G., Donahue, L. R., Rosen, C. R., Baylink, D. J., and Farley, J. R. (2000) *Calcif. Tissue Int.* **66,** 298–306
7. Kodama, Y., Dimai, H. P., Wergedal, J., Sheng, M., Malpe, R., Kutilek, S., Beamer, W., Donahue, L. R., Rosen, C., Baylink, D. J., and Farley, J. (1999) *Bone* (*NY*) **25,** 183–190
8. Akhter, M. P., Cullen, D. M., Pedersen, E. A., Kimmel, D. B., and Recker, R. R. (1998) *Calcif. Tissue Int.* **63,** 442–449
9. Robling, A. G., and Turner, C. H. (2002) *Bone* (*NY*) **31,** 562–569
10. Sheng, M. H.-C., Lau, K.-H. W., Beamer, W. G., Baylink, D. J., and Wergedal, J. E. (2004) *Bone* (*NY*) **35,** 711–719
11. He, X., Ku, D. N., and Moore, J. E., Jr. (1993) *Annu. Biomed. Eng.* **21,** 45–49
12. Lau, K.-H. W., Lee, M. Y., Linkhart, T. A., Mohan, S., Vermeiden, J., Liu, C. C., and

Baylink, D. J. (1985) *Biochim. Biophys. Acta* **840,** 56–68
13. Farley, J. R., and Jorch, U. M. (1983) *Arch. Biochem. Biophys.* **221,** 477–488
14. Li, X., Mohan, S., Gu, W., and Baylink, D. J. (2001) *Mamm. Genome* **12,** 52–59
15. Akhter, M. P., Raab, D. M., Turner, C. H., Kimmel, D. B., and Recker, R. R. (1992) *J. Biomech.* **25,** 1241–1246
16. Kesavan, C., Mohan, S., Oberholtzer, S., Wergedal, J. E., and Baylink, D. J. (2005) *J. Appl. Physiol.* **99,** 1951–1957
17. Sheng, M. H.-C., Baylink, D. J., Beamer, W. G., Donahue, L. R., Lau, K.-H. W., and Wergedal, J. E. (2002) *Bone* (*NY*) **30,** 486–491
18. Pavalko, F. M., Chen, N. X., Turner, C. H., Burr, D. B., Atkinson, S., Hsieh, Y. F., Qiu, J., and Duncan, R. L. (1998) *Am. J. Physiol.* **275,** C1591–C1601
19. DeFriend, D. J., Anderson, E., Bell, J., Wilks, D. P., West, C. M., Mansel, R. E., and Howell, A. (1994) *Br. J. Cancer* **70,** 204–211
20. Kapur, S., Chen, S.-T., Baylink, D. J., and Lau, K.-H. W. (2004) *Bone* (*NY*) **35,** 534–535
21. Wang, H. Y., and Malbon, C. C. (2004) *Cell. Mol. Life Sci.* **61,** 69–75
22. Westendorf, J. J., Kahler, R. A., and Schroeder, T. M. (2004) *Gene* (*Amst.*) **341,** 19–39
23. Hanai, J., Gloy, J., Karumanchi, S. A., Kale, S., Tang, J., Hu, G., Chan, B., Ramchandran, R., Jha, V., Sukhatme, V. P., and Sokol, S. (2002) *J. Cell Biol.* **158,** 529–539
24. Warren, S. M., Brunet, L. J., Harland, R. M., Economides, A. N., and Longaker, M. T. (2003) *Nature* **422,** 625–629
25. Cheng, M., Zaman, G., Rawlinson, S. C., Mohan, S., Baylink, D. J., and Lanyon, L. E. (1999) *J. Bone Miner. Res.* **14,** 1742–1750
26. Sakata, T., Halloran, B. P., Elalieh, H. Z., Munson, S. J., Rudner, L., Venton, L., Ginzinger, D., Rosen, C. J., and Bikle, D. D. (2003) *Bone* (*NY*) **32,** 669–680
27. Sakata, T., Wang, Y., Halloran, B. P., Elalieh, H. Z., Cao, J., and Bikle, D. D. (2004) *J. Bone Miner. Res.* **19,** 436–446
28. Kapur, S., Mohan, S., Baylink, D. J., and Lau, K.-H. W. (2005) *J. Biol. Chem.* **280,** 20163–20170
29. Robling, A. G., Li, J., Shultz, K. L., Beamer, W. G., and Turner, C. H. (2003) *FASEB J.* **17,** 324–326
30. Srivastava, A. K., Kapur, S., Mohan, S., Yu, H., Kapur, S., Wergedal, J., and Baylink, D. J. (2005) *J. Bone Miner. Res.* **20,** 1041–1050
31. Gu, W.-K., Li, X.-M., Roe, B. A., Lau, K.-H. W., Edderkaoui, B., Mohan, S., and Baylink, D. J. (2003) *Curr. Genomics* **4,** 75–102
32. Karjalainen, H. M., Sironen, R. K., Elo, M. A., Kaarniranta, K., Takigawa, M., Helminen, H. J., and Lammi, M. J. (2003) *Biorheology* **40,** 93–100
33. Segey, O., Samach, A., Faerman, A., Kalinski, H., Beiman, M., Gelfand, A., Turam, H., Boguslavsky, S., Moshayov, A., Gottlieb, H., Kazanov, E., Nevo, S., Robinson, D., Skaliter, R., Einat, P., Binderman, I., and Feinstein, E. (2004) *Bone* (*NY*) **34,** 246–260
34. Hughes-Fulford, M. (2004) *Sci. STKE 2004,* RE12
35. Lean, J. M., Jagger, C. J., Chambers, T. J., and Chow, J. W. (1995) *Am. J. Physiol.* **268,** E318–E327
36. Rawlinson, S. C., Mohan, S., Baylink, D. J., and Lanyon, L. E. (1993) *Calcif. Tissue Int.* **53,** 324–329
37. Klein-Nulend, J., Roelofsen, J., Sterck, J. G., Semeins, C. M., and Burger, E. H. (1995) *J. Cell. Physiol.* **163,** 115–119
38. Liegibel, U. M., Sommer, U., Bundschuh, B., Schweizer, B., Hilscher, U., Lieder, A., Nawroth, P., and Kasperk, C. (2004) *Exp. Clin. Endocrinol. Diabetes* **112,** 356–363
39. Tanaka, S. M., Sun, H. B., Roeder, R. K., Burr, D. B., Turner, C. H., and Yokota, H. (2005) *Calcif. Tissue Int.* **76,** 261–271
40. Sakai, K., Mohtai, M., and Iwamoto, Y. (1998) *Calcif. Tissue Int.* **63,** 515–520
41. Raab-Cullen, D. M., Thiede, M. A., Petersen, D. N., Kimmel, D. B., and Recker, R. R. (1994) *Calcif. Tissue Int.* **55,** 473–478
42. Bonewald, L. F. (2002) *J. Musculoskelet. Neuronal Interact.* **2,** 239–241
43. Damien, E., Price, J. S., and Lanyon, L. E. (2002) *J. Bone Miner. Res.* **15,** 2169–2177
44. Jessop, H. L., Sjoberg, M., Cheng, M. Z., Zaman, G., Wheeler-Jones, C. P., and Lanyon, L. E. (2001) *J. Bone Miner. Res.* **16,** 1045–1055
45. Lee, K., Jessop, H., Suswillo, R., Zaman, G., and Lanyon, L. (2003) *Nature* **424,** 389
46. Jessop, H. L., Suswillo, R. F., Rawlinson, S. C., Zaman, G., Lee, K., Das-Gupta, V., Pitsillides, A. A., and Lanyon, L. E. (2004) *J. Bone Miner. Res.* **19,** 938–946
47. Lee, K. C., Jessop, H., Suswillo, R., Zaman, G., and Lanyon, L. E. (2004) *J. Endocrinol.* **182,** 193–201
48. Johnson, M. L. (2004) *J. Musculoskelet. Neuronal Interact.* **4,** 135–138
49. Hens, J. R., Wilson, K. M., Dann, P., Chen, X., Horowitz, M. C., and Wysolmerski, J. J. (2005) *J. Bone Miner. Res.* **20,** 1103–1113
50. Canalis, E., Economides, A. N., and Gazzerro, E. (2003) *Endocr. Rev.* **24,** 218–235
51. von Bubnoff, A., and Cho, K. W. Y. (2001) *Dev. Biol.* **239,** 1–14
52. Paez-Pereda, M., Giacomini, D., Refojo, D., Nagashima, A. C., Hopfner, U., Grubler, Y., Chervin, A., Goldberg, V., Goya, R., Hentges, S. T., Low, M. J., Holsboer, F., Stalla, G. K., and Arzt, E. (2003) *Proc. Natl. Acad. Sci. U. S. A.* **100,** 1034–1039
53. Kapur, S., Baylink, D. J., and Lau, K.-H. W. (2005) *J. Bone Miner. Res.* **20,** Suppl. 1, S240 (Abstr. SU219)
54. Lai, C.-F., Chaudhary, L., Fausto, A., Halstead, L. R., Ory, D. S., Avioli, L. V., and Cheng, S. L. (2001) *J. Biol. Chem.* **276,** 14443–14450
55. Ponik, S. M., and Pavalko, F. M. (2004) *J. Appl. Physiol.* **97,** 135–142
56. Clemmons, D. R., and Maile, L. A. (2005) *Mol. Endocrinol.* **19,** 1–11
57. Kim, H., Laing, M., and Muller, W. (2005) *Oncogene* **24,** 5629–5636
58. Novak, A., Hsu, S. C., Leung-Hagesteijn, C., Radeva, G., Papkoff, J., Montesano, R., Roskelley, C., Grosschedl, R., and Dedhar, S. (1998) *Proc. Natl. Acad. Sci. U. S. A.* **95,** 4374–4379
59. Lai, C. F., and Cheng, S. L. (2005) *J. Bone Miner. Res.* **20,** 330–340
60. Rhee, S. T., and Buchman, S. R. (2005) *Ann. Plast. Surg.* **55,** 207–215

Appendix-5

SU219

The Canonical Wnt Pathway Is Downstream to the BMP Signaling Pathway in Mediating Fluid Shear Stress-Induced Osteoblast Proliferation.

S. Kapur, D. J. Baylink, K. H. W. Lau. Musculoskeletal Disease Center, J. L. Pettis Memorial VAMC, Loma Linda, CA, USA.

C57BL/6J (B6) inbred mice, but not C3H/HeJ (C3H) mice, responded to loading with an increase in bone formation. Our previous microarray study showed that genes of the Wnt, BMP/TGFβ, IGF-I, and Estrogen receptor (ER) pathways were upregulated in B6, but not in C3H, osteoblasts (Obs) 4 hrs after the 30-min steady shear strain of 20 dynes cm^2, suggesting that the Ob mitogenic response to shear stress may involve these 4 pathways. Since there is abundant evidence for the involvement of IGF-I and ER pathways in shear stress-induced Ob mitogenic response, the present study focused on the potential role of and crosstalk between the Wnt and BMP pathways. Obs isolated from B6 mice were subjected to a 30-min steady shear stress at 20 dyne/cm^2. Cell proliferation was assessed by [^{3}H]thymidine incorporation. Expression of genes of the Wnt and BMP pathways (normalized against β-actin) was measured with real-time PCR 4 hr after the stress. The stress significantly increased cell proliferation (by 2-fold, $p<0.005$) in B6 Obs but not in C3H Obs. It also significantly ($p<0.05$ for each) upregulated the expression of genes of the canonical Wnt pathway: Wnt1 (2.3-fold), Wnt3a (3.3-fold), β-catenin (3.4-fold), LEF-1 (2.8-fold), and Axin (3.5-fold) and that of the BMP pathway: BMPR (2.6-fold), BMP4 (1.7-fold), Necdin (1.4-fold), and DLX1 (1.6-fold), in B6 Obs. The upregulation of many of these genes was confirmed by immunoblots. This shear stress-induced Ob proliferation and BMPR expression was each completely abolished by the BMP pathway inhibitor, noggin (300 ng/ml), while it was only partially (~60%, $p<0.002$) blocked by endostatin (10 μg/ml), an inhibitor of the canonical Wnt pathway. The lack of a complete inhibition was not due to an incomplete blockage of the shear stress-induced upregulation of canonical Wnt pathway, since this dose of endostatin abolished the shear stress-mediated upregulation of β-catenin expression completely. To evaluate potential crosstalk between the canonical Wnt and BMP pathways, we examined the effect of the noggin pretreatment on shear stress-induced upregulation of genes of the canonical Wnt pathway. The shear stress-induced Wnt1, Wnt3a, and β-catenin expressions were completely blocked by the noggin pretreatment. The shear stress also upregulated Wnt5a expression (non-canonical Wnt pathway) by 1.7-fold ($p<0.01$), but noggin had no significant effect on the shear stress-induced Wnt5a expression. In conclusion, the canonical Wnt pathway is downstream to the BMP pathway in the shear stress-mediated Ob proliferation and the BMP pathway mediated the shear stress-induced Ob proliferation partially through the canonical Wnt pathway.

Disclosures: ***K.H.W. Lau****, None.*